INSTALLATION OF BOREHOLE STRAINMETERS TO MONITOR NORTH ANATOLIAN FAULT NEAR ISTANBUL

by

Osman Bal

B.S., Geodesy and Photogrammetry Engineering, Ondokuz Mayıs University, 2012

Submitted to the Kandilli Observatory and Earthquake Research Institute
in partial fulfillment of
the requirements for the degree of
Master of Science

Graduate Program in Geodesy
Boğaziçi University

2018

INSTALLATION OF BOREHOLE STRAINMETERS TO MONITOR NORTH ANATOLIAN FAULT NEAR ISTANBUL

APPROVED BY:

Prof. Dr. Haluk Özener ..... (Thesis Supervisor)

Assist. Prof. Dr. Fatih Bulut .....

Prof. Dr. Bahadır Aktuğ ..... (Ankara University)

DATE OF APPROVAL: 20.03.2018

ACKNOWLEDGEMENTS

I would like to thank my supervisor Prof. Dr. Haluk Özener for giving me to chance to be a participant in the ongoing projects in Geodesy Department of KOERI. Throughout my thesis-writing period, he provided me encouragement, good advice and helpful opportunities. I am also grateful to Assoc. Prof. Dr. Aslı Doğru who has been very kind to guide me from the beginning and help me organize my ideas.

I am very thankful to jury members Prof. Dr. Bahadır Aktuğ and Assist. Prof. Dr. Fatih Bulut for their time and constructive reviews. Their ideas and critics shaped my thesis magnificently.

I am grateful to Wade Johnson from UNAVCO who was always with me during the entire process. He was not only a colleague but also an instructive friend in every step we have taken together.

I am thankful to Dr. Kerem Halıcıoğlu who encourage me to write my thesis in latex, and helped me with any problem I encountered. I am also thankful to Prof. Dr. Semih Ergintav who always answers students's questions and sharing his resources.

I am very greatful to know Dr. Saed Moghimi and Dr. Yin Cheng as not only my home mates but also best friends in my life.

I am deeply thankful to my family. They have always trusted and believed in me. Lastly, and most importantly, I would like to thank my girlfriend Nesli Kocaalili for her endless support, patience and understanding along this period.

ABSTRACT

INSTALLATION OF BOREHOLE STRAINMETERS TO MONITOR NORTH ANATOLIAN FAULT NEAR ISTANBUL

The North Anatolian Fault Zone (NAFZ) , which forms the plate boundary between the Anatolian plate in the south and the Eurasian plate in the north, runs under the Marmara Sea and is located less than 20 km from the city of İstanbul. According to historical seismicity data and recurrence times; an earthquake, which is bigger than magnitude 7, is expected.

Geodesists have been doing many observations on the NAFZ with various techniques since 1972. Geodesy Department of Kandilli Observatory and Earthquake Research Institute (KOERI) plays a crucial role on deformation measurement on the NAFZ with its micro-geodetic networks since 1989. By using the developing technology in time, Geodesy Department of KOERI incorporated some other terrestrial deformation measuring techniques like creepmeters and strainmeters.

The aim of this thesis is to discuss, the need of the strainmeter, installation cases for two boreholes, solutions found for site specific problems and the result of installation. Installed strainmeters will allow us to monitor potential slow-slip events along the Marmara Seismic Gap.

ÖZET

İSTANBUL YAKININDA DERİN KUYU GERİNİM ÖLÇER KURULUMU VE KUZEY ANADOLU FAY HATTININ GÖZLENMESİ

Güneyde Anadolu ve kuzeyde Avrasya levhalarının sınırını oluşturan Kuzey Anadolu Fay Zonu (KAFZ) , İstanbul'un merkezine 20 km'den daha yakın bir mesafe ile Marmara Denizi'nin altından devam etmektedir. Tarihsel depremsellik verileri ve tekrarlama sürelerinde bakıldığında, 7 büyüklüğünden daha büyük bir deprem beklenmektedir.

1972'den beri jeodezi bilim insanları KAFZ üzerinde farklı tekniklerle birçok gözlem yapmaktadırlar. Kandilli Rasathanesi ve Deprem Araştırma Enstitüsü (KRDAE) Jeodezi Anabilim dalı ise 1989'dan beri oluşturduğu mikro-jeodezik ağlar ile, KAFZ üzerindeki deformasyon ölçümlerinde çok önemli bir rol oynamaktadır. KRDAE Jeodezi Anabilim Dalı zamanla gelişen teknoloji ile birlikte, levha sınırlarında kullanılan gerinim ölçer ve kripmetre gibi yersel deformasyon ölçüm tekniklerini bünyesine katmıştır.

Bu tezin amacı, Marmara Denizi altında bulunan sismik boşluk için gerinim ölçer gerekliliği, iki adet derinkuyu gerinim ölçer kurulum tecrübelerini, sahaya özel sorunların çözümlerini ve kurulum sonuçlarını tartışmaktır. Bu tez, aynı zamanda, önümüzdeki zaman içerisinde, Marmara Denizi'ndeki sismik boşlukta yavaş kayma hareketi olup olmadığı konusunda bilgimizi arttırmak için yapılacak derinkuyu gerinim ölçer kurulumları için bir örnek teşkil edecektir.

TABLE OF CONTENTS

ACKNOWLEDGEMENTS . . . iii
ABSTRACT . . . iv
ÖZET . . . v
LIST OF FIGURES . . . viii
LIST OF TABLES . . . x
LIST OF SYMBOLS . . . xi
LIST OF ACRONYMS/ABBREVIATIONS . . . xii
1. INTRODUCTION . . . 1
2. GLADWIN TENSOR STRAIN MONITOR AND ITS APPLICATION . . . 15
2.1. Site Selection Criteria . . . 16
2.2. Drilling Techniques . . . 17
2.3. Logging and Logging Tools . . . 20
2.3.1. Density, Porosity and Full Wave Sonic Tool . . . 20
2.3.2. Lithology and Acoustic Televiewer Tool . . . 22
2.3.3. Miscellaneous and Three Arm Caliper Logging Tool . . . 23
2.3.4. Resistivity and Multiparameter E-Logging Tool . . . 24
2.4. Installation . . . 26
2.4.1. Strainmeter Installation . . . 27
2.4.2. Seismometer Installation . . . 30
3. EXPERIMENTS AND RESULTS . . . 32
3.1. Discussion on Estimated Strain Levels Around TEPE and HALK Stations 33
3.2. TEPE Site . . . 38
3.2.1. Geology in the TEPE Site . . . 40
3.2.2. Drilling Experiments in the TEPE Site . . . 44
3.2.3. Logging in the TEPE Site . . . 48
3.2.4. Installations in the TEPE Site . . . 49
3.3. HALK Site . . . 55
3.3.1. Geology in the HALK Site . . . 56
3.3.2. Drilling Experiments in the HALK Site . . . 60

3.3.3. Logging in the HALK Site 64
3.3.4. Installations in the HALK Site 64
4. CONCLUSION 69
REFERENCES 71
APPENDIX A: LOGS OF HALK SITE 80
APPENDIX B: LOGS OF TEPE SITE 88

LIST OF FIGURES

Figure 1.1. Measuring techniques of borehole strainmeter types (modified from Ishii et al, 2015). 8

Figure 1.2. Seismic gap in the Sea of Marmara and historic earthquakes along the NAF (modified from USGS,2000). 12

Figure 1.3. Coverage of the strain measuring equipments by UNAVCO. 13

Figure 1.4. Effective detection capabilities of seismometer, borehole strainmeter and GPS (modified from GTSM Technologies). 14

Figure 2.1. Strainmeter parts modified from Gladwin 16

Figure 2.2. Rotary drilling equipment (modified from Liao,Chien-Min,et al.). 18

Figure 2.3. Full wave sonic tool (modified from Century Geophysical Corp.)..... 21

Figure 2.4. Acoustic televiewer tool (modified from Century Geophysical Corp.) 23

Figure 2.5. Three arm caliper tool (modified from Century Geophysical Corp.)..... 24

Figure 2.6. Multiparameter e-logging tool (modified from Century Geophysical Corp.).. 25

Figure 3.1. Estimated GPS velocities from a block model by Reilinger (modified from Reilinger et al, 2006). 35

Figure 3.2. TEPE and HALK site's distance from the NAF. 36

Figure 3.3. Strain detectability of TEPE and HALK sites. 37

Figure 3.4. Location of the TEPE site. 39

Figure 3.5. Cutting samples for the first 84 meters in TEPE site. 40

Figure 3.6. Cutting samples from 84 meters to 97 in TEPE site 41

Figure 3.7. Last cutting samples in TEPE site.. 42

Figure 3.8. Geological formation in TEPE Site. 43

Figure 3.9. Danismen formation in the European side of Istanbul (modified form IBB Geological Map). 44

Figure 3.10. 6 and 7 inches casing, 6 inches drill bit and reduction. 45

Figure 3.11. Site visiting before the second drilling.. 46

Figure 3.12. Drilling and casing properties in TEPE site. 47

Figure 3.13. Trap mechanism and dump bailor setting.. 49

Figure 3.14. Mixing Masterflow 1206. 50

Figure 3.15. Cooled strainmeter. 51

Figure 3.16. Obtaining the magnetic compass value 52

Figure 3.17. Strainmeter installation in TEPE site. 52

Figure 3.18. Seismometer installation in TEPE site. 53

Figure 3.19. TEPE site in a container. 54

Figure 3.20. Location of the HALK site. 55

Figure 3.21. Mr. Arpat is examining the cuttings. 57

Figure 3.22. Last samples of HALK site. 58

Figure 3.23. Geological formation in HALK Site. 59

Figure 3.24. Cekmece formation around HALK site (modified from IBB Geological Map). 60

Figure 3.25. Drilling truck in the HALK site. 61

Figure 3.26. Borehole cleaning operation in the HALK site. 62

Figure 3.27. Drilling and casing properties in HALK site. 63

Figure 3.28. Dump bailor test in the HALK site. 65

Figure 3.29. Seismometer installation in the HALK site. 66

Figure 3.30. HALK site after installations. 67

Figure 3.31. Cable cut in HALK site. 67

Figure 3.32. HALK site in the container. 68

Figure A.1. Raw data of HALK site during Iran-Iraq earthquake in 12.11.2017 at 18.18 UTC. 81

Figure B.1. Raw data of TEPE site during Iran-Iraq earthquake in 12.11.2017 at 18.18 UTC. 89

LIST OF TABLES

Table 1.1. Components of measuring instruments. 7

Table 1.2. GTSM installations around the world by installation years. 15

LIST OF SYMBOLS

AC	Alternating Current
f	Frequency
ft	Feet
Hz	Hertz
kgs	Kilograms
m	Meters
r	Radius
V	Voltage
ϵ	Strain Rate
η	10^{-9}
θ	Rotation Angle
μ	10^{-6}

LIST OF ACRONYMS/ABBREVIATIONS

ABD	Amerika Birleşik Devletleri
CORP	Corporation
EAFZ	East Anatolian Fault Zone
GPS	Global Positioning System
GTSM	Gladwin Tensor Strain Monitor
HALK	Halkalı Strainmeter Station
InSAR	Interferometric Syntetic Aperture Radar
KAFZ	Kuzey Anadolu Fay Zonu
KOERI	Kandilli Observatory and Earthquake Research Institute
KRDAE	Kandilli Rasathanesi ve Deprem Araştırma Enstitüsü
NAFZ	North Anatolian Fault Zone
SLR	Satellite Laser Ranging
TEFZ	Thrace Eskişehir Fault Zone
TEPE	Tepekent Strainmeter Station
US	United States
USA	United States of America
VLBI	Very Long Baseline Interferometry

1. INTRODUCTION

Topography and surface specifications of the earth are highly related to rheology. Rheology is the manner of a material or a specific rock how it deforms under pressure, heat and other factors. Materials consist of the earth surface are separated into three groups as fragile, ductile and elastic respectively. Deformation styles are significantly related to deformation speed. A material can show elastic behaviour when it is deformed fast. However, the same material can show ductile behaviour in the same temperature and pressure and constraints when it is deformed slower. Mainly, the behaviour of materials under different stress and temperature is divided into three groups as elastic behaviour, plastic behaviour and viscose behavior respectively. There are three different transforming sections within these main groups as elastoplastic, viscoplastic and elasticoviscose [1].

Elastic deformation is convertible. Material under pressure gets deformed and keeps its position when the pressure goes on. However when the pressure goes off the material comes back to its first position and deformation clears away. Plastic deformation is not convertible. For a finite value of stress, if the deformation is increasing even the stress is the same, the material is called plastic. The other behaviour a material can show is viscosity. If a material comes back to its form deferred when the stress goes off, it is called the viscose behaviour [2].

Confining pressure, loading rate, temperature, solutions, time, pore pressure, anisotropy and in-homogeneity are crucially important factors for the rock behaviour. Confining pressure increases direct proportion to depth. As the confining pressure increases, rocks in deeper parts become more strong than their condition on the surface [3] [4].

Resistance of the rocks is inversely proportional to temperature and in the deeper parts of the surface as the temperature increases, the resistance of the rock decreases. Therefore, the rock tends to show plastic behaviour. During the deformation of the

rocks, the water in the empty spaces and the rock itself interacts each other. This interaction is mostly seen in metamorphic rocks. The solution inside of the rock effects the resistance of the rock and conveys the volume of the change in shape. The denser the liquid gets, the easier the rock deforms. The deformation of the materials inside the surface may change by the speed of the applied stress. The Earth is elastic and rigid under the short period of response, where it shows plastic behaviour under long period of response. Empty spaces inside of the rock or the liquid fulfills these empty spaces stands against the response of the confining pressure and decreases the confining pressure. Rocks may change in every other sections, so it must not be assumed that the rock would show the same response everywhere .

Determination of deformations is a research base on an existent movement derived from factoral forces. Crust deformations can be measured by several techniques which are categorized in two main groups as space and terrestrial techniques. In this thesis, VLBI (Very Long Baseline Interferometry), SLR (Satellite Laser Ranging) , GPS (Global Positioning System), InSAR (Interferometric Synthetic Aperture Radar) will be mentioned as space techniques and Tiltmeter, Creepmeter and Strainmeter as terrestrial techniques.

VLBI is used to determine earths spin speed, rotational axes movements and crust deformations. Coordinates can be obtained with under 1 cm precision by using radio signals. Because it is not affected from the weather conditions it is used in determining the crustal movements, earths spin speed, rotational axes movements and preparing base for space coordinate system and lots of tectonic movements and seismic deformations. It is used on determining the kinematics of the San Andreas fault in California with GPS measurements.

SLR is a space technique to determine spherical crustal movements. In this technique a laser shot's travel time is observed precisely which is send from the station point to the satellite. The distance from station point to satellite equals to half of the multiplication of the difference of the travel time and the light speed. SLR stations are used for modelling the spherical crustal movements, earths spin, acquiring the some

parameters related to gravitational field and building terrestrial reference systems.

InSAR is a technique where topographic elevation, changes on surface and actions on lands are tracked by using radar images which are obtained from satellites, plains or similar vehicles. InSAR is used on the research of subsurface collapse, land slides and volcanoes in coseismic and postseismic times.

GPS is consist of three main segments as space, control and user. Space segment has GPS satellites with two frequencies broadcasting module and atomic clock module. This satellites send messages including the location information. Second segment of GPS is control segment. This segment's purpose is observing the satellites's broadcasting and defining orbit parameters, calibrating the atomic clock and updating the location information messages periodically [5].

In all terrestrial methods, displacement has to be measured. As the deformations are small, displacements are even smaller. There are some improved electronic and optical sensors are produced to make this measurements, which are used in tiltmeters and strainmeters. The optical method is used in some of the earliest crustal deformation measurements and still in use today. The basic principle is using a reflected light beam to magnify the rotation of a mirror. If the mirror's rotation is θ , the beam will be displaced by $2r\theta$ at a distance r. The other and the most sensitive displacement transducers used in tiltmeters and strainmeters, measure changes in capacitance caused by the displacement of one part of the transducer [6].

Tiltmeters are designed for measuring very little differences in the horizontal axis in buildings and on the earth surface. They measure the amount and the direction of the movement on or inside of a mass. Tiltmeters are easy to use which have been used in tunnels, deep excavations, reservoirs and other engineering structures. Sensitivity of the tool can be decided for the purpose thus there are many kind of tiltmeters are available. Tilt meausurements are mostly done with a bubble sensor, horizontal pendulum or water tubes. In the modern borehole tiltmeters capacitive transducers are used to measure the displacements [6].

Creepmeters are the tools which is used where tensions occur because of the tectonic sources to measure very slow and continuous displacement. Creepmeter is located on the two cross sides of the fault and measures the displacement in the local area. A niclad wire is stretched from side to side and the length of this wire changes changes related to the movement in the fault. Displacement can be measured from this change in the length. Creepmeters are easy to set, low costed tools. Their sensitivity is in microns [7].

Strainmeters are measuring tools for linear, areal, volumetrical or creep deformations in a time average. They can be placed as horizontal or vertical for the purpose. In this thesis, strainmeters which are used for tectonic research purposes will be handled. Strainmeters, used for tectonic purposes, can be categorized into four groups by their operating principle. Which are wire strainmeters, laser strainmeters, hydraulic strainmeters and rod strainmeters respectively. The strainmeter types will be explained in this order. In the explanations, the chronological order is taken into consideration [6].

Wire strainmeters consist of an invar wire held in tension by a frictionless balance. The displacement transducers are used to measure strain which appears as rotations of the balance. The instruments used this basic design are built by Sydenham in 1969 [8], Bilham and King in 1970 [9] and Gerard in 1971 [10]. The most widely used design is developed by Cambridge University by King and Bilham which includes a servo motor to reset the distance of the weight from the pivot, stretching the wire to keep the instrument on scale for strains up to 10^{-4}. Wire strainmeters are installed in shallow trenches.

Laser strainmeters work with the principle of optical interferometry. The development of laser technology lets us to build strainmeters by using interferometry. Even several groups have studied on laser strainmeters, three groups have very significant results which are Berger and Lovberg from University of California, San Diego in 1970 [11], Goulty from Cambridge University and Levine and Hall from U.S. National Bureau of Standards in 1972 [12].

Benioff, the inventor of the strainmeter, suggested that broadening strains might be measured by burying a large container of liquid with a small opening. However, Sacks and Evertson have done it after 30 years where it is descripted in Evertson's thesis [13]. The principle is the same as that suggested by Benioff with the sensing volume cylindrical so that it fits in a borehole. The outher case of this strainmeter consists of two parts which are the actual sensing volume which is completely filled with liquit, and the second part is a smaller backing volume which is partly filled with inert gas. Sacks and Evertson strainmeters are widely used in the USA and Japan.

The first rod strainmeter is made in 1882 by Dewey and Byerly [14] however the first useful strainmeter was built 50 years later by Benioff in 1935 [15] for seismometry. The first strainmeter Benioff designed was a 20-m iron pipe which is attached to a pier and the other end to a reluctance transducer which drove a recording galvanometer. His strainmeter measured the strain rate because of the velocity transducer he used. Significant changes have been made by Benioff in 1959 by using 3-m sections of fused-quartz tubing cemented together to a length of 24 m. This renewed strainmeter is installed in California, New Jersey and Peru. It produced free oscillation data after the 1960 Chilean Earthquake. Some other designs, emphasized the use of strainmeters as seismometers. In 1966, Shopland [16] installed for 20-m strainmeters in shallow thrench to build an array at the Wichita Mountain. Shopland also installed 6-m strainmeters around the Nevada Test Site to measure strains released from nuclear explosions in 1970 [17]. In 1970, Fix and Scherwin [18] installed strainmeters in an abandoned mine at Queen Creek, Arizona. They wanted to build the most sensitive seismic system possible, so they took the advantage of the low noise level of this location. Using moving-coil transducers with a very high generator constant, this design allowed detection of small teleseismic events in 1973 [19]. After Benioff's design several quartz-rod systems were built in the USA, which required underground installation. By using a re-entrant aluminum coupling, Major [20] attempted to build instruments with temperature compensation so that they could run in shallow trenches. In Japan, the largest number of strainmeters have been installed to build a national network for crustal deformation observatories [21]. Some strainmeters are also installed in China. Many earlier systems used optical sensors, in which the end of the rod tilt a horizontal

pendulum.In 1968, a less sensitive strainmeter system also used in the Soviet Union [22] which rest the end of the rod on a small roller, motions of the rod turned the roller and an attached mirror. More recent Japanese strainmeters have used capacitive or inductive sensors.

Rather than shallow trenches, borehole installations have seen advantageous. Flexibility of deployment and possible long term stability leaded scientists to build strainmeters for borehole installation. In 1974, a 0.14-m quartz-rod length borehole strainmeter is designed [23]. A simpler designed strainmeter in the similar design has been built in China by Chi [24]. Details of the used electronics are not given but it is said that the instrument allows to detect displacements of $3x10^{-12}$ m. Instruments in China were installed in soil at depths of 20 to 40 m, and coupled to the earth by packing soil around them. After about one month's stabilization the instruments recorded tides and small local earthquakes. Another Chinese strainmeter is developed by Wang [25]. It uses a stretched wire to measure strain changes. The resolution of the strainmeter is said to be about $3n\epsilon$. An installation of this strainmeter in a shallow hole in a mine shows tides and annual cycle of amplitude $2\mu\epsilon$.

The other strainmeter is developed by Gladwin [26], which is used in our installation. Gladwin strainmeters are designed to be installed in boreholes at depths of 100-200 m. The resolution of the transducer 30pm, or $0.3n\epsilon$. In the strainmeters Gladwin designed, capacitance transducers are used as strain sensors. Basically it consist of a three-plate differential capacitor, with the center plate movable and the outer ones fixed. If a voltage V is applied to the top plate, and an opposite voltage to the bottom plate electric field between the plates is constant, and the voltage level is a linear function of position. However in this system, measuring the voltage on the center plate would vary only at the frequencies of interest, and at such low frequencies all electronic devices become more noisy than their thermal limits. These excess noises mostly have a spectrum that rises as f^{-1} for frequencies below 1 Hz and so to get the best performance, measurements should be made at high frequencies.

All kinds of deformation measuring instruments must include some kind of ref-

erence system, an instrument frame, a way to measure the displacement of the frame relative to the reference and some kind of attachment to the deforming object . In geodetic deformation monitoring, our GPS, tiltmeter and strainmeter systems are attached to the Earth by using different systems (Table 1.1).

Table 1.1. Components of measuring instruments

	GPS	**Tiltmeter**	**Strainmeter**
Reference	Whole Earth	Vertical	Length / Volume
Frame	Antenna	Body	Body
Displacement	Radio/ Software	Transducers	Transducers
Attach	Monument	Borehole / Anchor	Borehole / Anchor

Today, there are three known borehole strainmeter types available. They are the Carnegie, GTSM and Sakata (Ishii) type strainmeters. Carnegie strainmeters are Sacks and Evertson strainmeters, which are now being produced by Carnegie Institution for Science. GTSM is made by Mike Gladwin and Sakata type strainmeters are developed by Hiroshi Ishii and used in Japan.

Carnegie (Sacks and Evertson) Strainmeters can be used to observe changes in the volumetric strain only. The principle of this strainmeter is to convert the movement of siliconade oil sealed inside a cylindrical vessel into changes in strain. Sakata developed another strainmeter type applying Sacks-like principle, however Sakata's strainmeter is a three-component strainmeter. These strainmeters are sensitive to temperature changes. GTSM is based on the principle of measuring changes in the diameter of a cylindrical vessel by using a capacitance conversion sensor.

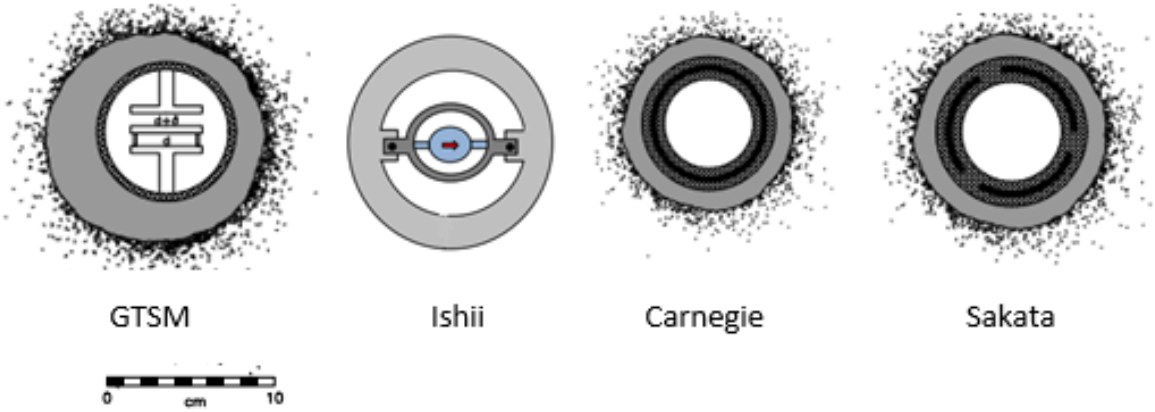

Figure 1.1. Measuring techniques of borehole strainmeter types (modified from Ishii et al, 2015).

Ishii [27] developed a strainmeter that had improved sensitivity as a result of mechanically expanding the deformation of the cylindrical vessel. Also Ishii [28] developed a comprehensive device with strainmeters, seismometers, tiltmeters and other components. Japanese strainmeters are mainly used for subduction zones. Being too far from the fault line, makes it harder to eliminate noises. Therefore, Japanese scientists decided to install borehole strainmeters up to 1 km depth. As it is mentioned in their papers, installing deeper than 500 meters, eliminate most of the noises. Japanese instruments are mostly used in Japan except 2 borehole installations in a mine in South Africa. GTSM and Carnegie strainmeters are relatively cheaper than the Ishii strainmeters however Ishii strainmeters are quite comprehensive. GTSM is mainly used for PBO project where it is located by San Andreas fault which is a strike slip fault. However GTSM is also used in Cascadia, where a subduction zone is available. The number of the kind of installed strainmeters are mostly the matter of trade and production.

Anatolia has not only been the cradle of civilizations but also the tectonic movements. These movements mostly originated from the northward movements of Arabian and African plates. The most attractive zone in the Anatolian plate has been the North Anatolian Fault Zone. Due to containing the most active zones in world, it constitutes

a natural laboratory for the geoscientists. There have been many studies on the North Anatolian Fault Zone, in addition to this many papers have been written. Since 1972, geodetic observations have been done in various parts of North Anatolian Fault Zone where Geodesy Department of Kandilli Observatory and Earthquake Institute takes a crucial role since 1989 [29].

During and after the 17 August 1999 Izmit Earthquake, GPS observations have been made by several institutions to determine coseismic and postseismic fault slip [30]. Furthermore, estimates of seismic potential in the Marmara Sea are made by using GPS measurements where a secular velocity field in the north-western Turkey geodetically observed with a block model that accounts for recoverable elastic-strain accumulation [31]. Time dependent crustal movements of the Izmit earthquake are also been studied by using different methodologies with linear, quadratic and exponential kinematic models [32]. Being a result of Africa-Arabia-Eurasia continental collision, North Anatolian and East Anatolian faults also been studied for plate interactions [33]. The most seismically active region in Western Eurasia, the Aegean Region, has been studied with a geodetic network for disaster management on the active Tuzla Fault which is close to the third biggest city in Turkey, Izmir [34]. Another study has been done with a new GPS campaign and strain accumulation has been calculated [35]. The Earth is being monitored every moment by many kinds of sensors where GPS receivers are being used as geodetic instruments to precisely detect crustal motion in the Earth's surface. Strain rates are a key factor in seismic hazard analyses, and a study has done by KOERI Geodesy department on generating strain maps by using data from continuous GPS stations for seismic hazard analysis [36]. The western part of NAF bifurcates around Mudurnu into two fault segments as northern and southern branches. The latter bifurcates again at west of Pamukova and creates middle strand. The middle strand is near Iznik which is considered as inactive fault where a microgeodetic network is available called General Command of Mapping and Istanbul Technical University network. Adding the GPS campaigns held in between 2004 and 2007, the triangulation measurements between 1941 and 1963 and trilateration measurements in 1981 are used for investigation of long period crustal deformation on the inactive branch of NAFZ [37]. Monitoring the NAFZ after Izmit and Izmit-Duzce earthquakes went on and 7 years

of postseismic deformation measurements are done by using continuously recorded and survey mode GPS observations [38]. Lack of geodetic information about the present tectonics of eastern parf of NAFZ is resolved by the GPS campaigns made in an area of 350 km x 200 km where the NAFZ and the EAFZ intersects. In this study results show that strain is accumulating between the NAFZ and EAFZ along small secondary fault branches [39]. Another study has been done by using the combination of geodetic and seismological data around the Karliova Triple Junction. GPS-derived geodetic slip rates suggest that it has the potential to produce an earthquake of Mw 7.5 across an 80-km rupture zone in Yedisu segment [40]. Precise leveling can also be used to determine vertical displacement. Using GPS and presize levelling displacement of the Tuzla Fault has been determined [41]. The geodesy department of KOERI established three micro-geodetic network in the eastern Marmara region which are Akyazi, Sapanca and Iznik networks. In these networks, GPS data have been collected since 1994 [42]. Another well known creeping segment Ismetpasa is observed by the General Command of Mapping from the 5 pillars established in 1972. Geodesy department of KOERI also carried out GPS campaigns in these 5 pillars annually between 2005 and 2011. Finding the creep rate less than half of the annual average rate, it is indicated that significant strain is being accumulated on the fault [43]. An evidence for aseismic fault reactivation has found after Mw 7.2 23 October 2011 Van earthquake [44]. Another study has been done on the locking depth variation along central and easternmost segments of NAFZ [45]. The major seismic gap along the NAFZ is under the Sea of Marmara. To estimate strain accumulation on the fault segments in the Marmara Sea seismic gap 20 years of GPS observations has been used. It has seen that Princes' Islands segment is most likely to generate the next M>7 earthquake along the Sea of Marmara segment of the NAFZ [46]. The East Anatolian Fault Zone is the second major fault system in Turkey, following the North Anatolian Fault Zone. Geodesy deparment of KOERI is also concerned about NAFZ and survey-type GPS data and homogeneously combined published velocities from other studies are collected for a study [47]. Being a part of observatory, Geodesy department is also interested in astro-geodetic camera systems for the measurement of the vertical deflections [48]. As a kind of deformation, coastline deformation is also seen often in Turkey peninsula. Carrying out a geodetic survey in

the Kilyos Campus of Bogazici University between 2001 and 2002, shoreline change has been studied using Landsat imagery between the years 1986-2015 [49]. One of the terrestrial deformation measuring techniques, creepmeter, has also been used recently in KOERI's projects. Installing creepmeters in well known creeping Ismetpasa segment, various kind of measurements have been studied and surface creep has been determined between the years 1944 and 2016 [50].

Tectonic geodesy studies in Turkey mainly made by using GPS. A lot of effort spent on measuring slip rates not only around the active fault zones but also all around the country. In virtue of the studies mentioned above, the slip rates of main fault zones driving Turkey's neotectonics determined and block deformation models are formatted through geodetic methods in a recent project. Surrounded by active faults Marmara Region has crucial importance for geosciences. Furthermore, current seismic activity in the eastern Marmara Sea indicates a complex fault network at the transition between the western end of the Izmit earthquake rupture and the assumed seismic gap south of Istanbul, below the Sea of Marmara, where a major earthquake is expected to occur in the near future [51].

The North Anatolian Fault Zone is one of the largest plate-bounding transform faults separating the Anatolia and Eurasian plates and extending for about 1600 km between Eastern Anatolian and Northern Aegean. A series of earthquakes starting from 1939 near Erzincan and propagated westward toward the Marmara region where 1999 Izmit earthquake occured. The seismic gap is between 1912 Ganos and 1999 Izmit ruptures where there is no rupture since 1766 [52] (Figure 1.2).

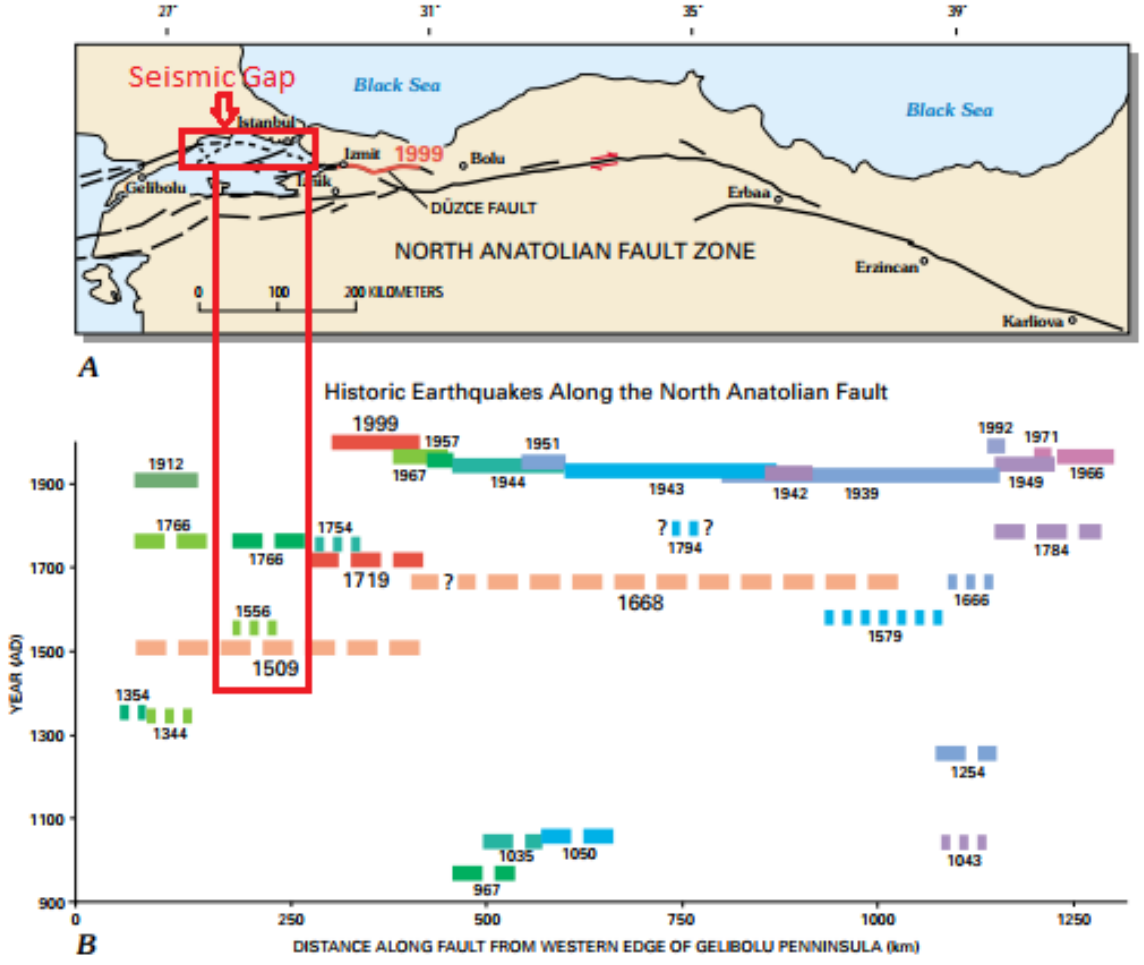

Figure 1.2. Seismic gap in the Sea of Marmara and historic earthquakes along the NAF (modified from USGS,2000).

However, existing seismic observations lack the spatial and temporal resolution required to accurately distinguish between locked and creeping segments. For this reason, more sensitive tools are needed for acquiring the strain rates.

The continuous tectonic motion measurements have rates of $10^{-14}s^{-1}$ thus it requires extremely high instrument stability. However more rapid motions like tides and seismic waves are even smaller and are not observable easily. For the tectonic purposes the sensitivity of strain rate is around 10^{-9} [6] 1.3.

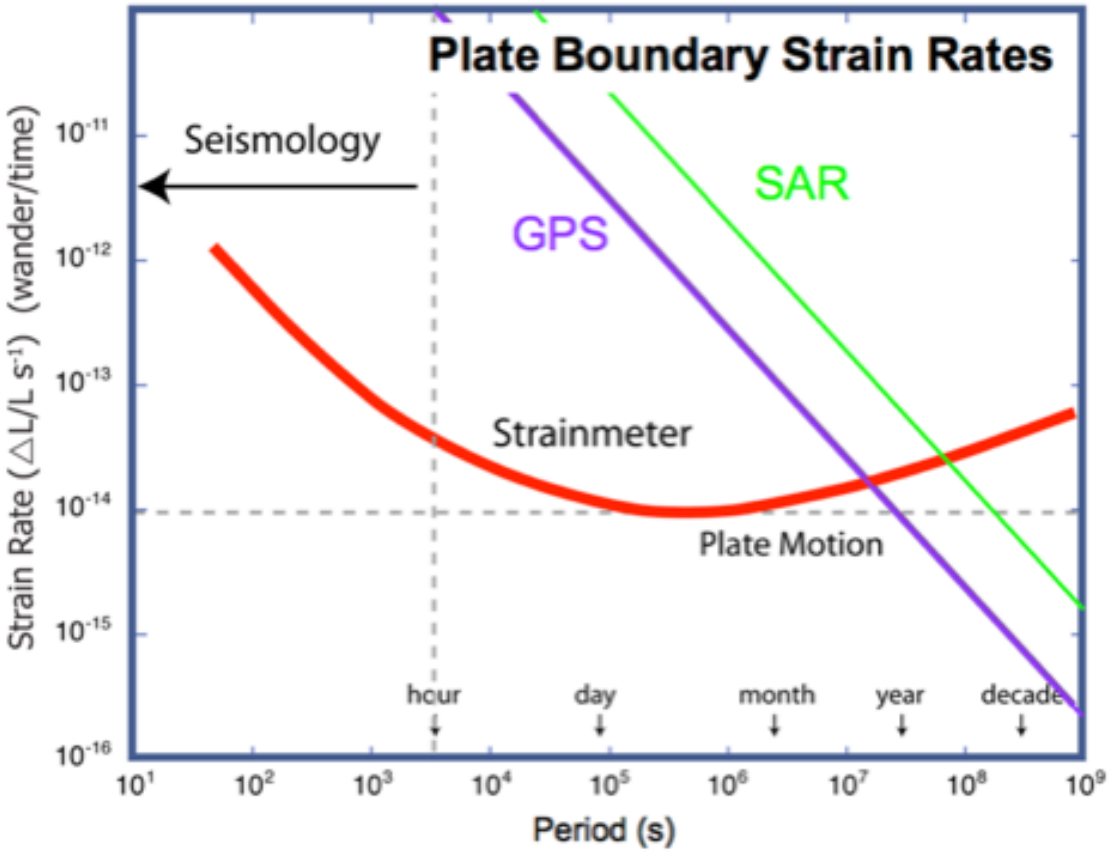

Figure 1.3. Coverage of the strain measuring equipments by UNAVCO.

Downhole sensors provide substantial benefit to signal quality. Sensors which are installed downhole have the advantage of absence of near-surface noise. Strainmeters are highly sensitive instruments with precision of 1 part per billion which is suitable for tectonic purposes (Figure 1.4). They are usually installed in boreholes where surface noise is greatly reduced. Besides, strainmeters are supplementary in tectonic studies between seismology and GPS studies (Figure 1.3) [53] [54].

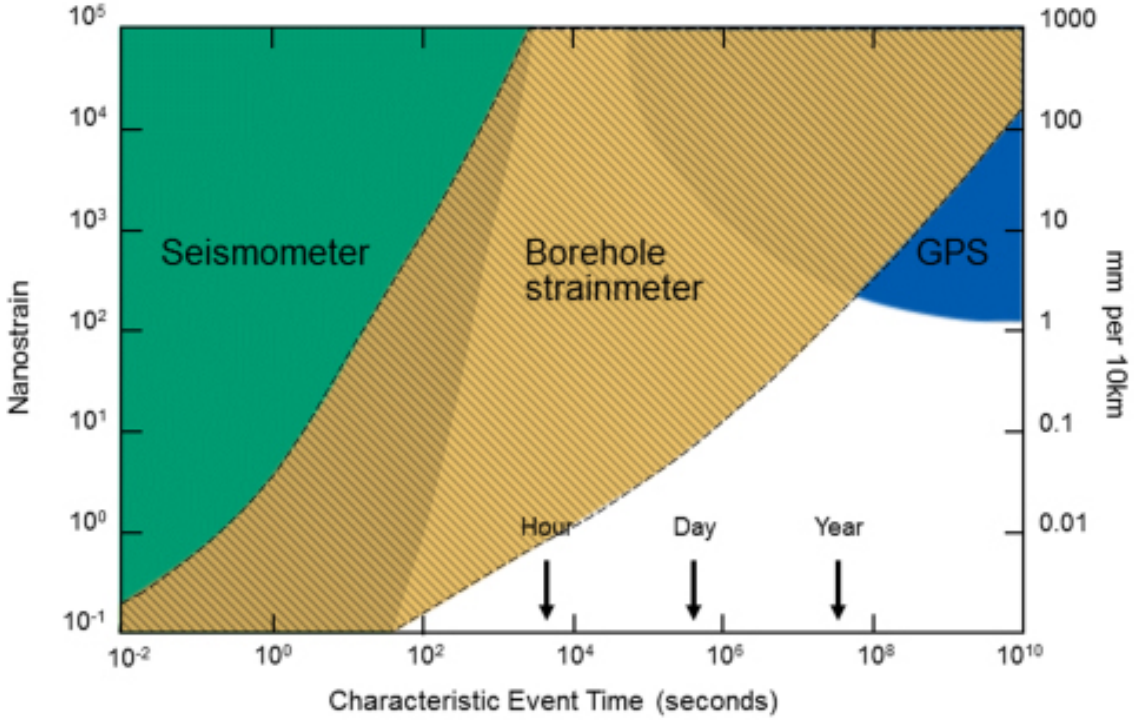

Figure 1.4. Effective detection capabilities of seismometer, borehole strainmeter and GPS (modified from GTSM Technologies).

Fullfilling the gap between seismology and GPS studies (Figure 1.4), borehole strainmeters are used in plate boundaries in Japan and USA. In order to monitor NAFZ passing under the Marmara Sea, strainmeters were great needs. Increasing the number of strainmeters as a network, the western part of NAFZ would be more observable. This thesis is also aimed to be a manual for the future strainmeters installations in Turkey.

2. GLADWIN TENSOR STRAIN MONITOR AND ITS APPLICATION

Gladwin Tensor Strain Monitor so called GTSM is a rod type borehole strainmeter. It started as a graduate work of Michael Gladwin in 1969. It is firstly installed in 1972 in Queensland and the test of the instrument on the tectonic strain measurement is held after the installation in the Praesidio fault in San Francisco. As it is understood that the instrument covers a big lack of the observations and it even overlaps with seismic and GPS studies, starting from 1983 the system has been installed in thirteen places over the first fifteen years. In 2004 the system has been begun to used by US Plate Boundary Observatory and in five years, 70 systems have been installed in the USA. Furthermore, the system has started to get in use in the other countries. Between the years 2003 and 2010, thirteen systems have been installed in Taiwan, four installed in Japan in 2009, five systems in Australia between 1991 and 1992, two in Korea in 2010 and six in Turkey between 2014 and 2015 (Table 2.1).

As it is told above GTSM is a rod type in shape and installed in a borehole which is specifically drilled for it. It is an instrument that has three strain cells located 120 degrees from each other. In every strain cell there is a three element capacitance with a fixed gap reference. The move of the moving plate in this strain cells can be monitored to a few picometers. Three strain cells are used for the stability of the

Table 2.1. GTSM installations around the world by installation years

Country	**Installation Year**	**Amount of GTSM**
USA	1983-2005	78
Australia	1991-1992	5
Taiwan	2003-2010	13
Japan	2009	4
Korea	2010	2
Turkey	2014-2015	6

measurement system and its independence to environmental perturbations. There is also a module for orientation where a magnetic compass encoded to determine the attained instrument orientation when it is placed in the borehole. The parts of the strainmeter are shown in the figure below. (Figure 2.1).

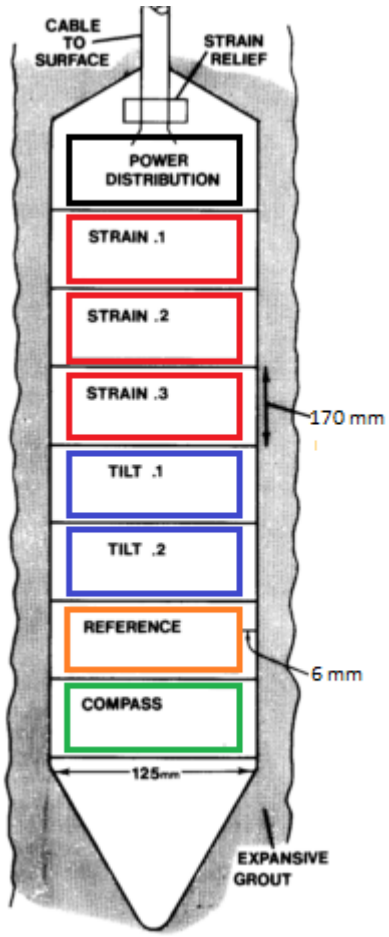

Figure 2.1. Strainmeter parts modified from Gladwin.

2.1. Site Selection Criteria

Site selection so called siting, depends on three technical conditions which are scaling the array, hydrology and topography. Due to the fact that only two strainmeters installed, an array geometry has not been considered. Nevertheless being in the a linear line parallel to the fault with in an approximate distance has been considered.

Topography is an observable anisotropy imposed on the tectonic field. Topographic issues may cause 30% of the departures from ideal tidal calibrations and are often subject to rotations of the measured field [55] .

Instruments should be installed above the average topographic profile because the effects on data quality are obvious. This happens because some of the topography may follow the underlying geology, so the search for the quality rock moves the targets away from recent sedimentary materials. The location of 200 meters bore-holes in 2000 meters topographic relief compromises the coupling of the instrument in the deep bore-hole. The sides of steep topography should be avoided both for topographical reasons and for the related thermoelastic response of the hill site.

2.2. Drilling Techniques

Drilling means to make a hole in order to get access to the earth's subsurface. Drilling may be done for three basic purposes which are gaining information about subsurface, production of materials under earth's surface, or monitoring subsurface properties. Drilling can be done in three basic methods which are percussion drilling, rotary drilling and combined drilling. Percussion drilling is a very basic manual drilling method. In percussion drilling a heavy cutting or hammering bit is attached to a cable or a rope in an open hole or a temporary casing. This method can be used in many conditions but the keeping the orientation of the borehole in some limits and a smooth drilling is hardly possible. Combine drilling method is not a unique method like percussion and rotary drilling. Instead it is a collocation of these methods. In some cases, where the layers are too hard to pass or for economic reasons, percussion drilling and rotary drilling can be used together.

The rotary drilling can be applied in unconsolidated and consolidated formations. It is economical for large diameter holes, needs minimal drilling fluid and holes can be drilled with one or two passes. In this technique the drilling fluid passes through the drilling rigs, flow out the well, is filtered on site and reused for the same purpose. It is called rotary drilling because of the rotaries are in every part of drilling progress.

Rotary drilling equipment can be moved separately or there are special trucks for rotary drilling where drill rods, water tanks, drilling tower and the other necessary equipment can be carried on the truck haulage.

In Turkey, the rotary drilling is mostly made with drilling trucks. In the drilling truck we used, there is a twelve meter long tower which allows the kelly bar and drill rod settings in it. Drill rods are 10 meter long iron rods ,which are connected to each other as deep as the borehole goes. In the end of these drill rods, there is a drill bit which consists of three revolving cutting bits. The inside of the drill rods is empty so water can be pumped in for the drill bit. Drill bit cuts the layers while the water is circulated in the borehole. This system helps to cool the drill bit and softens some material while drilling. For the need of power, there is a generator on the drill truck with a gear which also controls the spin speed of drilling rods. There are also ropes and cables to lower the kelly bar and other systems attached to the tower. In the upper sections, bentonite, a special kind of clay can be used to stabilize the borehole walls. A simple figure of drilling equipment is shown below [56] (Figure 2.2).

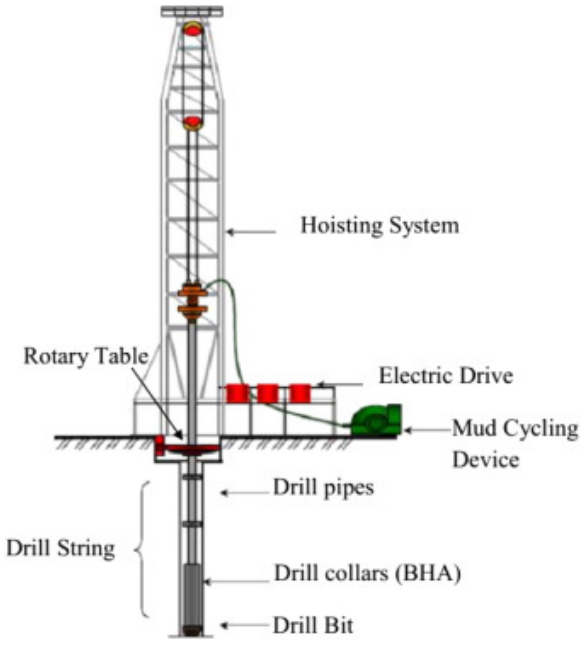

Figure 2.2. Rotary drilling equipment (modified from Liao, Chien-Min, et al.).

Drilling boreholes for strainmeter installations have some specifications. As it is mentioned in Gladwin's notes for drilling there are some criteria where some are different for UNAVCO and also in our cases. Every installation has its own story and specifications thus unique in problem cases. Basically, Gladwin has suggested the items below for the drilling specifications.

- Access
- Use of open hole and air hammer to get to near target
- Identification of when to begin coring
- Stabilization of the uncased section of the open hole with casing
- Core recovery
- Types of mud allowed
- Verticality
- Cleaning and preparation of the target zone

The drilling site has to be in an accessible place because there is always need to carry many equipment to the site. Thus rotary drilling used in our installations, there have been no need for an air hammer. As also Gladwin mentioned in his notes, UNAVCO have decided not to core before installation. Casing has been a crucial problem in our installations because of the different system used in Turkey than the USA. Experiences on casing will be shared in every installation in the next chapter. Recovery of the uncased section is also crucial for installations. The installation zone has to be so clean that there must not be any material like mud or clay between the expansive grout, strainmeter and installation zone. Thus the upper segments of the borehole consist of loose material, special kind of clay (bentonite) has to be used to keep the borehole in form. Even mud is not allowed in the core, it is a need in the beginning of drilling before casing. The point has to be concerned is cleaning all the mud before installation. Verticality is another crucial subject because the strainmeter has to stand in vertical position. Conventionally drilled boreholes are claimed to be vertical, but are commonly found to deviate by as much as 5 to 15 degrees. In our installations, the drilling company contracted to keep boreholes within 5 degrees from

the vertical. Properly drilled holes has to be cased by using metal casing. After the casing and logging if the installation section seems fine, the borehole has to be cleaned from mud and clay. If necessary cleaning foam can also be used in this progress.

2.3. Logging and Logging Tools

Electrical coring has been the term for logging when it is invented in 1927. It is also be translated as a record of characteristics of rock formations traversed by a measurement device in the well bore. Well logging started with petrol researches on the world where it is used for many other purposes for geosciences.

2.3.1. Density, Porosity and Full Wave Sonic Tool

Density is described as the mass per volume of a material. For a completely homogeneous material density can be calculated straightforward 2.1 .

$$Density = \frac{Mass}{Volume} \tag{2.1}$$

Nonetheless, earth materials are combined of several supplements. Rocks especially consist of many kinds of materials and so they are porous, and porosity is closely related to density 2.2.

$$Porosity = \frac{PoreVolume}{TotalVolume} \tag{2.2}$$

Several logging techniques are available to measure density and porosity. These indirect techniques have some considerable errors determined by borehole conditions

but they provide a measure of the in-situ properties. Gamma ray logs bombard the formation with radiation from an active source. Radiation spreaded back to the logging tool depends on the electron density of the material. Formation density is extracted from the amplitude of these back-scattered gamma rays.

In our installations, the full wave sonic tool has been used which is designed by the Century Geophysical Corp (Figure 2.3). The full wave form data is also recorded simultaneously, along with near and far travel times, borehole-compensated delta time, calculated sonic porosity, receiver gains, near/far amplitudes and natural gamma.

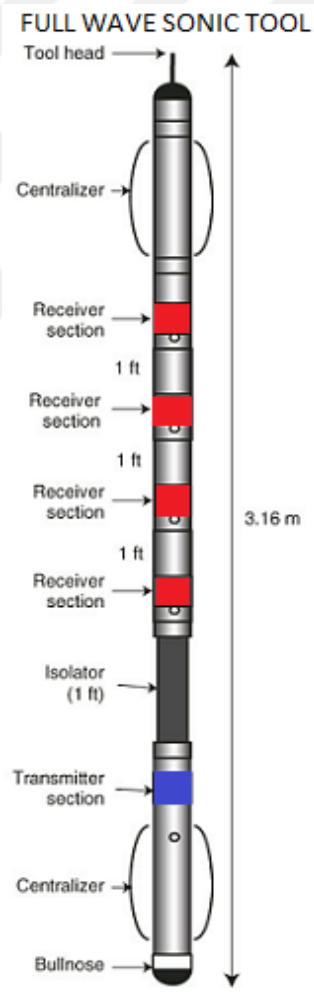

Figure 2.3. Full wave sonic tool (modified from Century Geopyhsical Corp.).

The sonic or acoustic log uses the basic principle of sound waves travelling through

a media. The century sonic system uses a single transmitter and dual receiver system for recording the travel times of the formation. The receivers are spaced approximately 2 and 4 feet, from the transmitter. Therefore, a 0.3 m (1 foot) calculation can be made to measure this interval transit time.

2.3.2. Lithology and Acoustic Televiewer Tool

Lithology is a term used as a gross identification for a rock layer in the subsurface. In a very basic way lithology uses familiar names such as sandstone, limestone, dolostone, claystone, chert, coal, shale, diatomite, halite, anhydrite, gypsum and tuff.

Lithology mainly focuses on grains where the direct determination can be made. Obtaining a sample of the reservoir is the surest way to unambiguously determine lithology and rock type. The mud logs are the first chose however the size of the individual rock sample examined at the surface is rather small because it is limited by the size of drill cuttings and rock strength.

Another case is the indirect determination where no direct rock sample is available in a given zone, log responses must be used alone to simultaneously determine lithology. Acoustic velocity is primarily a function of the rock matrix and can be used to identify different lithologies and stratigraphic correlations.

The Acouistic televiewer loging tool can be used in the indirect determination method. This tool takes an oriented picture of the borehole using high-resolution sound waves. This acoustic data is displayed in both amplitude and travel time. Moreover the data is used to detect bedding planes, fractures and other hole anomalies without the need to have clear fluid filling the boreholes. The televiewer digitizes 256 measurements around the borehole at each high-resolution sample interval. The sample interval refers to 0.005 meters or 0.02 feet.

In our loggings 9804UG model of Acoustic Televiewer is used which is produced by Century Geopyhsical Corp (Figure 2.4).

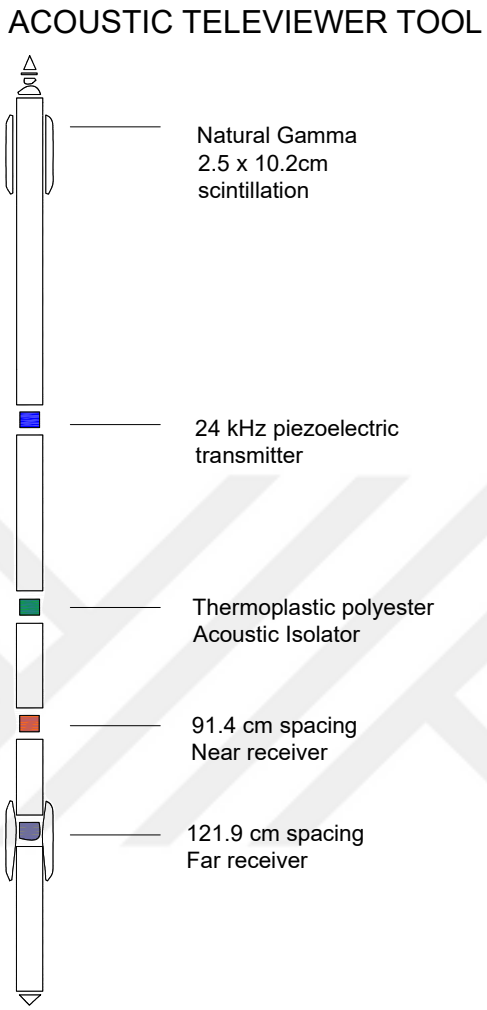

Figure 2.4. Acoustic televiewer tool (modified from Century Geophysical Corp.).

2.3.3. Miscellaneous and Three Arm Caliper Logging Tool

Miscellaneous of the borehole refers to deformation of the borehole's diameter in our case.

Three arm caliper, has three metal arms to detect the change in the diameter. The caliper send to the end of the borehole in closed position and the arms get opened by a electro motor inside of the caliper. While the caliper travels to the head of the borehole, metal arms collect data by touching the sides of the borehole. Deflection of

the arms are turn into a dataset by a potantiometer (Figure 2.5).



Figure 2.5. Three arm caliper tool (modified from Century Geophysical Corp.).

2.3.4. Resistivity and Multiparameter E-Logging Tool

Resistivity logging in a borehole gives us information to characterize the rock or sediments by measuring its electrical resistivity. Electrical resistivity can be measured

Resistivity logging is the recording in uncased sections of a borehole ,which means

the lower installation sections in our case, of the resistivites of the subsurface formations. This recording is giving us information about the quantitive evolution of possible installation zone.

In our fieldwork, a multiparameter E-logging tool has been used. The tool has three sensor for natural gamma, temperature and fluid resistivity respectively (Figure 2.6).

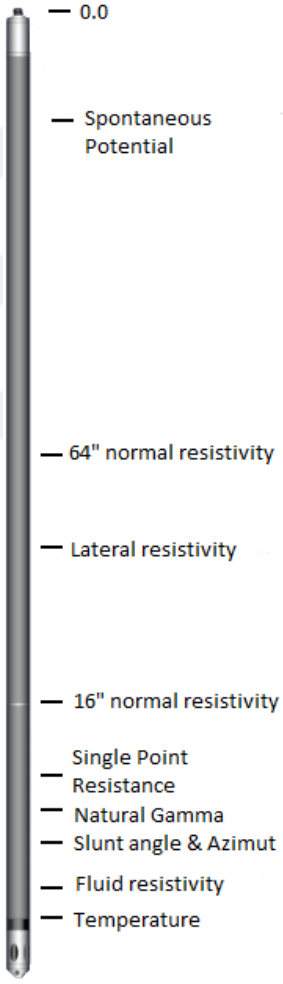

Figure 2.6. Multiparameter e-logging tool (modified from Century Geophysical Corp.).

The 9044 model E-logging tool has been produced by Century Geophysics Corp.

2.4. Installation

The role of the strainmeter in the deformation measurements is covered in the previous sections. As it is mentioned, there are many types of strainmeters therefore many types of installations are available. In our case, the Gladwin Tensor Strain Monitor is installed with a 2 Hz 3-C seismometer in every borehole. In this section generally the needs of installation and installation program will be explained.

After field research, drilling, geological decisions and casing, the installation step begins. The installation have a procedure which contains logging, grouting and installing the equipment. In every other step of this procedure special engineering techniques are used which are necessary for a successful strainmeter installation and coupling.

At first, the borehole has to be checked in terms of porosity, lithology, miscellaneous and resistivity of the installation zone. These measuments are done by using special logging tools which are mentioned in the previous section. Before the logging operations, the borehole has to cased to protect logging tools from a possible collapse in the borehole walls. Therefore, the most of the logs are taken from the uncased section which is also the candidate installation zone.

Before logging operations the borehole does not have to be clean, however if the section which is logged is suitable for the installation the borehole has to be cleaned very well to provide and opportunity for the best coupling.

Grouting is also done by using a special equipment which is called dump bailor with a trap mechanism embedded. Dump bailor is a 10 meter long aluminum tube with 5 inches width. The trap mechanism is consist of steel and aluminum parts which works as a button when it is pressed in the end of the borehole, it lets the grout flow out of the dump bailor and fill in the borehole. By using a dump bailor and trap mechanism the borehole is grouted in the deeper sections.

Installation is the last step for this progress. Welding the quarter block to the well head, strainmeter is slowly slides in the borehole with its own cable. When it reaches the desired depth, the cable is tied to the well head until the set of concrete. The seismometer installation is easier and done with a sliding rope which is marked with the desired distance. The grout is send by using a regular hose which is strapped to the seismometer.

2.4.1. Strainmeter Installation

There are many designs for strainmeters and other deformation-measuring instruments where the transducers are improved in time. However another crucial issue is how it is to be attached to the earth. Attachment is a difficult problem because it must be done in the field rather than a laboratory. Many coupling methods have been tried but the coupling problem remains unsolved. A properly coupled equipment would record only the deformations that are physically present without distortion.

The real deformations are assumed to be in greater depths which are seismic waves, earth tides, surface loads, and crustal deformation. We can auspiciously explain the observations by assuming the earth to be a nearly uniform elastic body, we commonly take this assumption to be generally valid; thus we expect a properly coupled instrument to be one that records the deformation physically present near the surface of an elastic sphere. This assumption may be broken down for slow crustal deformation and assuredly does over geological time scales [57]. Scientific theoretical preconceptions are so weak and it is hardest to decide whether or not an instrument is measuring the real deformations.

Three general attachment method can be considered in the coupling deformation-measuring instruments as attachments near the surface, attachments in the caves and tunnels and boreholes. Attaching the instrument near the surface or depths easily reached is accessible at low cost but the surface deformations may not follow the real deformations at all. Loose and partially fractured material at the surface can be decoupled from deeper motions. The best evidence for this the borehole stress measurements

in California [58]. They show stress changes with depth which are consistent with a purely elastic model. However the best evidence against this are the seismic, tidal and geodetic measurements which are made at the surface and exactly show the motion at depth. If the borehole stress measurements and shallower measurement show a similar stress direction, it can be said that the effects of tectonic forces are propagated to the surface [59].

Tiltmeters and strainmeters can also be installed deep in the ground to reduce thermal effects on the instrument. Until the development of the borehole instruments, strainmeters are attached into the caves, mines and tunnels. However the main problem is, the instruments get installed in an opening and opening distorts the deformation field. Furthermore, these cavities are not mostly available where the measurement is needed. Borehole installation is the other method where the more excavation and budget needed. Nevertheless, in the limited space of boreholes, special designs are needed for measuring equipment and all the data has to be sent to the surface. In the borehole installation, the azimuth of the instrument has to be found by using the magnetic compass. Furthermore, as it is not possible to level the instrument in a deep borehole, at least the tilt angle has to be known.

Installing a rod type strainmeter in a borehole needs some specifications. After the site selection and drilling properly, the subsurface screening begins. Well logging is the other step has to be taken right after the casing. The logging operation is done after the casing because any collapse in the borehole cause to loose of logging tools. Before the logging operation, cuttings have been observed. Cuttings give us some information about the type of the rock has been drilled, however it is impossible to understand whether there are fractures in the rock. After the logging operation if it is necessary to drill deeper, drilling operation should go on inside of the casing until reaching the target zone. If the logs and the other observations show that the installation zone has been reached, the borehole has to be cleaned by using only water or if necessary some foam may be added to the cleaning water.

After the borehole has been cleaned, a well head has to be welded to the beginning

of the casing which is used for the quarter block attaching. The welding has to be done before the cementing because there will not be enough time for strainmeter lowering after the grout has been sent. Dump bailor and trap mechanism has to be set and tested outside. The other test with the dump bailor is made in the borehole. The trap mechanism has a special design which allows the grout to pour out when it crashes to the end of the borehole. Thus this test has to be done with water fulfilled dump bailor. The test has to be done twice to see whether the trap mechanism work properly. After these tests, grout has to be prepared. As it is mentioned in the introduction, in deformation monitoring attaching the equipment in a proper way that the physically existing deformation can be monitored, is the most crucial subject.

In other words, everything can be made properly until attaching the equipment to the installation zone; if the installation is made with a wrong material for a tool which works in nanostrains, the real deformation will be lost on the way to the sensors. Installation with different cements have been tested in many boreholes. There is not a perfect way of coupling the tool, however cementing technology is getting improved day by day. In our installations, Masterflow 1206 high-strength grout has been used which is produced by BASF. Masterflow 1206 is a cement based product with specially graded spherical aggregate that produces a pumpable non-bleeding high-strenght grout. It is bleed free for vertical heights up to 100 ft (30.5 m). It is compatible with high-strength steel and can be pumped for long periods of time. It can be used over a wide range of mixed grout and placement temperatures. Surfaces that the grout will be applied should be oil free and clean. Mixing this grout also needs some care. For a 25 kgs bag 6.8 to 7.9 liters of water should be used and the water has to be potable and preferably alkaline. In our installations ASE MIX 15 mixer is used which is produced for special kind of concrete mixtures.

Strainmeter installation needs some preliminary preparations. Hence there will not be enough time after dump bailer crush, strainmeter cable has to be unwrapped and marked with a marker tape in advance.

The cable has to be marked with a piece of tape for every ten meters which is

easy to follow. In the mean time strainmeter lies in its casing where it gets cooled by water. Because of the lower temperature of the borehole, the strainmeter has to be cooled before the installation in case of any quick temperature changes .

After setting down the dump bailer, strainmeter has to be carried carefully near the borehole. In the mean time a roller must be installed on the well head because the cable has to be centralized and not to be rubbed to the well head.

Before the crush, strainmeter sensors has to be checked by oscilloscope and the gravity value has to be checked on the ground from strainmeter where it is to be installed. In order to read the gravity value from the stainmeter, it has to be connected with the cable head and rotated clock wise and counter clockwise in its own orbit to catch the gravity value in the oscilloscope.

2.4.2. Seismometer Installation

Seismometer installation subjects to second part of installations. As the strainmeter installed, most of the progress has been done. Seismometer installation is very basic with cementing and lowering steps.

Three day after the strainmeter installation, the seismometer installation progress begin. For the seismometer cementing special kind of cement is not needed. Firstly a pipe, which is going to be used for the cement's travel in the hole, is prepared as one of the sides in the deepest part of the hole and the other part arranged like a cone to pour the grout. Right before pouring the grout, some amount of water has to be send into the pipe for vacuuming the grout to the other end which is at the bottom. After mixing the cement and water and sending some amount of water, the grout is sent via the pipe.

After cement has been poured into the borehole, seismometer has to be lowered gently by using a sliding rope. This rope has to be as long as the deepest point of the borehole after the strainmeter installation. The rope has to marked with a highlighter

to be sure about the installation depth. The seismometer has to be send as deep as possible. Setting the seismometer into the grout finishes the installation. At the end, the rope has to be tied to the well head and the seismometer cable is folded near the borehole.

3. EXPERIMENTS AND RESULTS

In the previous chapters, some information is given about the tectonic studies, studies held in Turkey, type of deformation measuring techniques, strainmeter types, different drilling methods, several installation methods, various logging applications and devices which are installed in our study.

The knowledge we obtain from the previous chapters show a century of experience lies under the installations have been happening today. Scientist from all around the world, studied on tectonics and built many kinds of deformation measuring equipment and many types of installation skills followed it. Applying the modern technology into their studies, earth scientists outreached the dynamics of the planet earth.

In this section, two borehole installations held in Istanbul will be focused on. Even the techniques have been tried and the deformation measuring equipment have been using for many years, every installation is a unique experience. Furthermore, much more practical experiences have been obtain from these installations since they were the first strainmeter installations in Turkey.

In the subsections, the study have been divided to four parts by the specifications of the fieldwork before and during installations. After the site have been selected by the criteria, fieldwork begins. As the drilling team begin to work, sampling from the cuttings begin to come off where we can interpret the geology of the site. When the samples show that it is the installation zone, the borehole is cased and logging operation is done. Observation details are given in logging sections. When the borehole is ready,

strainmeter, seismometer and rain gauge are installed respectively.

3.1. Discussion on Estimated Strain Levels Around TEPE and HALK Stations

Istanbul province encompasses rock units with a complex structural evolution extending in age from the Early Paleozoic to present. Istanbul mainly consist of two large lithostratigraphic units, which are Istranca and Istanbul Units, metamorphic and non-metamorphic respectively. Only a few units of the Istranca metamorphic assamblage lie within the province of Istanbul to the west and north of the Çatalca district. They form a high grade metamorphic basement. The Eocene contractional movements, which dominated the tectonics of Anatolia, led to intense pre-Lutetian folding and faulting in the Marmara region including the Istanbul area. These movements resulted in the thrusting of the Paleozoic and Mesozoic units over the Upper Cretaceous-Lower Eocene sequences during the Early Eocene. During the Middle Eocene there was a new transgression in the region and the Çatalca and Şile regions were transgressed by a sea in which sands and reefs where formed in the coastal parts (Koyunbaba Formation, Yunuslubayır Formation, Soğucak Limestone), and shales in the internal parts (Ceylan Formation). Landslides are common in the European coastal parts of Istanbul. Most of the landslides have developed within the shales of the Gürpınar and Güngören formations, which have low shear resistance, especially when they are overlying by the poorly consolidated conglomerates and coarse sandstones of the Kıraç member [60].

In our installation zones, two different kind of formation has been detected, which are Cekmece and Danismen Formations for HALK and TEPE sites respectively.

Marmara region is substantially important for the tectonic studies about NAFZ. However, the tectonic evolution of the Marmara Sea begins from early miocene epoch with Thrace-Eskişehir fault zone. Moreover, the NAFZ and its branches forms the tectonic evolution of Marmara Sea since the late pliocene epoch. The Thrace-Eskişehir fault and its westward branching secondary fault systems are claimed to be defining the early neotectonic signature in the Marmara region. The late neotectonic period

started at the end of the early pliocene when the NAFZ divided the TEFZ into four parts [61].

The conventional seismic data collected in 1997, by R/V Sismik-1 of the Mineral Research and Exploration Institute of Turkey, interpreted by three different working groups; where they ended up with different conclusions. The position and character of the NAFZ have been studied by them. In the first study it is proposed that a master fault bordering the southern part of the western Marmara Sea is a northeast-southwest thrust fault to the east of the West Marmara Through. Also in the same study it is claimed that there is a normal fault in the middle of the through and a north-thrusting dextral fault to the west of the through land [62]. Another research claimed that an east-west trending normal faults caused the evolution of the Marmara Sea. The other study interpreted the data after the 1999 eastern Marmara earthquakes alleges that there is a buried master fault extending through the Marmara Sea [63]. Three models have been created as pull-apart, en echelon and master fault models for the Marmara Sea.

Understanding the neotectonics of the Marmara Sea depends on the tectonic evolution and the surroundings of it. A detailed mapping of bathymetry and faulting shows that there is a active branch of the NAFZ in the Marmara Sea [64]. Moreover, GPS studies show that pre-seicmic and post-seismic deformation for the 1999 earthquake sequence were symmetric about the fault [33]. It is also claimed that the eastern segment has significantly shallower seismicity than the western segment [65].

The observations in Marmara region raise the possibility that central segment of the Main Marmara Fault in the Marmara Sea may be creeping at shallow depths. The absence of strain in the north of the north branch of the fault is unexpected, so this situation promotes the creeping event. For further studies, any detected creep may help to determine fault dynamics. In the north of the Marmara Sea no strain is observed even at distance within 10 km of the north segment of MMF. It shows that existing models for Marmara Sea do not account for the rheological and kinematic complexity of this releasing bend.

Acknowledging a block model defined by Reilinger [33], GPS velocities are estimated for the MMF. Using these GPS velocities, backslip displacement and annual strain rates are calculated for a station 20 km away from the fault zone which coincide with the HALK and TEPE sites situation.

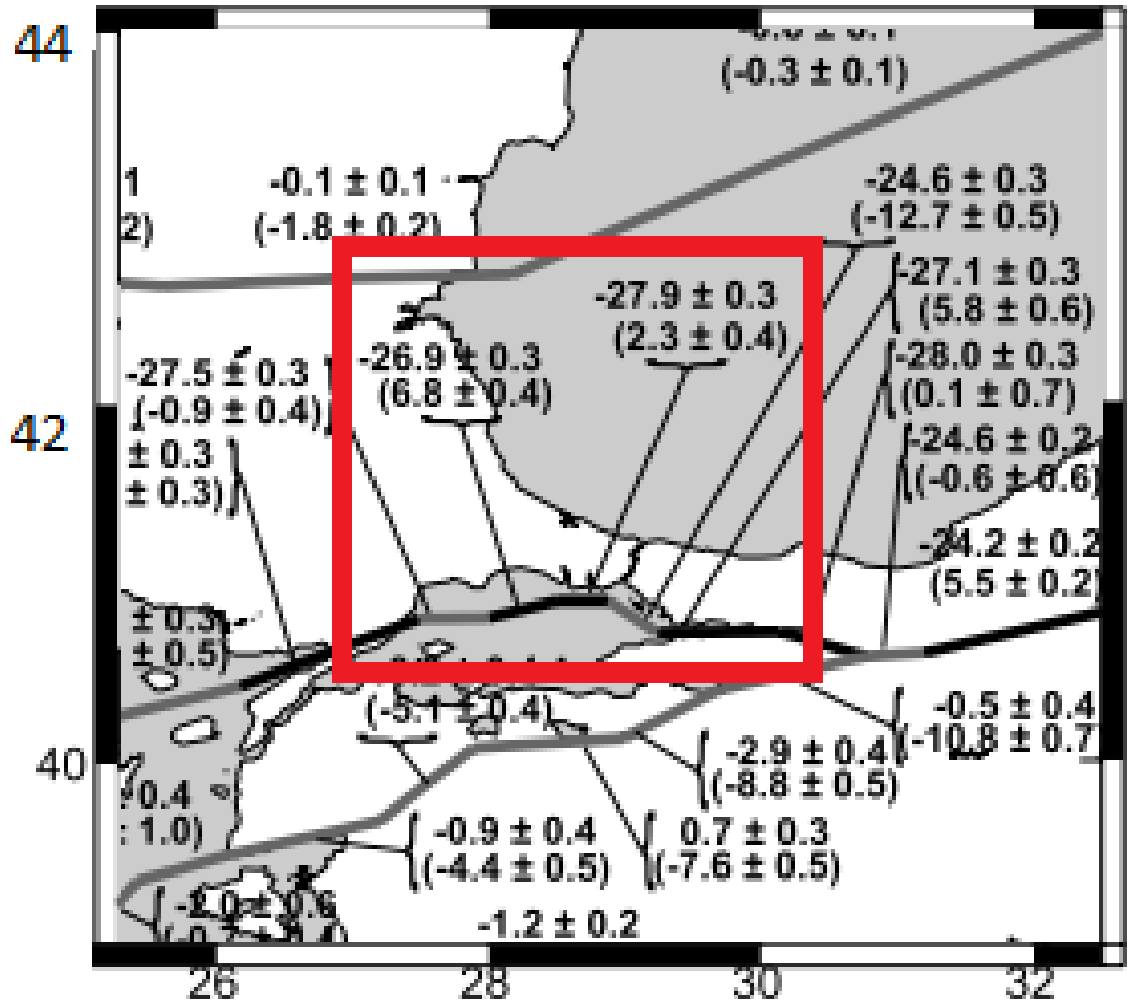

Figure 3.1. Estimated GPS velocities from a block model by Reilinger (modified from Reilinger et al. 2006).

In the light of these GPS velocities, an average velocity for MMF is calculated as 27.4 mm/yr. Using this information, strain detectability of HALK and TEPE stations are calculated (Figure 3.3) [66].

TEPE and HALK sites located about 20 km far away from the NAF (Figure 3.2).

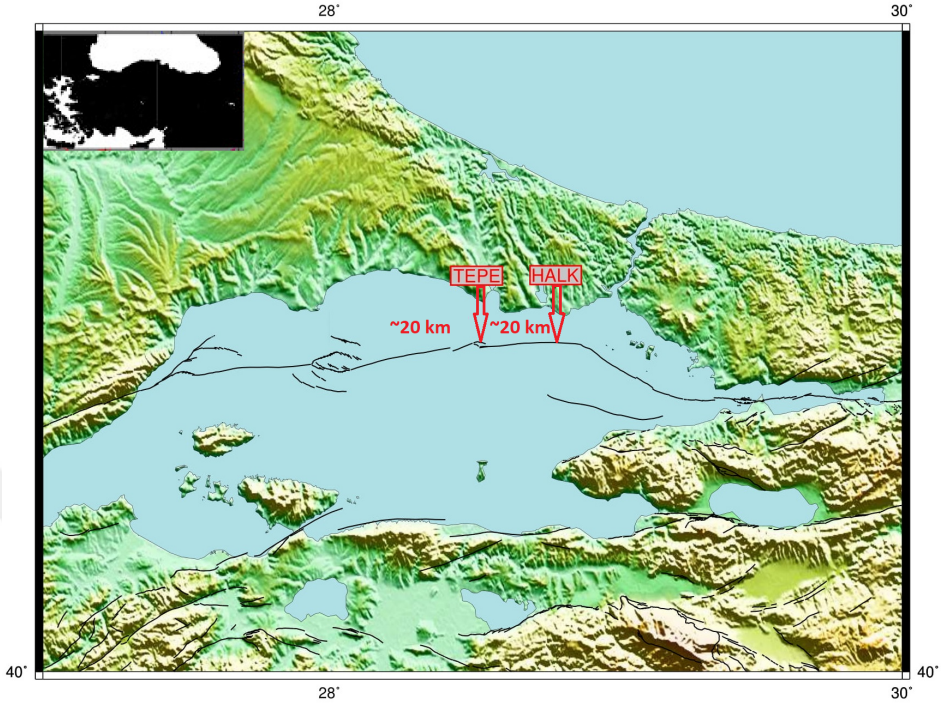

Figure 3.2. TEPE and HALK site's distance from the NAF.

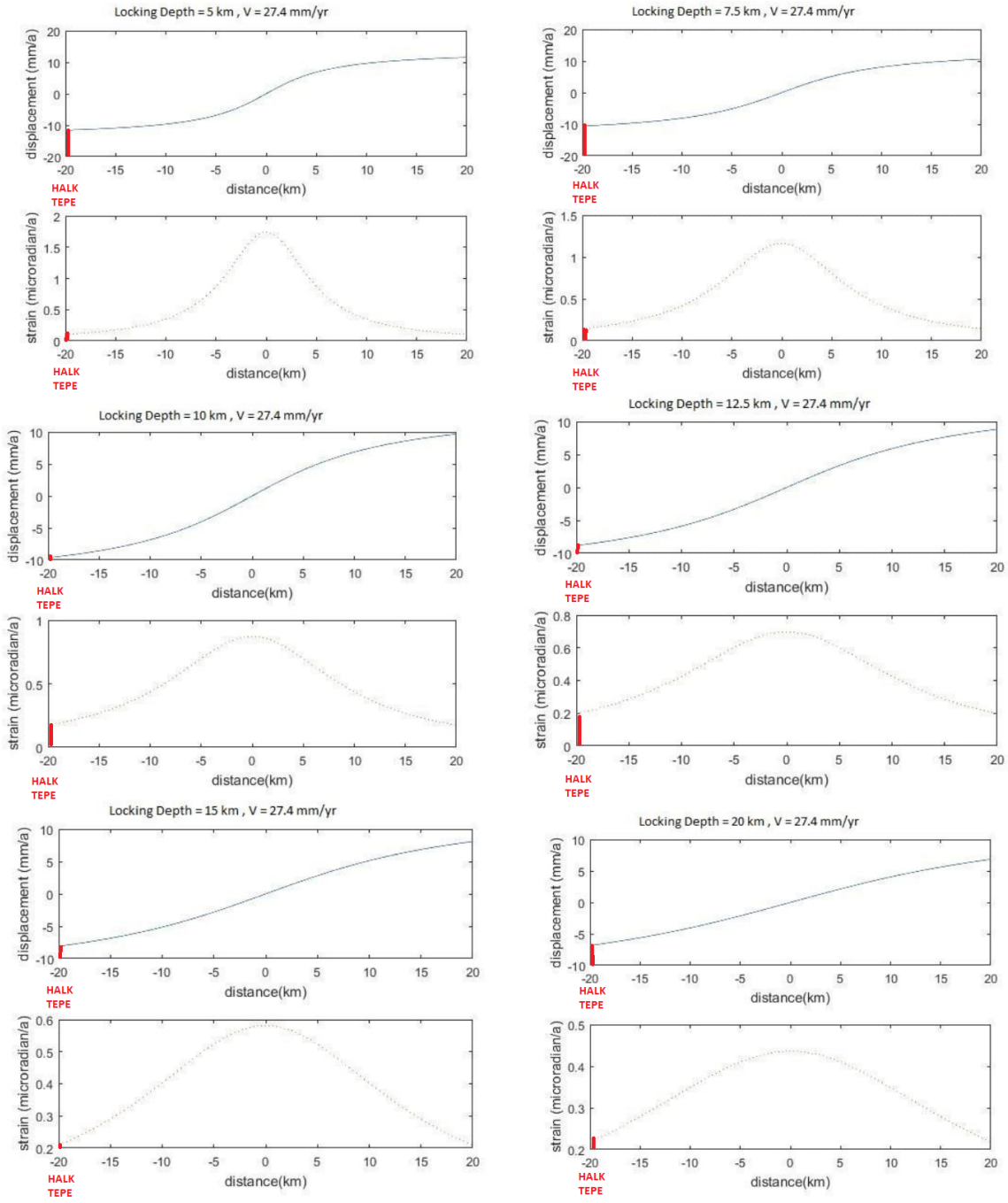

Figure 3.3. Strain detectability of TEPE and HALK sites.

HALK and TEPE stations located about 20 km away from the NAF. Possible displacements and strain rates are calculated for the locking depths from 5 to 20 km. The minimum and the maximum strain rates expected in HALK sites are $0.1x10^{-6}$ and

$0.21x10^{-6}$ respectively. Expected displacements are between 11 mm/yr and 7 mm/yr which are inversely proportional to the locking depth.

There have been many models of plate motion about Marmara Sea however existing models of plate motion do not account for the rheological and kinematic complexity of this releasing bend. The absence of strain north of the north branch of the fault is unexpected, so there might be some other constraints.

The north segment of the fault, MMF, can not be inactive because detailed mapping of the bathymetry and faulting in the Marmara Sea shows that the MMF is the active branch of the fault [64]. The MMF can not be dipping southward skewing the locus of the surface shear strain to the south because the seismicity along the MMF defines a vertical plane, although the eastern segmnet has significantly shallower seismicity than the western segment [65]. The other possibility is that the central segment of the MMF is creeping to very shallow depths preventing a slip deficit from accumulating.

Strainmeters are powerful tools for measuring creep. Detectability of strainmeters are up to 10^{-9} so if slow slip events are occuring in the Marmara sea, the observation insterspace correspond for the accumulated strain in TEPE and HALK sites.

3.2. TEPE Site

Tepe site has taken its name from the private villa site where it is located, Tepekent which is located in Büyükçekmece district in the European side (Figure 3.4).

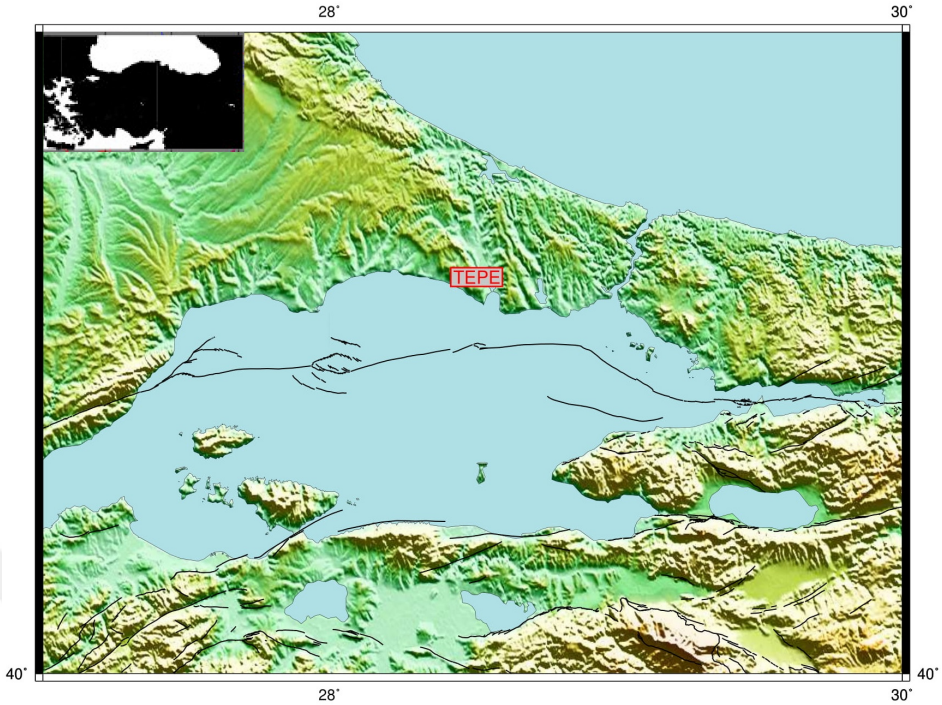

Figure 3.4. Location of the TEPE site.

TEPE is located on a hill which in 124 meters altitude. From the former water well drillings around this site showed us, it is likely to cut a massive sandstone around 100 meters.

The site was quite comfortable for the drilling because of the private security, a water well of a neighbour garden and easy reaching platform where it is possible to drive near the borehole.

There had been a water well in a neighbour villa that we could use all over the field work. The installation site is quite secure with 7/24 security guards in the every entrance of the villa site.

3.2.1. Geology in the TEPE Site

In TEPE site, it is anticipated that a hard sandstone segment is to be cut in a short distance from the surface. To understand in what formation we are, cuttings have been collected by the drilling team. As it is a close system, the water circulation have been made from the mud pool. Thus, some mud may be seen in the samples. The first ten meters are soil and sand. From the eleven to twenty five meters a soft sandstone goes on. In the twenty fifth meter, clay and sand mixture goes on until eighty (Figure 3.5).



Figure 3.5. Cutting samples for the first 84 meters in TEPE site.

After the eigthy four meters, drilling bit has broken because of the hard stone. It has given us signals that we are in the segment that we are looking for. As we go forward the segment got stronger and the last seven meters have been drilled in three days. In the picture below cuttings are sampled from eighty four ninety seven are seen as separated sampling (Figure 3.6). As it is told the drillers hardest segments must be sampled separately and washed well.



Figure 3.6. Cutting samples from 84 meters to 97 in TEPE site.

Last samplings have not been taken but have been looked while drilling. As it is seen in hand, hard sand stone has been drilled in very small pieces (Figure 3.7).



Figure 3.7. Last cutting samples in TEPE site.

Casing have been done after reaching 97 meters. The first logging have been done right after the casing and been seen that the installation zone is deeper as we have seen in the second hole. And the last loggings have been done in when the hole has reached 103 meters (Figure 3.8).

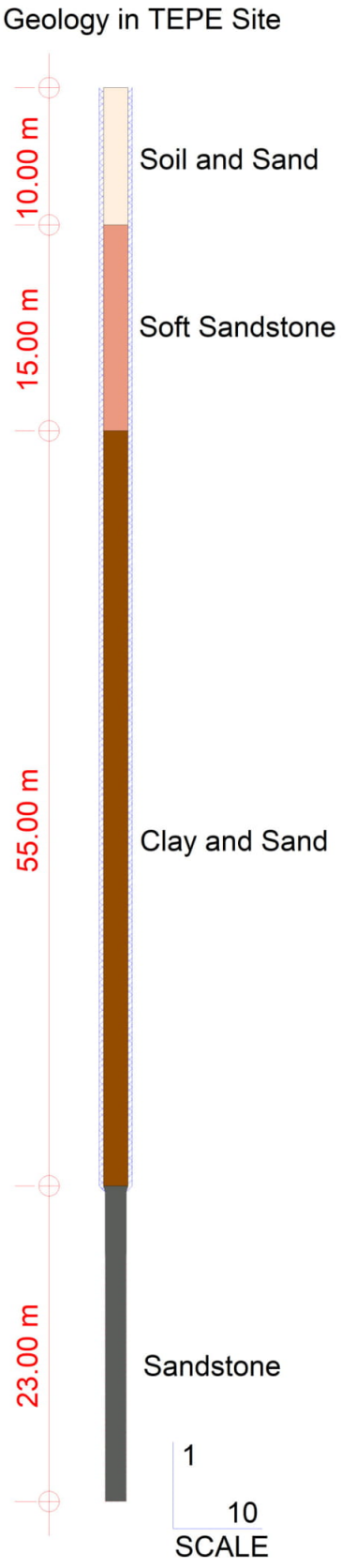

Figure 3.8. Geological formation in TEPE Site.

Matching with the IBB Geological Map, TEPE site is a typical Danismen Formation which is formed in upper Oligocene. TEPE sits on Silivri Member of Danismen formation which is about 40 meter thick sandstone (Figure 3.9).

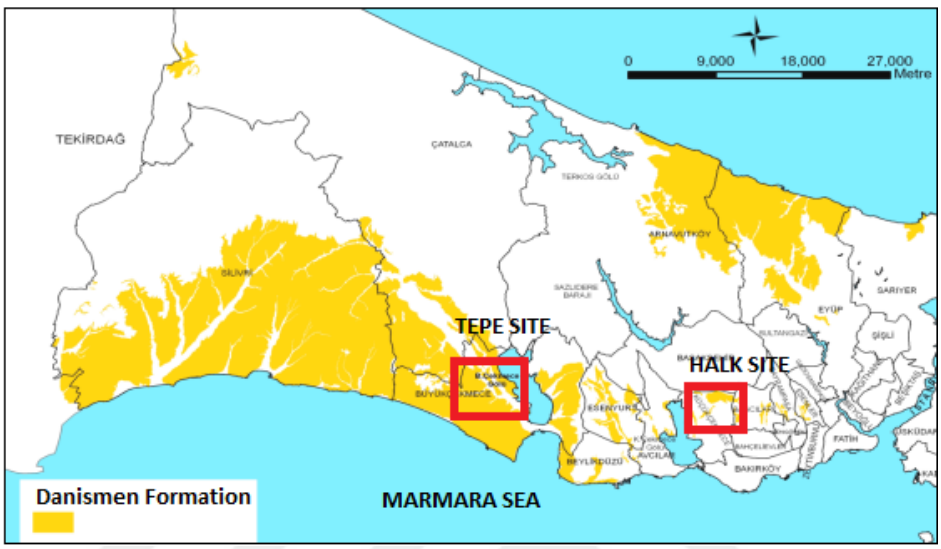

Figure 3.9. Danismen formation in the European side of Istanbul (modified form IBB Geological Map).

3.2.2. Drilling Experiments in the TEPE Site

TEPE site is the first installation site where three boreholes are drilled and two of them are abandoned.

In the first borehole; the size of the well and casing have been discussed by project members and drillers. Technically it hasn't been seen the six-inch-hole can be drilled with six-inch-bit in standards used in Turkey. The other case is, if the logs doesn't show good results we had to keep drilling until the good installation zone, where we have cased the below section with the six-inch-casing. The equipment drillers have does not allow to continue six inches hole in six-inch-casing because of the kelly bar where it was possible to continue drilling in seven-inch-casing with six-inch drill bit (Figure 3.10). The solution found for it is reducing the casing in the lower sections. The borehole is drilled with 9.5 inch drilling bit to 80 meters. Reaching 80 meters, drilling progress

went on with a 6 inch drill bit to 90 meters and the hole is cased with 80 meters of 7 inch casing and 2 meters of 6 inch casing with a reducer. After cementing the casing, the first logging operation has done. As seen in the logs, it is needed to drill deeper. As it is argued with the drillers, drilling went deeper to 100 meters. When the second logging has been done, it is seemed that the reduction part of the casing is broken and bent to inside of the borehole which does not allow us to install. As drillers suggested, the casing has been tried to taken out, however it has been an unsuccessful operation. The only good news about the first borehole was that we were in the installation zone in 100 meters.



Figure 3.10. 6 and 7 inches casing, 6 inches drill bit and reduction

Abandoning the the first borehole, the second borehole drilling operation begin. Unlike the first borehole, drillers has suggested to use a PVC pipe for the casing. As the logs have been taking from the borehole nearby, it is approved to use a PVC pipe for the borehole casing. Asking for a deeper drilling, the second drilling has finished in 110 meters as 7 inches borehole and 6 inches PVC casing to 75 meters. In the logs

it is seemed that the 103 meters look good for the installation. The last 7 meters has to be cemented. The grout calculation is given to the drillers and preparations begin to installation. When it came to the last logging before installation, logging tools could not go deeper than 45 meters because the borehole was clogged. Thus there was no possibility to drill inside the PVC piping, the second borehole is also abandoned. Finding another work, drillers are also lost with the borehole (Figure 3.11).



Figure 3.11. Site visiting before the second drilling.

The third and the last hole begin with a new drilling team. Going through all the experiences with the old team, the new team used the same system as it is done in the first borehole which is easier to go on if it is not the installation zone. Drilling went on to 95 meters where drillers said it was too hard. Suggesting the drilling team to go to 105 meters, drillers wanted to have a log before they go deeper. The first 80 meters is cased with a 7 inches casing and a reduction with 5 meters 6 inch casing. It is seem that the logs are so similar to first two boreholes, the drilling went on 10 more meters to 105 meters inside of the casing. The miscellaneous log have taken with the tree arm caliper tool and it is interpreted as the installation zone. After cleaning of the borehole, drilling is finished (Figure 3.12).

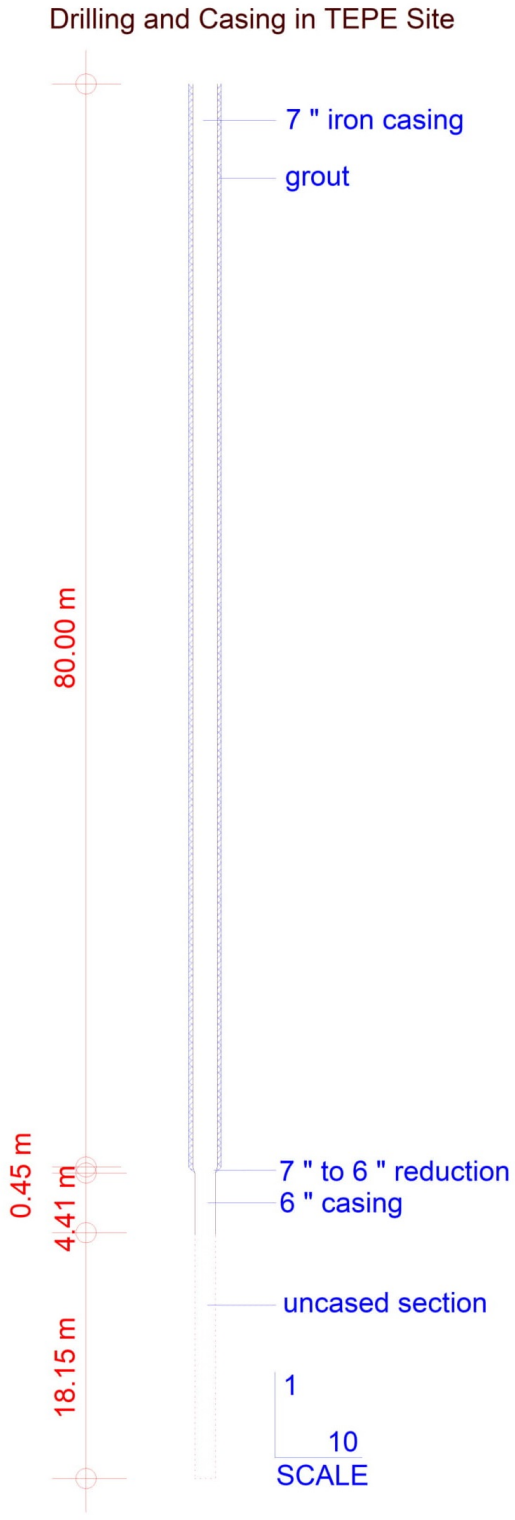

Figure 3.12. Drilling and casing properties in TEPE site.

3.2.3. Logging in the TEPE Site

As it is mentioned above, there are three boreholes drilled in TEPE site and the logs of each borehole are given in the appendix.

Logs have been numbered with their drilling order.

In TEPE 1 borehole, there were numerous aquifers in this borehole which can be detected by changes in temperature. The most obvious is the temp change at 77m. There is also a obvious fracture on the FWS at this depth. There is also a clay rich formation around 79.5m at indicated by the natural gamma. No adequate install zones were foind in this borehole. Had the borehole been installed we would have most likely put the instrument on the bottom of the borehole. A casing issue caused the abandonment of the borehole.

In TEPE 2 borehole, we were not able to get the FWS tool past 108.75 so there were incomplete logs of the bottom of the borehole. The Caliper also shows potential fractures at 105m and 106.4 m. the logs between 100-105 m show very consistent material with no fractures and very competent material. This would have been an outstanding install zone. No install due to loss of hole after cementing. This hole did have a good installzone between 100 to 105 m.

In TEPE 3 borehole, The borehole strainmeter was installed at 103m based primarily on the caliper and full wave sonic (FWS) data. The FWS does show a potential fracture at 102.9m which shows up as an anomaly on the DELTAT. The DELTAT is the difference in the arrival time of the near and far sensors on the FWS. The site was not installed deeper due to the caliper showing a rougher surface and the deviation of the borehole goes up to 7 degrees at the bottom of the borehole which is outside of the instruments specifications. GTSM21 Strainmeter installed at 103 m.

3.2.4. Installations in the TEPE Site

Right after the cleaning last logs are taken before the installation. Even the borehole looks pretty clean, it was crocked as 7 degrees which is not seen in the tree arm caliper tool because it has no inclinometer built in. Understanding that didn't break our plans but some changes had to made because the dump bailor is a 10 meter solid tool which will not be able to reach to the end of the borehole and stuck in the crocked part. Because of this, it is decided to lower dump bailer in two times. As it is told, it is not suggested but in requisite conditions it can be used.

At first, the dump bailor has to be tested if it fits in the crocked section and the trap mechanism work. To do this tests, dump bailor has to be set and the trap mechanism has to be cleaned and set. After setting the dump bailor, the deepest point it reaches has to be exercised, thus the wire used for dump bailor lowering has to be marked before the dumpbailor test (Figure 3.13).



Figure 3.13. Trap mechanism and dump bailor setting.

The experience we obtain here was unique. Because of a leakage in the upper uncased section, some clay flew to the end of the borehole. In the second and the third test, it seemed like we were loosing the hole because of the difluence in the upper sections or the section around the casing. But the length was not changing so it is thought that it would be some clay leaked after the cleaning and stopped. The solution found for it is putting some gravels onto the clay. We found some medium size round shaped gravels and send them one by one to the end of the borehole. Due to the buoyancy of the water, it may take a while to wait until the gravels gravitated. In the forth test the trap mechanism worked and preparations for the strainmeter installation begin. The strainmeter cable in the cable reel is unfasten as 150 meters and from the connecting part, every ten meter is marked with a marker tape. So that it is understood whether the strainmeter is in the deepest point.

After measuring the strainmeter cable, the grout has to be mixed. In the grout mixture, 7.5 kgs of potable water has been used for a 25 kgs of bucket. In total 8 buckets of Masterflow 1206 and 60 liters of potable water is used (Figure 3.14).



Figure 3.14. Mixing Masterflow 1206.

Buckets are used to carry the grout to the dump bailer where it is poured into it through a funnel. After the half of the grout dump bailor has sent to the end of the borehole in free fall. The successful dump is followed by another successful dump so

the last 7 meters of the borehole is fulfilled with grout. Connecting the quarter block onto the well head strainmeter gets ready for installation. To decrease the temperature change, the strainmeter is cooled in some water before it gets installed (Figure 3.15).



Figure 3.15. Cooled strainmeter.

Another crucial issue is, strainmeter has to run before the installation to obtain the magnetic compass value on the ground (Figure 3.16). And also it has to run right after the installing to see if there is something wrong with the sensors. If there is something wrong, the strainmeter has to be pulled up from the borehole.



Figure 3.16. Obtaining the magnetic compass value.

Hanging the strainmeter by using a piece of sliding rope to the crown on the truck, strainmeter is lowered to the head of the borehole. After entering the borehole, the rope around the strainmeter is cut and strainmeter is slowly slid in the borehole to the end (Figure 3.17).



Figure 3.17. Strainmeter installation in TEPE site.

Seismometer installation has to be made one day after the strainmeter installation. Seismometer installation is quite easier than the strainmeter installation. Tying

the seismometer with a sliding rope, seismometer cable has to be wrapped to the rope. Because the seismometer cable is weak, it must not be lowered by using its cable. Grouting the seismometer is made by using a hose which is wrapped to the seismometer while lowering down. The cement does not have to be an expansive cement like it is used in strainmeter installation. However, having more cement in stocks, it is decided to use Masterflow 1206 for seismometer installation. In seismometer installation, more water is added to the cement because it would flow from a tight hose. A crucial issue here is sending some water right before the grout because the water helps the cement to vacuum into the borehole (Figure 3.18).



Figure 3.18. Seismometer installation in TEPE site.

After the electronical setup of data logger in the enclosure, a rain gauge is installed at the top of the enclosure which helps us to get information if the strain change happened because of the heavy rain which caused the fulfill the borehole.

The installation of the TEPE site ended with setting up a container over the borehole (Figure 3.19).



Figure 3.19. TEPE site in a container.

3.3. HALK Site

HALK site takes its name from Halkali, the name of the neighbourhood where the strainmeter is located (Figure 3.20). The site is located in a crowded area in Istanbul thus a good installation location has been hard to find. Reconnaissance has been made with the Küçükçekmece Municipality officers. Five candidate sites has been visited. The installation site has been chosen in municipality's property near by a residential site. The site has a container, solar panel and AC power supplied by the municipality.

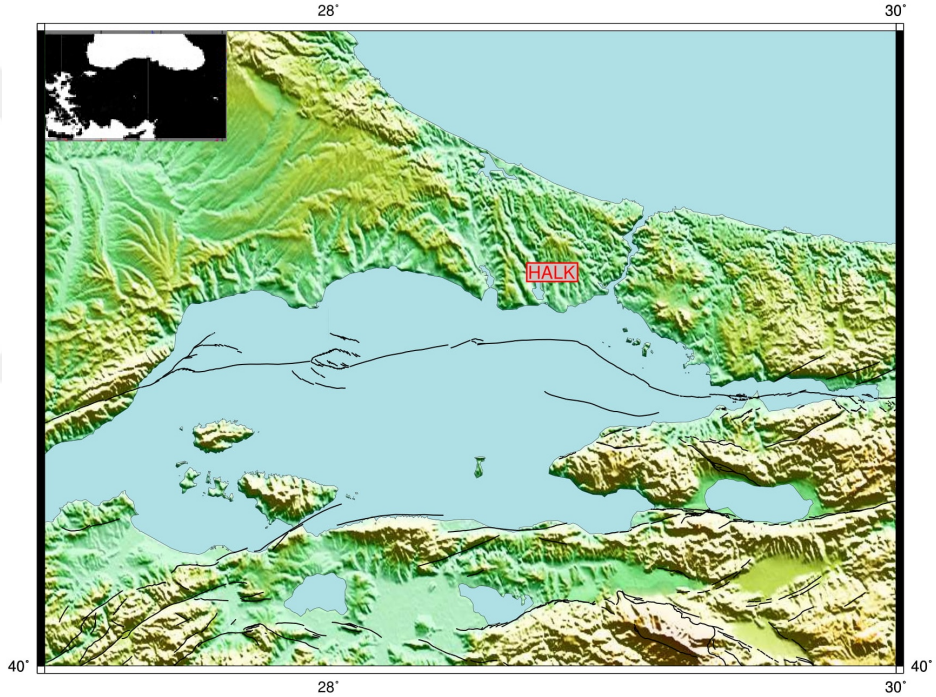

Figure 3.20. Location of the HALK site.

The residential site has a guard building near the container which is also important for the data logger's security.

Thus this is the second installation site, , it is thought to be installed in a parallel line to the fault in the Marmara Sea. While doing the site research, they were important conditions to not to go far from the fault and being in the same parallel line with TEPE station.

The site is in a easy reachable position and GSM operators work fine there. During the installation, the municipality has sent a water truck with two workers to the site, which is very crucial while working with the grout.

3.3.1. Geology in the HALK Site

In HALK site the strainmeter has been installed into limestone. Another borehole had been drilled in this area and information about cuttings has been achieved. As it is learned from the borehole nearby, upper segment is full of clay and it is assumed to cut fragmented limestone in 80 meters and massive limestone starts around 100 meters. Site has been visited with a well known geologist Mr. Esen Arpat before the start and during drilling (Figure 3.21).

In the HALK site, as it is expected, the samples up to 100 meters indicated very thick clay deposit over limestone. In the clay layer it has been easy and fast to drill. Beginning from 110 meters some limestone pieces appeared in the cuttings and it came with mixed clay. In 120 after flooding some water in to the borehole, cuttings have been taken. These cuttings are examined by Mr. Esen Arpat and also from UNAVCO engineers.



Figure 3.21. Mr. Arpat is examining the cuttings.

Being too close to the clay layers, it is decided to drill 10 meters more and start casing. As it is planned, the borehole has been drilled to 130 meters and casing is applied to its 120 meters. In the last samples, the formation was too strong and the last 3 meters took one day to drill (Figure 3.22).



Figure 3.22. Last samples of HALK site.

Looking at the samples, it is understood that we reached to the massive limestone because the cuttings were in very little pieces and drilling it took a long time.

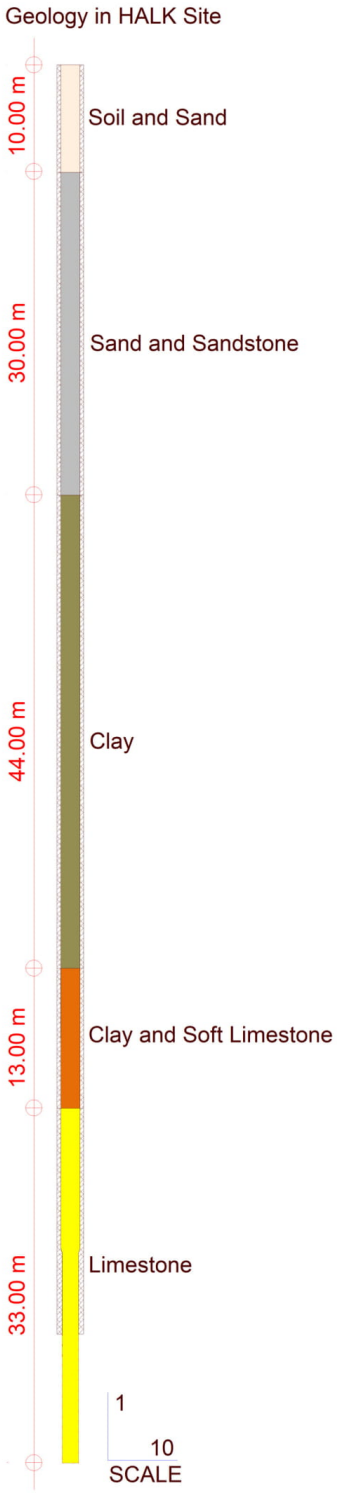

Figure 3.23. Geological formation in HALK Site.

Matching with the IBB Geological Map, HALK sits on Bakırköy member of

Çekmece formation. Bakırköy member of Çekmece formation mostly consist of clay and limestone.This can also be seen in the cutting samples of the HALK site (Figure 3.24).

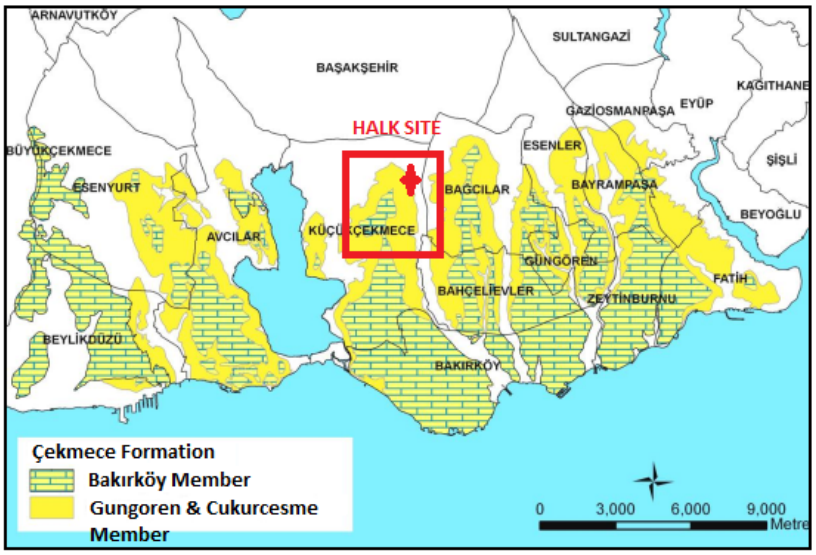

Figure 3.24. Cekmece formation around HALK site (modified from IBB Geological Map).

3.3.2. Drilling Experiments in the HALK Site

In this site another drilling team has worked (Figure 3.25). Going through all the experiences together, a meeting is held on site before starting to drill. In this borehole, because of the drilling system we had, it is decided to use a reducer after 7 inches casing to 6 inches casing at the end. The team has started with a very good leveling of the truck. Having a larger bit, the borehole started with 9 inches drill bit. During drilling, samples have been taken every other meter. In the first 100 meters the drilling went very soft and fast. After this point, with some of limestone, it took longer to go deeper.



Figure 3.25. Drilling truck in the HALK site.

After casing the hole, logging operation has been done. Logs have shown that there had been so much mud and clay in the borehole. Drillers are told to clean the borehole. After they have cleaned, another logging operation have been done which is not good at all because of the mud inside. The borehole has not been cleaned well by only the water. It had to be cleaned an other way which drillers suggested. The borehole has to be cleaned by using foam. As we agreed on it, an older drilling truck came to site for cleaning the borehole (Figure 3.26).



Figure 3.26. Borehole cleaning operation in the HALK site.

After a successful cleaning in the borehole, logging operation has been done for the last time and the result were seen suitable for installation. The borehole has cleaned very well and the installation zone stays safe and sound (Figure 3.27).



Figure 3.27. Drilling and casing properties in HALK site.

3.3.3. Logging in the HALK Site

In the HALK site, the install zone is in a layered limestone formation. This can be seen in the caliper and FWS data. The Natural Gamma is relatively low indicating little to no clay between the limestone layers. We ran multiple caliper logs due to clay adhering to the walls of the bore hole. This clay was intruding from a clay rich formation in the cased section on the borehole. There was no obvious aquifers in this borehole

The logs of the borehole is given in the appendix.

3.3.4. Installations in the HALK Site

After a very successful cleaning the borehole seemed quite install able for a strain-meter. The borehole has a very good verticality with 89 degrees which allow us to use dump bailor in a full length. In the cleaning operation, the drilling truck left the site and for the installation and grouting a lorry loader have been used. The dump bailor set and the trap mechanism is control for several times. The dump bailor test is done with fulfilled of water for two times (Figure 3.28).



Figure 3.28. Dump bailor test in the HALK site.

After the dump bailor test, by using masterflow 1206 cement, grout is mixed with 7.5 kgs of potable water per 25 kgs bucket. As in the other site, 8 buckets of cement is used. Fulling dump bailor with the grout mixed, a successful dump is made. In the mean time, a cable stand for the strainmeter cable is made for an easier install. Strainmeter is ran to obtain magnetic compass value. Hanging the strainmeter to the carring wire by a piece of sliding rope, the strainmeter is sent to the bottom of the borehole. Because the last half a meter of the borehole seemed may have fractures, the strainmeter is stopped half a meter before the end and the cable is tied to the well

head by using the sliding rope. As the strainmeter install finished, all the equipment is put in order to deploy to truck in the feature and the site has been left for one day before the seismometer installation.

Arriving early in the site, the seismometer cable is wrapped to the sliding rope and measured for installation. As it is seen the cable is just enough for the installation right under the casing, more cement is needed. Some old masterflow 1206 cement was moisten which were spared to use in seismometer installation and it is decided to buy new cement for seismometer installation (Figure 3.29. For the seismometer installation normal cement is used. Nine 50 kgs bags of cement is mixed with 135 liters of water.



Figure 3.29. Seismometer installation in the HALK site.

After installation of the seismometer equipment in the site area is loaded to the truck, the electronical setup has been done and site leaved running (Figure 3.30).



Figure 3.30. HALK site after installations

In a site cleaning operation, the cable of the HALK site has been cut by an excavator. Right after getting a container, the cable has been repaired and the site went on working and collecting data in the container (Figures 3.31 3.32).



Figure 3.31. Cable cut in HALK site



Figure 3.32. HALK site in the container

4. CONCLUSION

The main purpose of this thesis is to explain installation of two strainmeters in Istanbul. Beginning with the deformation measuring techniques, the evolution of strainmeters are explained. Since the GTSM is the type of strainmeter installed in Istanbul, a special importance has given with priority.

Recent studies of Geodesy Department of KOERI has been concerned as a fund of knowledge. In the light of the tectonic studies about western part of NAFZ, especially in Istanbul, using a more sensitive terrestrial measurement technique has been a great need.

The biggest advantage of strainmeters is that strainmeters offer a complementary and, for many natural phenomena of interest, required measurement. For geophysical events that are longer than 1 second and less than 1 year, strainmeters offer the best signal to noise ratio [67]. Moreover, strainmeters hold out valuable and sensitive measurements and have been utilized for critical discoveries in the past like slow slip events [68]. Disadvantages of strainmeter depends on its installation difficulty. Though it is not the major impediment, strainmeters are also expensive. The primary difficulty and disadvantage about installation is its coupling which is a combination of the grout and host rock. Checking this combination for this coupling in the borehole is very difficult to test and control. About 20% of boreholes drilled do not present adequate host rock and are abandoned. Another 20% of boreholes installed exhibit grout issues, but still present usable data. Contrast a seismometer, strainmeter's coupling coefficient can be mechanically coupled and removed.

At the high sensitivity of the GTSM instruments, where local hydrological and loading signals are appreciable and can even dominate, it is important that events are detected on multiple instruments separated by distances near the wavelength of the event of interest to discriminate site-specific environmental signals from the tectonic signal of interest. This is one of the main reasons for selecting sites with inter-site spac-

ing of 10-20 km. Noise generated by load tides, atmospheric events and hydrological phenomena will be on the order of tens of nanostrain. To solve this issues a network of four instruments is considered the minimum viable network to detect and use the data generated from such sources with six installation is ideal. Because, in case of İstanbul, the Marmara Sea will be an obvious and very large signal source.

A well known borehole strainmeter system, GTSM, has been decided to install under coordinating of UNAVCO and Geodesy Department of KOERI. The project has been a transfer of know-how between these institutions for the future installations.

In conclusion, the need of the strainmeter, installation cases for two boreholes, solutions found for site specific problems and the result of installation are discussed in this thesis. The detection capability of the strainmeters in HALK and TEPE sites are in the interspace of the expected strain accumulation on the seismic gap.

Installed strainmeters will allow us to monitor potential slow-slip events along the Marmara Seismic Gap. An array of strainmeters will be beneficial for Istanbul in these reasons and this thesis can be used as a manual for future installations.

REFERENCES

1. Hatcher, R. D., *Structural geology: principles, concepts, and problems*, Merrill Pub. Co., 1990, https://books.google.com.tr/books?id=n51OAQAAIAAJ.

2. Dirik, K., *Yeraltı Jeolojisi Ders Notları*, 2006.

3. Paterson, M. S., "Experimental Deformation and Faulting in Wombeyan Marble", *GSA Bulletin*, Vol. 69, No. 4, pp. 465–476, apr 1958, http://dx.doi.org/10.1130/0016-7606(1958)69[465:EDAFIW]2.0.COhttp://0.0.0.2.

4. Badgley, P. C., "Structural and tectonic principles.", , 1965.

5. Aktug, B., J. M. Nocquet, a. Cingöz, B. Parsons, Y. Erkan, P. England, O. Lenk, M. a. Gürdal, a. Kilicoglu, H. Akdeniz and a. Tekgül, "Deformation of western Turkey from a combination of permanent and campaign GPS data: Limits to block-like behavior", *Journal of Geophysical Research: Solid Earth*, Vol. 114, No. 10, pp. 1–22, 2009.

6. Agnew, D. C., "Strainmeters and tiltmeters", *Reviews of Geophysics*, Vol. 24, No. 3, pp. 579–624, 1986.

7. King, G. and R. Bilham, "A Geophysical Wire Strainmeter", *Bulletin of the Seismological Society of America*, Vol. 66, No. 6, pp. 2039–2047, 1976.

8. Sydenham, P. H., "A tensioned-wire strain seismometer", *Journal of Physics E: Scientific Instruments*, Vol. 2, No. 12, p. 1095, 1969.

9. Bilham, R. G. and G. C. P. King, "Strain gauges for geophysics", *Commun. Obs. R. Belg., Ser. A*, Vol. 13, pp. 258–278, 1971.

10. Gerard, V. B., "An invar wire earth strain meter", *Journal of Physics E: Scientific*

Instruments, Vol. 4, No. 9, p. 689, 1971.

11. Berger, J. and R. H. Lovberg, "Earth strain measurements with a laser interferometer", *Science*, Vol. 170, No. 3955, pp. 296–303, 1970.

12. Goulty, N. R., G. C. P. King and A. J. Wallard, "Iodine stabilized laser strainmeter", *Geophysical Journal International*, Vol. 39, No. 2, pp. 269–282, 1974.

13. Evertson, D. W., "Borehole Strainmeters For Seismology", , 1977.

14. Dewey, J. and P. Byerly, "The early history of seismometry (to 1900)", *Bulletin of the Seismological Society of America*, Vol. 59, No. 1, pp. 183–227, 1969.

15. Benioff, H., "A linear strain seismograph", *Bulletin of the Seismological Society of America*, Vol. 25, No. 4, pp. 283–309, 1935.

16. Shopland, R. C., "Shallow strain seismograph installation at the Wichita Mountains Seismological Observatory", *Bulletin of the Seismological Society of America*, Vol. 56, No. 2, pp. 337–360, 1966.

17. Shopland, R. C. and R. H. Kirklin, "Application of a vertical strain seismograph to the enhancement of P waves", *Bulletin of the Seismological Society of America*, Vol. 60, No. 1, pp. 105–124, 1970.

18. Fix, J. E. and J. R. Sherwin, "A high-sensitivity strain/inertial seismograph installation", *Bulletin of the Seismological Society of America*, Vol. 60, No. 6, pp. 1803–1822, 1970.

19. Fix, J. E., *Strain/Inertial Seismograph Complexes.*, Tech. rep., 1974.

20. Major, M. W., "Strainmeters", *ESSA Symposium on earthquake prediction*, pp. 69–71, 1966.

21. Okada, Y., S. Watanabe and K. Kasahara, "Observation of crustal deformation at

the Fujigawa Observatory, Central Honshu, Japan (1). l Geod", *Soc. Jap*, Vol. 21, pp. 179–190, 1975.

22. Latynina, L., E. Starkova, B. Podgornykh and R. Karmalyeva, "Deformations of the earth's crust at the Kondara station of the Tadzhik Socialist Soviet Republic", *Izv. Acad. Sci. USSR, Phys. Solid Earth (Engl. Transl.)*, pp. 184–189, 1968.

23. Moore, T. C., L. H. Rorden, R. L. Kovach and S. W. Smith, *Deep Borehole Strainmeter to Measure Earth Strain*, Tech. rep., 1974.

24. Shunliang, C., "Preliminary Experimental Result of a Capacitance-type Borehole Strainmeter", *Acta Seismologica Sinica*, Vol. 1, pp. 98–101, 1982.

25. Hongjun, W. Q. F. X. M. A., "A String Frequency Borehole Strainmeter", *Acta Seismologica Sinica*, Vol. 3, p. 12, 1983.

26. Gladwin, M. T., "High[U+2010]precision multicomponent borehole deformation monitoring", *Review of scientific instruments*, Vol. 55, No. 12, pp. 2011–2016, 1984.

27. ISHII, H., "Development of high sensitivity bore hole strain meters and application for rock mechanics and earthquake prediction study", *Rock Stress*, pp. 253–258, 1997, https://ci.nii.ac.jp/naid/10025367896/en/.

28. Ishii, H. and Y. Asai, "Development of a borehole stress meter for studying earthquake predictions and rock mechanics, and stress seismograms of the 2011 Tohoku earthquake (M 9.0)", *Earth, Planets and Space*, Vol. 67, No. 1, p. 26, Feb 2015, https://doi.org/10.1186/s40623-015-0197-z.

29. Özener, H., B. Turgut, A. Dogru, K. Halicioglu and O. Gürkan, "Kuzey Anadolu Fay Zonu Batı ve Doğu Kesimlerinde Güncel Kabuk Hareketlerinin Jeodezik Yöntemlerle Belirlenmesi", *11. Türkiye Harita Bilimsel ve Teknik Kurultayı*, pp. 1–8, 2007.

30. Reilinger, R. E., S. Ergintav, R. Burgmann, S. McClusky and e. al, "Coseismic and postseismic fault slip for the 17 August 1999, M = 7.5, Izmit, Turkey earthquake", *Science*, Vol. 289, No. 5484, pp. 1519–1524, Sep 01 2000, https://search.proquest.com/docview/213589112?accountid=9645.

31. Meade, B. J., B. H. Hager, S. C. McClusky, R. E. Reilinger, S. Ergintav, O. Lenk, A. Barka and H. Özener, "Estimates of seismic potential in the Marmara Sea region from block models of secular deformation constrained by global positioning system measurements", *Bulletin of the Seismological Society of America*, Vol. 92, No. 1, pp. 208–215, 2002.

32. Dogan, U., S. Ergintav, H. Demirel, R. Çakmak and H. Özener, "Estimation of the time-dependent crustal movements of the İzmit Earthquake", *Journal of Geodynamics*, Vol. 36, No. 5, pp. 615 – 632, 2003, http://www.sciencedirect.com/science/article/pii/S0264370703000905.

33. Reilinger, R., S. McClusky, P. Vernant, S. Lawrence, S. Ergintav, R. Cakmak, H. Ozener, F. Kadirov, I. Guliev, R. Stepanyan, M. Nadariya, G. Hahubia, S. Mahmoud, K. Sakr, A. ArRajehi, D. Paradissis, A. Al-Aydrus, M. Prilepin, T. Guseva, E. Evren, A. Dmitrotsa, S. V. Filikov, F. Gomez, R. Al-Ghazzi and G. Karam, "GPS constraints on continental deformation in the Africa-Arabia-Eurasia continental collision zone and implications for the dynamics of plate interactions", *Journal of Geophysical Research: Solid Earth*, Vol. 111, No. B5, pp. n/a–n/a, 2006, http://dx.doi.org/10.1029/2005JB004051, b05411.

34. Halicioglu, K. and H. Ozener, "Geodetic Network Design and Optimization on the Active Tuzla Fault (Izmir, Turkey) for Disaster Management", *Sensors*, Vol. 8, No. 8, pp. 4742–4757, 2008, http://www.mdpi.com/1424-8220/8/8/4742.

35. Dogru, A., E. Gorgun, H. Ozener and B. Aktug, "Geodetic and seismological investigation of crustal deformation near Izmir (Western Anatolia)", *Journal of Asian Earth Sciences*, Vol. 82, No. Supplement C, pp. 21 – 31, 2014, http://www.sciencedirect.com/science/article/pii/S1367912013006287.

36. Ozener, H., A. Dogru and A. Unlutepe, "An Approach for Rapid Assessment of Seismic Hazards in Turkey by Continuous GPS Data", *Sensors*, Vol. 9, No. 1, pp. 602–615, 2009, http://www.mdpi.com/1424-8220/9/1/602.

37. Akay, G. and H. Ozener, "Investigation of long period crustal deformation on the inactive branch of the North Anatolian Fault Zone", *Natural Hazards and Earth System Sciences*, Vol. 9, No. 3, p. 663, 2009, https://search.proquest.com/docview/912152504?accountid=9645, copyright - Natural Hazards and Earth System Sciences 2009; Last updated - 2012-06-29.

38. Ergintav, S., S. McClusky, E. Hearn, R. Reilinger, R. Cakmak, T. Herring, H. Ozener, O. Lenk and E. Tari, "Seven years of postseismic deformation following the 1999, M = 7.4 and M = 7.2, Izmit-Düzce, Turkey earthquake sequence", *Journal of Geophysical Research: Solid Earth*, Vol. 114, No. B7, pp. n/a–n/a, 2009, http://dx.doi.org/10.1029/2008JB006021, b07403.

39. Ozener, H., E. Arpat, S. Ergintav, A. Dogru, R. Cakmak, B. Turgut and U. Dogan, "Kinematics of the eastern part of the North Anatolian Fault Zone", *Journal of Geodynamics*, Vol. 49, No. 3, pp. 141 – 150, 2010, http://www.sciencedirect.com/science/article/pii/S0264370710000165, wEGENER 2008 - Proceedings of the 14th General Assembly of Wegener.

40. Aktug, B., U. Dikmen, A. Dogru and H. Ozener, "Seismicity and strain accumulation around Karliova Triple Junction (Turkey)", *Journal of Geodynamics*, Vol. 67, No. Supplement C, pp. 21 – 29, 2013, http://www.sciencedirect.com/science/article/pii/S0264370712000695.

41. Ozener, H., A. Dogru and M. Acar, "Determination of the displacements along the Tuzla fault (Aegean region-Turkey): Preliminary results from GPS and precise leveling techniques", *Journal of Geodynamics*, Vol. 67, No. Supplement C, pp. 13 – 20, 2013, http://www.sciencedirect.com/science/article/pii/S026437071200097X.

42. Ozener, H., O. Yilmaz, A. Dogru, B. Turgut and O. Gurkan, "GPS-derived velocity field of the Iznik-Mekece segment of the North Anatolian Fault Zone", *Journal of Geodynamics*, Vol. 67, No. Supplement C, pp. 46 – 52, 2013, http://www.sciencedirect.com/science/article/pii/S026437071200107X.

43. Ozener, H., A. Dogru and B. Turgut, "Quantifying aseismic creep on the Ismetpasa segment of the North Anatolian Fault Zone (Turkey) by 6 years of GPS observations", *Journal of Geodynamics*, Vol. 67, No. Supplement C, pp. 72 – 77, 2013, http://www.sciencedirect.com/science/article/pii/S0264370712001172.

44. Dogan, U., D. O. Demir, Z. Cakir, S. Ergintav, H. Ozener, A. M. Akoglu, S. S. Nalbant and R. Reilinger, "Postseismic deformation following the Mw 7.2, 23 October 2011 Van earthquake (Turkey): Evidence for aseismic fault reactivation", *Geophysical Research Letters*, Vol. 41, No. 7, pp. 2334–2341, 2014, http://dx.doi.org/10.1002/2014GL059291, 2014GL059291.

45. Aktuğ, B., A. Doğru, H. Özener and M. Peyret, "Slip rates and locking depth variation along central and easternmost segments of North Anatolian Fault", *Geophysical Journal International*, Vol. 202, No. 3, pp. 2133–2149, 2015, +http://dx.doi.org/10.1093/gji/ggv274.

46. Ergintav, S., R. E. Reilinger, R. Çakmak, M. Floyd, Z. Cakir, U. Doğan, R. W. King, S. McClusky and H. Özener, "Istanbul's earthquake hot spots: Geodetic constraints on strain accumulation along faults in the Marmara seismic gap", *Geophysical Research Letters*, Vol. 41, No. 16, pp. 5783–5788, 2014, http://dx.doi.org/10.1002/2014GL060985, 2014GL060985.

47. Aktug, B., H. Ozener, A. Dogru, A. Sabuncu, B. Turgut, K. Halicioglu, O. Yilmaz and E. Havazli, "Slip rates and seismic potential on the East Anatolian Fault System using an improved GPS velocity field", *Journal of Geodynamics*, Vol. 94-95, No. Supplement C, pp. 1 – 12, 2016, http://www.sciencedirect.com/science/article/pii/S0264370716300102.

48. Halicioglu, K., R. Deniz and H. Ozener, "Digital astro-geodetic camera system for the measurement of the deflections of the vertical: tests and results", *International Journal of Digital Earth*, Vol. 9, No. 9, pp. 914–923, 2016, https://doi.org/10.1080/17538947.2016.1189612.

49. Sabuncu, A., A. Dogru, H. Ozener and B. Turgut, "Detection of Coastline Deformation Using Remote Sensing and Geodetic Surveys", *ISPRS - International Archives of the Photogrammetry, Remote Sensing and Spatial Information Sciences*, pp. 1169–1174, Jun. 2016.

50. Bilham, R., H. Ozener, D. Mencin, A. Dogru, S. Ergintav, Z. Cakir, A. Aytun, B. Aktug, O. Yilmaz, W. Johnson and G. Mattioli, "Surface creep on the North Anatolian Fault at Ismetpasa, Turkey, 1944–2016", *Journal of Geophysical Research: Solid Earth*, Vol. 121, No. 10, pp. 7409–7431, 2016, http://dx.doi.org/10.1002/2016JB013394, 2016JB013394.

51. U.S. Department of the Interior; U.S. Geological Survey, "Implications for earthquake Risk Reduction in the United States from the Kacaeli, Turkey, Earthquake of August 17, 1999", *Usgs*, pp. 1–64, 1999, http://pubs.usgs.gov/circ/2000/c1193/c1193.pdf.

52. Bulut, F., M. Bohnhoff, W. L. Ellsworth, M. Aktar and G. Dresen, "Microseismicity at the North Anatolian Fault in the Sea of Marmara offshore Istanbul, NW Turkey", *Journal of Geophysical Research: Solid Earth*, Vol. 114, No. 9, pp. 1–16, 2009.

53. Prevedel, B., F. Bulut, M. Bohnhoff, C. Raub, R. F. Kartal, F. Alver and P. E. Malin, "Downhole geophysical observatories: best installation practices and a case history from Turkey", *International Journal of Earth Sciences*, Vol. 104, No. 6, pp. 1537–1547, Sep 2015, https://doi.org/10.1007/s00531-015-1147-5.

54. Soh, I. and C. Chang, "A Feasibility Study of Earthquake Monitoring Using a High-resolution Borehole Strainmeter", *The Journal of Engineering Geology*, Vol. 26,

No. 2, pp. 177–185, 2016.

55. Gladwin, M., *Frequently Asked Questions*, 2017.

56. Liao, C.-M., B. Balachandran, M. Karkoub and Y. L. Abdel-Magid, "Drill-string dynamics: reduced-order models and experimental studies", *Journal of Vibration and Acoustics*, Vol. 133, No. 4, p. 041008, 2011.

57. Bilham, R. and R. Beavan, "Strains and tilts on crustal blocks", *Tectonophysics*, Vol. 52, No. 1, pp. 121 – 138, 1979, `http://www.sciencedirect.com/science/article/pii/0040195179902166`, recent Crustal Movements.

58. McGarr, A., M. D. Zoback and T. C. Hanks, "Implications of an elastic analysis of in situ stress measurements near the San Andreas Fault", *Journal of Geophysical Research: Solid Earth*, Vol. 87, No. B9, pp. 7797–7806, 1982, `http://dx.doi.org/10.1029/JB087iB09p07797`.

59. Sbar, M. L., R. M. Richardson, C. Flaccus and T. Engelder, "Near-surface in situ stress: 1. Strain relaxation measurements along the San Andreas Fault in southern California", *Journal of Geophysical Research: Solid Earth*, Vol. 89, No. B11, pp. 9323–9332, 1984, `http://dx.doi.org/10.1029/JB089iB11p09323`.

60. Municipality, I. M., *Istanbul Il Alaninin Jeolojisi*, 2011.

61. Yaltırak, C., "Tectonic evolution of the Marmara Sea and its surrondings", *Marine Geology*, Vol. 190, pp. 493–529, 2002.

62. Okay, A. I., E. Demirbağ, H. Kurt, N. Okay and Å. KuşçU, "An active, deep marine strike-slip basin along the North Anatolian fault in Turkey", *Tectonics*, Vol. 18, pp. 129–147, Feb. 1999.

63. Le Pichon, X., T. Taymaz and A. M. C. Sengor, *The Marmara Fault and the Future Istanbul Earthquake*, 01 1999.

64. Armijo, R., B. Meyer, A. Hubert and A. Barka, "Westward propagation of North Anatolian fault into the northern Aegean:Timing and kinematics: Comment and Reply: REPLY", *Geology*, Vol. 28, No. 2, p. 188, 2000, +http://dx.doi.org/10.1130/0091-7613(2000)28<188:WPONAF>2.0.CO;2.

65. Karabulut, H., J. Schmittbuhl, S. Özalaybey, O. Lengline, A. Komec Mutlu, V. Durand, M. Bouchon, G. Daniel and M. Bouin, "Evolution of the seismicity in the eastern Marmara sea a decade before and after the 17 August 1999 Izmit Earthquake", Vol. 510, pp. 17–27, 09 2011.

66. Sandwell, D. T., "Elastic Solutions for Strike-Slip Faulting", pp. 1–19, 2001.

67. Barbour, A. and D. Carr Agnew, "Detection of Seismic Signals Using Seismometers and Strainmeters", Vol. 102, pp. 2484–2490, 12 2012.

68. Sacks, I. S., A. T. Linde, A. R. B. and J. A. Snoke, "Shallow seismicity in subduction zones", *Geophysical Research Letters*, Vol. 5, No. 11, pp. 901–903, https://agupubs.onlinelibrary.wiley.com/doi/abs/10.1029/GL005i011p00901.

APPENDIX A: LOGS OF HALK SITE

Logs of HALK site has been added as an appendix.

As it is seen in the legend Caliper Data, Temperature, Delta T and Acoustic Televiewer Data is available in the above the log data.

The first column in the logging data is refer to three arm caliper tool where the change in the diameter can be obtain. The second column is the temperature inside of the borehole. Rapid change in the temperature gives signals to underground water sources. The last, forth, column is the acoustic televiewer data which shows the travel time of the acoustic waves inside of the borehole. Interpreting this data allow us to detect discontinuance in the borehole walls.

The logging data in the borehole can be used in future studies or can be obtained as a sample for other geoscientists working in this area.

After the installations, data loggers of strainmeters are connected to a GPRS modem to send the data to UNAVCO and Kandilli Observatory. The data is in open access in UNAVCO's web site where the raw data, processed data, static plots, interactive plots, station notes and drilling logs available to download. The raw data of HALK and TEPE sites during the M 7.3 Iran-Iraq Earthquake in 12.11.2017 at 18.18 UTC (Figure A.1).

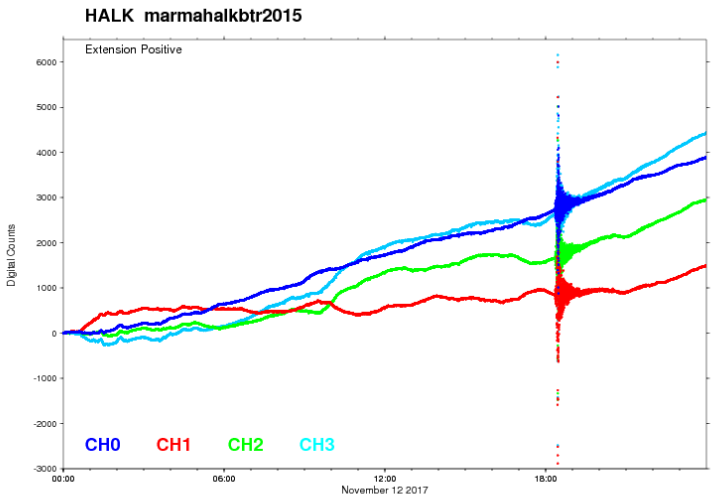

Figure A.1. Raw data of HALK site during Iran-Iraq earthquake in 12.11.2017 at 18.18 UTC

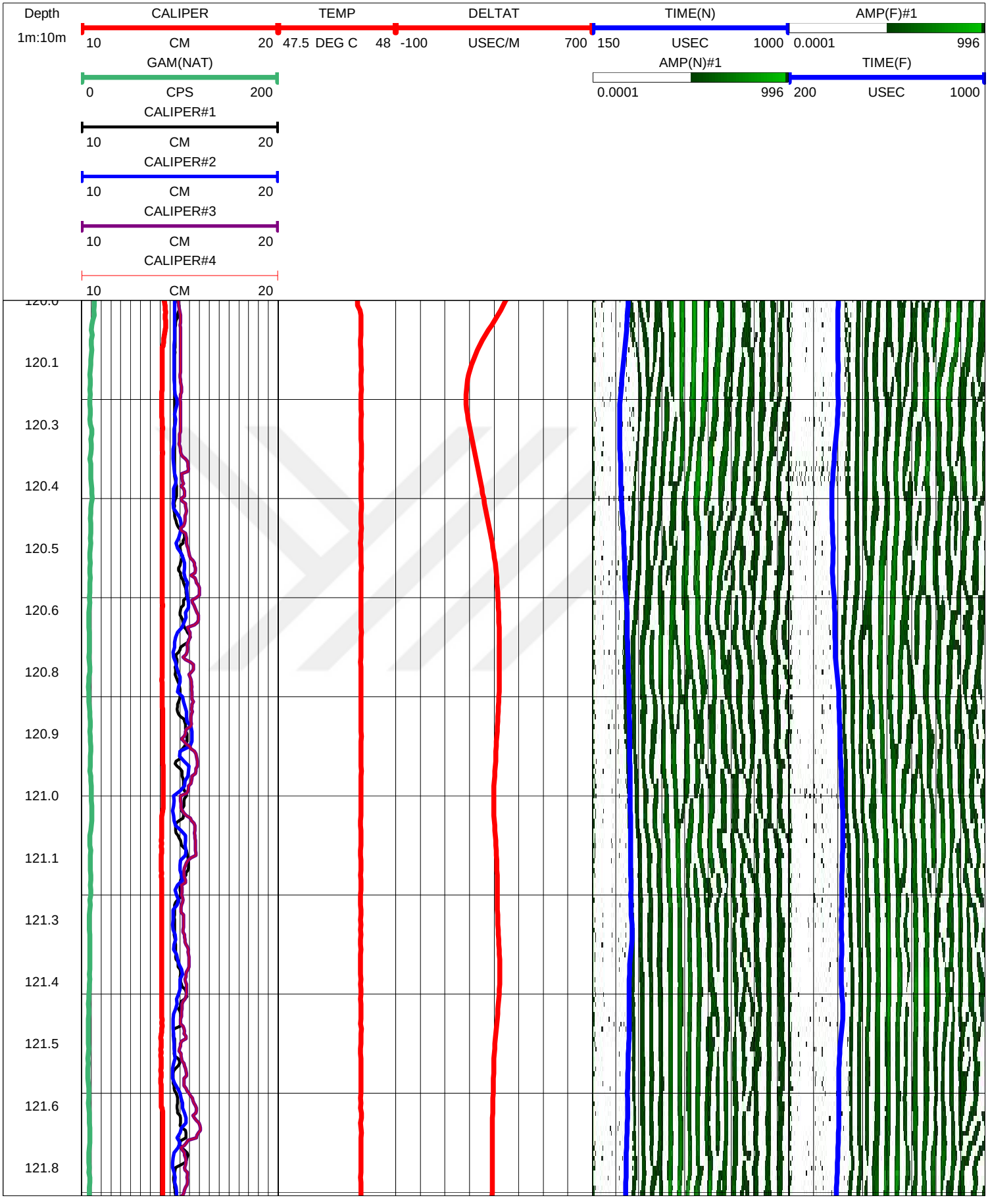
Depth
1m:10m
CALIPER
10 CM 20
TEMP
47.5 DEG C 48
DELTAT
-100 USEC/M 700
TIME(N)
150 USEC 1000
AMP(F)#1
0.0001 996
GAM(NAT)
0 CPS 200
AMP(N)#1
0.0001 996
TIME(F)
200 USEC 1000
CALIPER#1
10 CM 20
CALIPER#2
10 CM 20
CALIPER#3
10 CM 20
CALIPER#4
10 CM 20
120.1
120.3
120.4
120.5
120.6
120.8
120.9
121.0
121.1
121.3
121.4
121.5
121.6
121.8

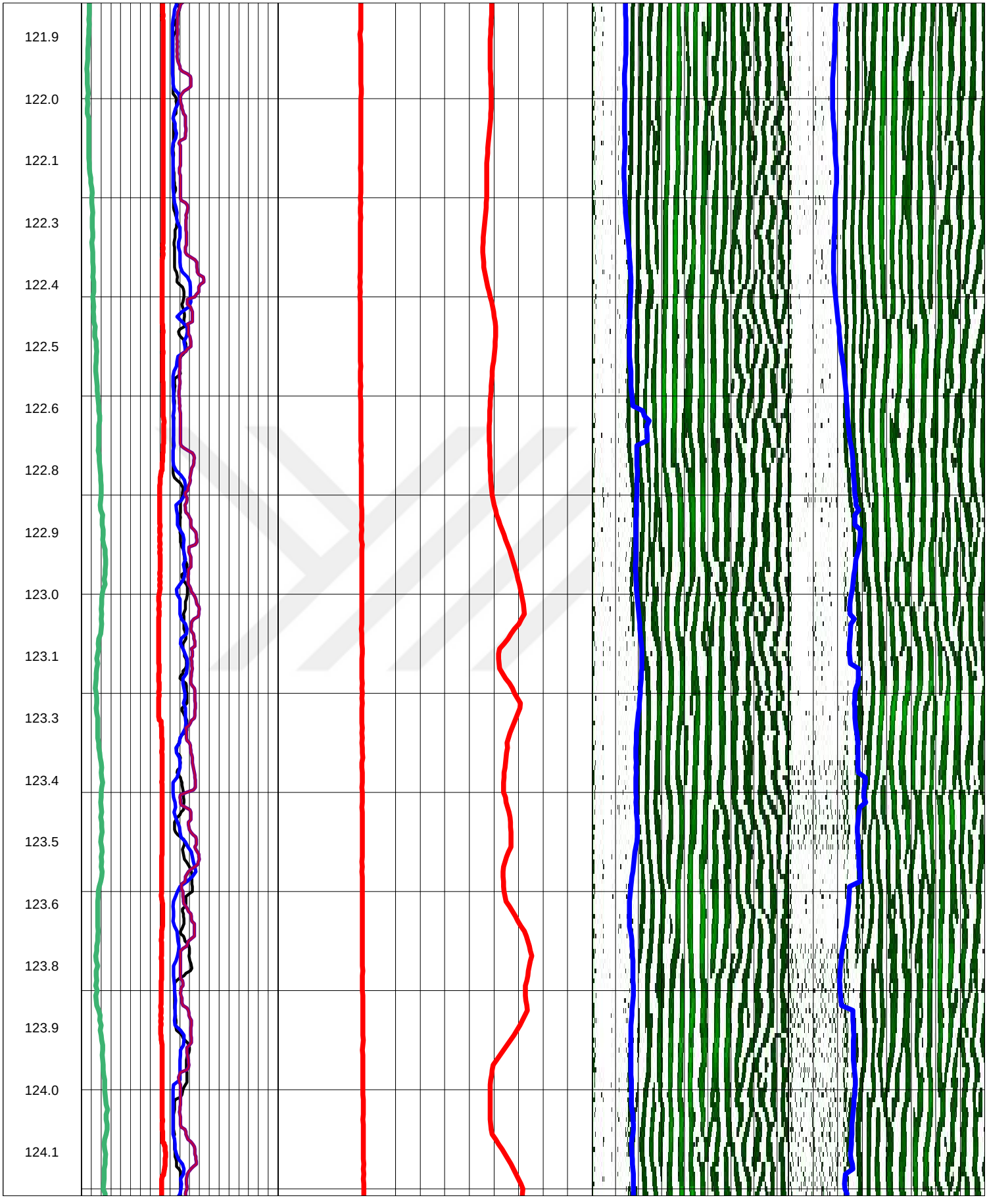
121.9
122.0
122.1
122.3
122.4
122.5
122.6
122.8
122.9
123.0
123.1
123.3
123.4
123.5
123.6
123.8
123.9
124.0
124.1

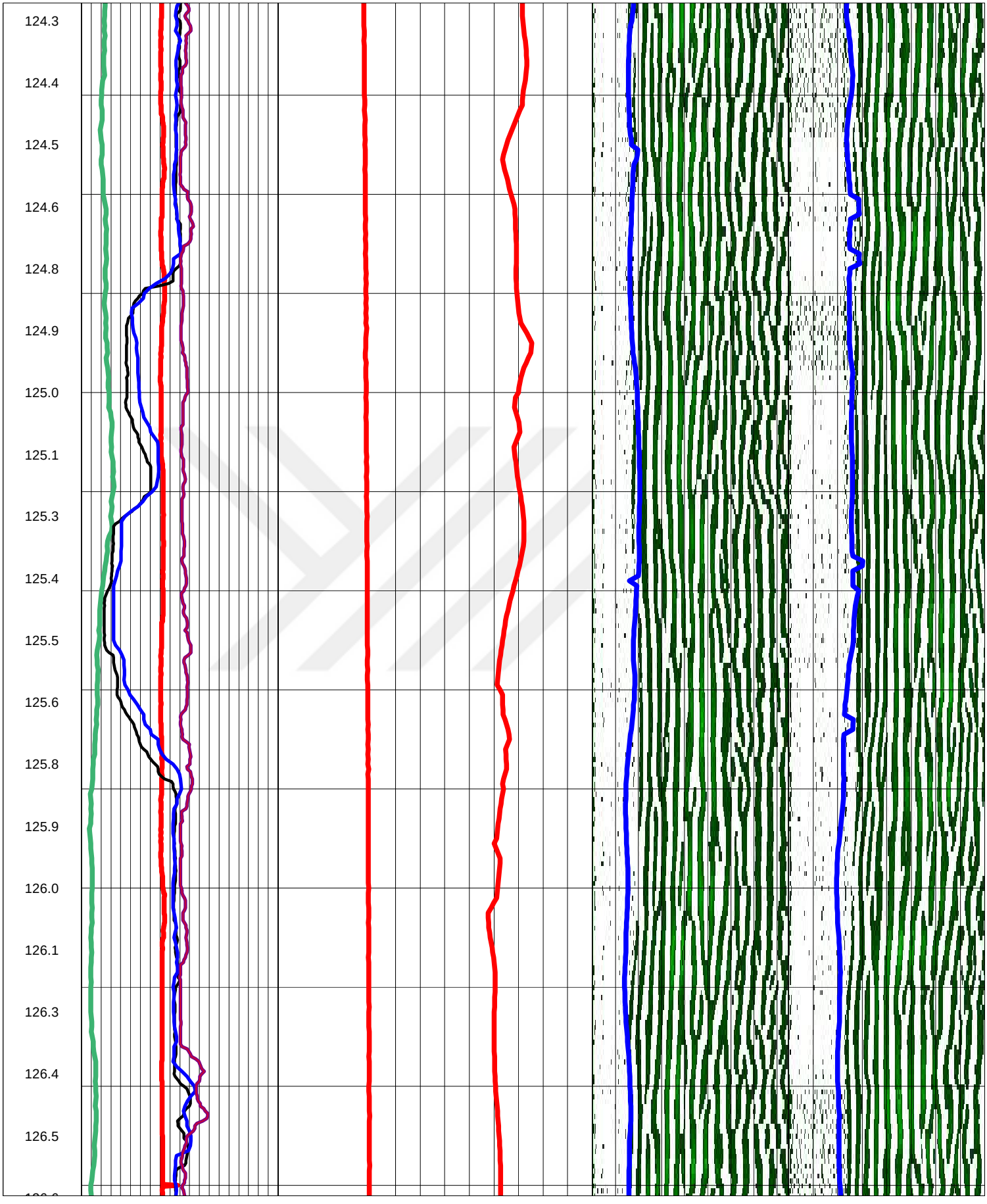
124.3
124.4
124.5
124.6
124.8
124.9
125.0
125.1
125.3
125.4
125.5
125.6
125.8
125.9
126.0
126.1
126.3
126.4
126.5

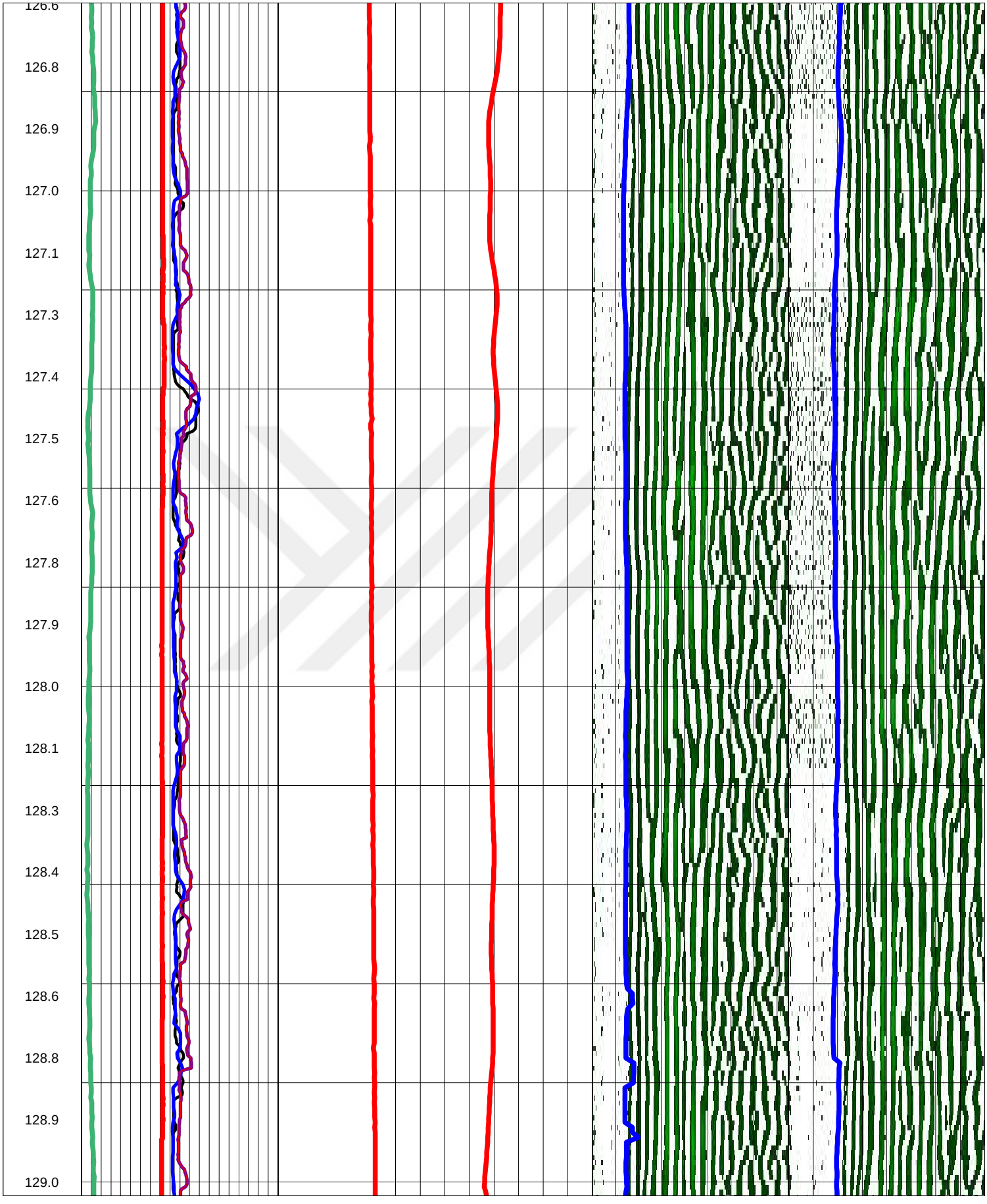
126.6
126.8
126.9
127.0
127.1
127.3
127.4
127.5
127.6
127.8
127.9
128.0
128.1
128.3
128.4
128.5
128.6
128.8
128.9
129.0

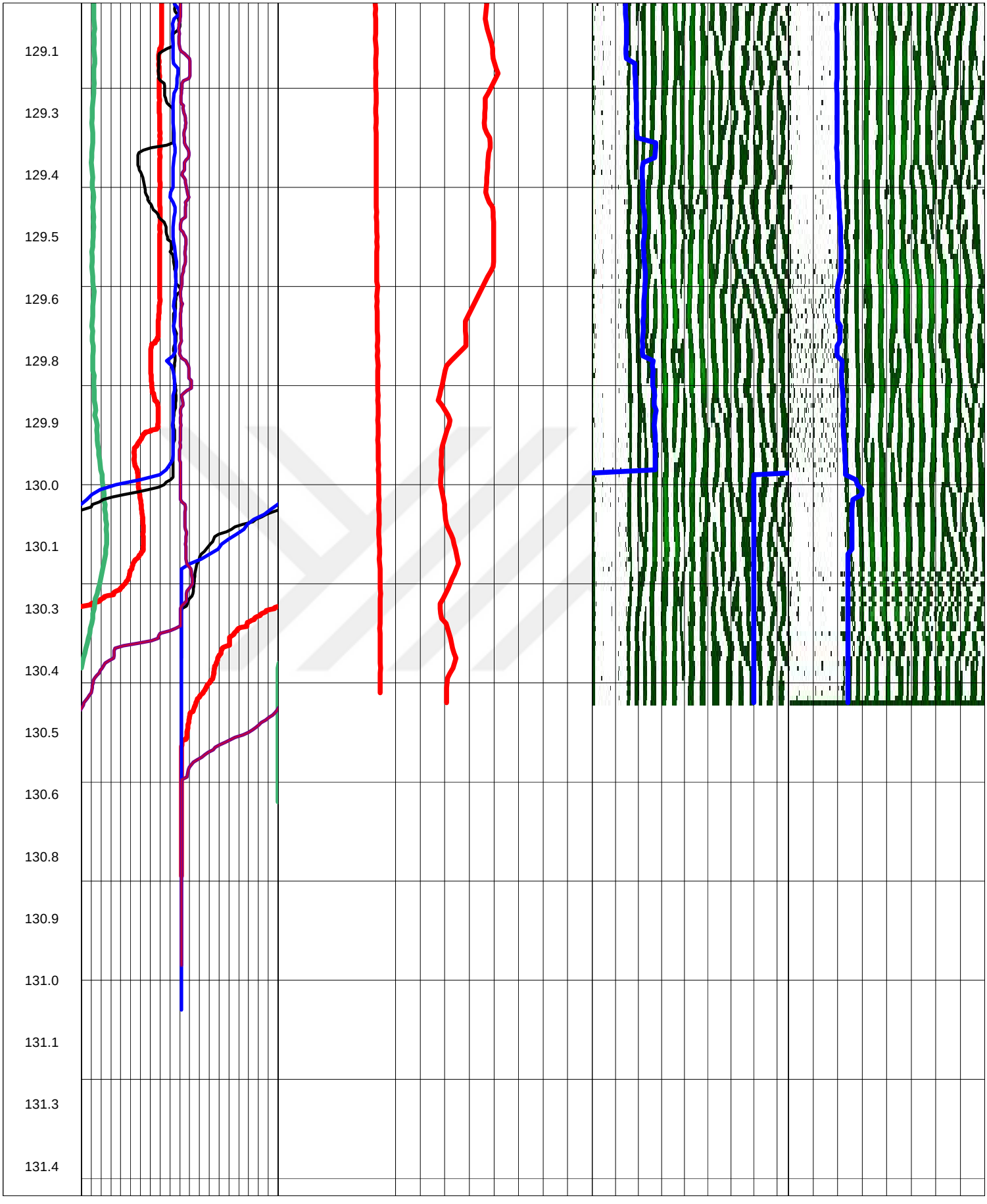
129.1
129.3
129.4
129.5
129.6
129.8
129.9
130.0
130.1
130.3
130.4
130.5
130.6
130.8
130.9
131.0
131.1
131.3
131.4

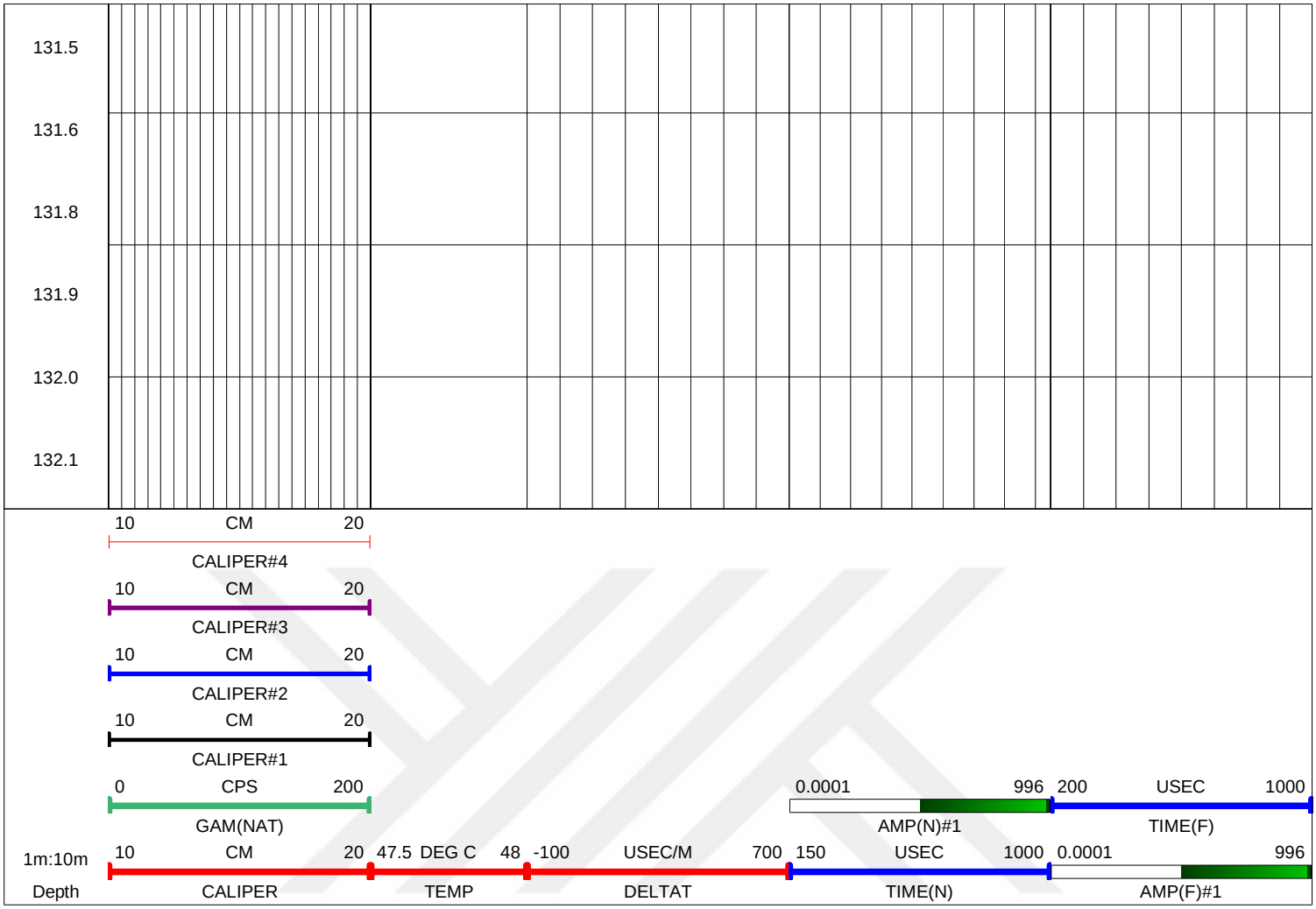
131.5
131.6
131.8
131.9
132.0
132.1
10 CM 20
CALIPER#4
10 CM 20
CALIPER#3
10 CM 20
CALIPER#2
10 CM 20
CALIPER#1
0 CPS 200
GAM(NAT)
0.0001 996
AMP(N)#1
200 USEC 1000
TIME(F)
1m:10m
Depth
10 CM 20
CALIPER
47.5 DEG C 48
TEMP
-100 USEC/M 700
DELTAT
150 USEC 1000
TIME(N)
0.0001 996
AMP(F)#1

APPENDIX B: LOGS OF TEPE SITE

Logs of TEPE site has been added as an appendix.

In the logs below the explanation in the title as numbers refer to the holes drilled accordingly.

As it is seen in the legend Caliper Data, Temperature, Delta T and Acoustic Televiewer Data is available in the above the log data.

The first column in the logging data is refer to three arm caliper tool where the change in the diameter can be obtain. The second column is the temperature inside of the borehole. Rapid change in the temperature gives signals to underground water sources. The last, forth, column is the acoustic televiewer data which shows the travel time of the acoustic waves inside of the borehole. Interpreting this data allow us to detect discontinuance in the borehole walls.

The logging data in the borehole can be used in future studies or can be obtained as a sample for other geoscientists working in this area.

After the installations, data loggers of strainmeters are connected to a GPRS modem to send the data to UNAVCO and Kandilli Observatory. The data is in open access in UNAVCO's web site where the raw data, processed data, static plots, interactive plots, station notes and drilling logs available to download. The raw data of HALK and TEPE sites during the M 7.3 Iran-Iraq Earthquake in 12.11.2017 at 18.18 UTC (Figure B.1).

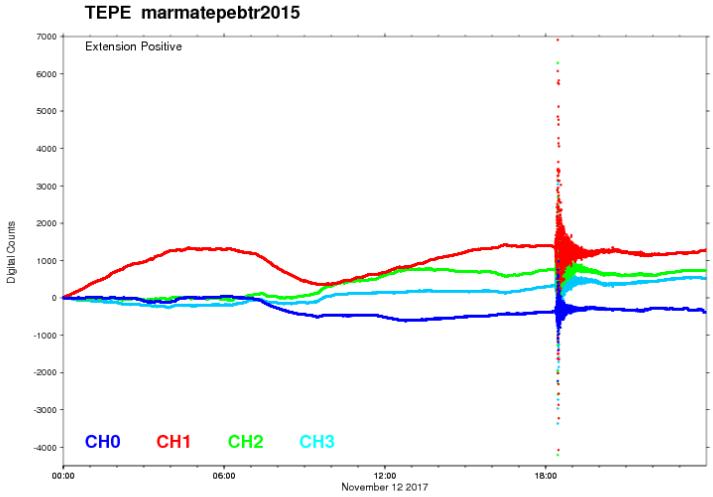

Figure B.1. Raw data of TEPE site during Iran-Iraq earthquake in 12.11.2017 at 18.18 UTC

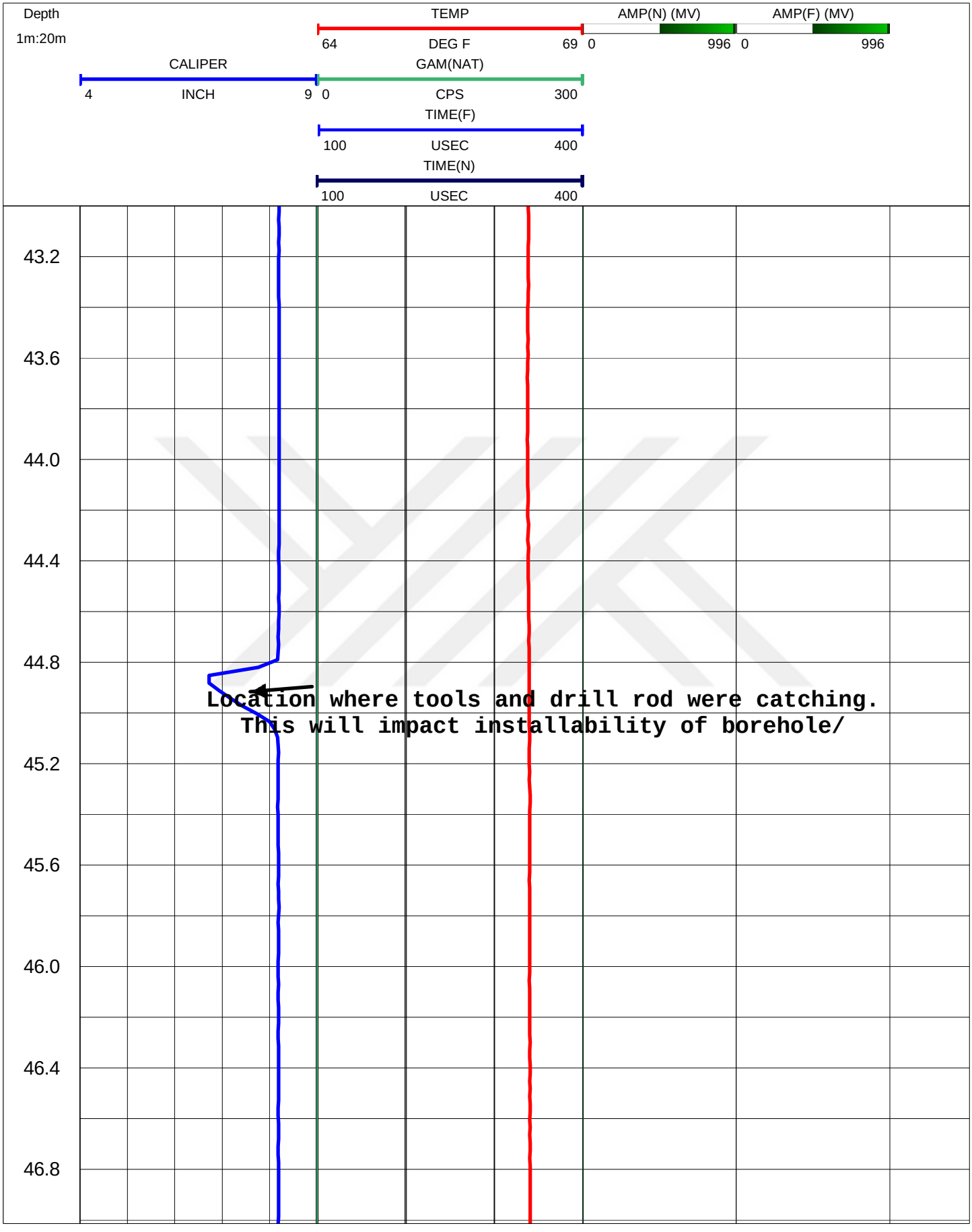
Depth
1m:20m
TEMP
64
DEG F
69
AMP(N) (MV)
0
996
AMP(F) (MV)
0
996
CALIPER
4
INCH
9
GAM(NAT)
0
CPS
300
TIME(F)
100
USEC
400
TIME(N)
100
USEC
400
43.2
43.6
44.0
44.4
44.8
45.2
45.6
46.0
46.4
46.8
Location where tools and drill rod were catching.
This will impact installability of borehole/

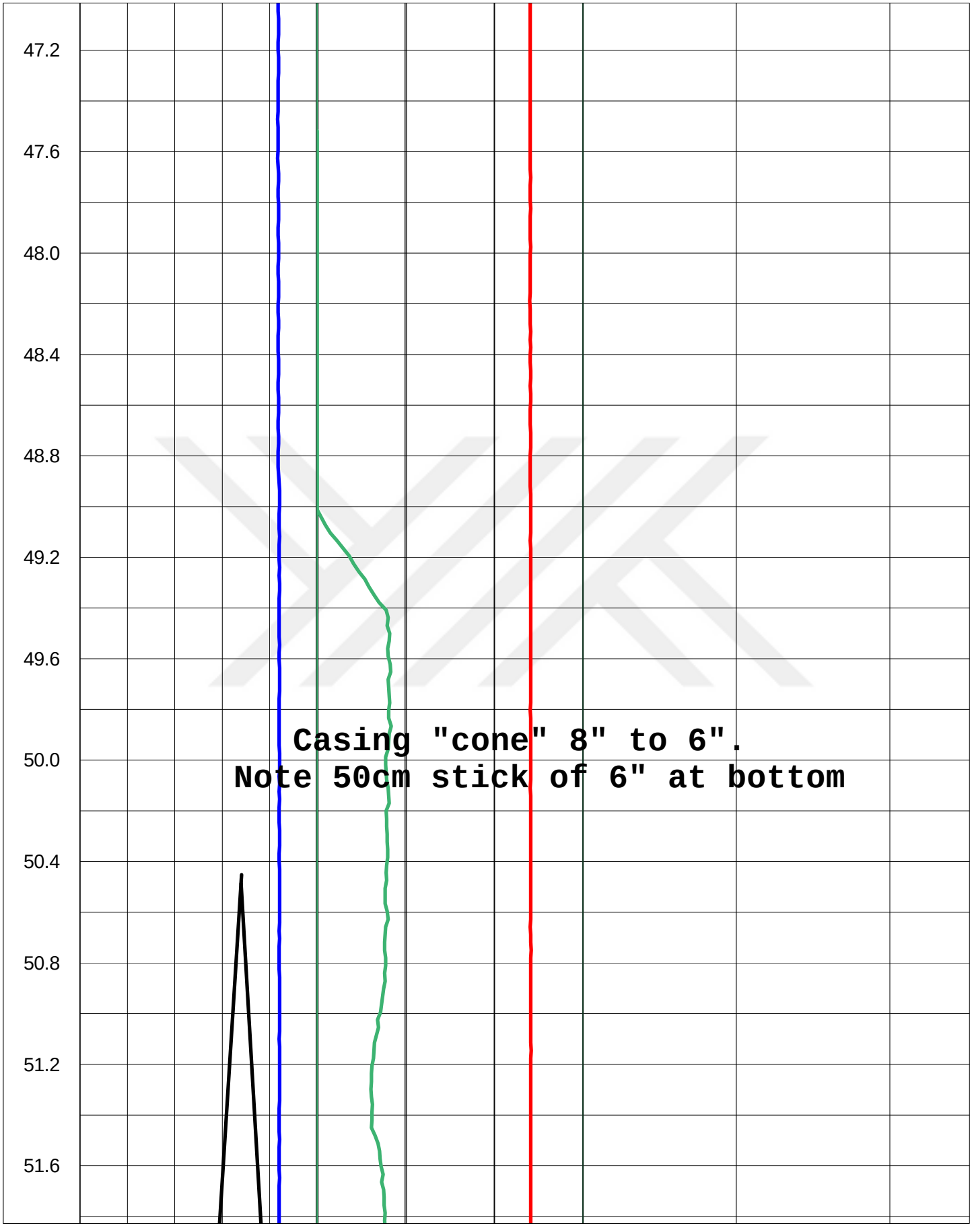
47.2
47.6
48.0
48.4
48.8
49.2
49.6
50.0
50.4
50.8
51.2
51.6
Casing "cone" 8" to 6".
Note 50cm stick of 6" at bottom

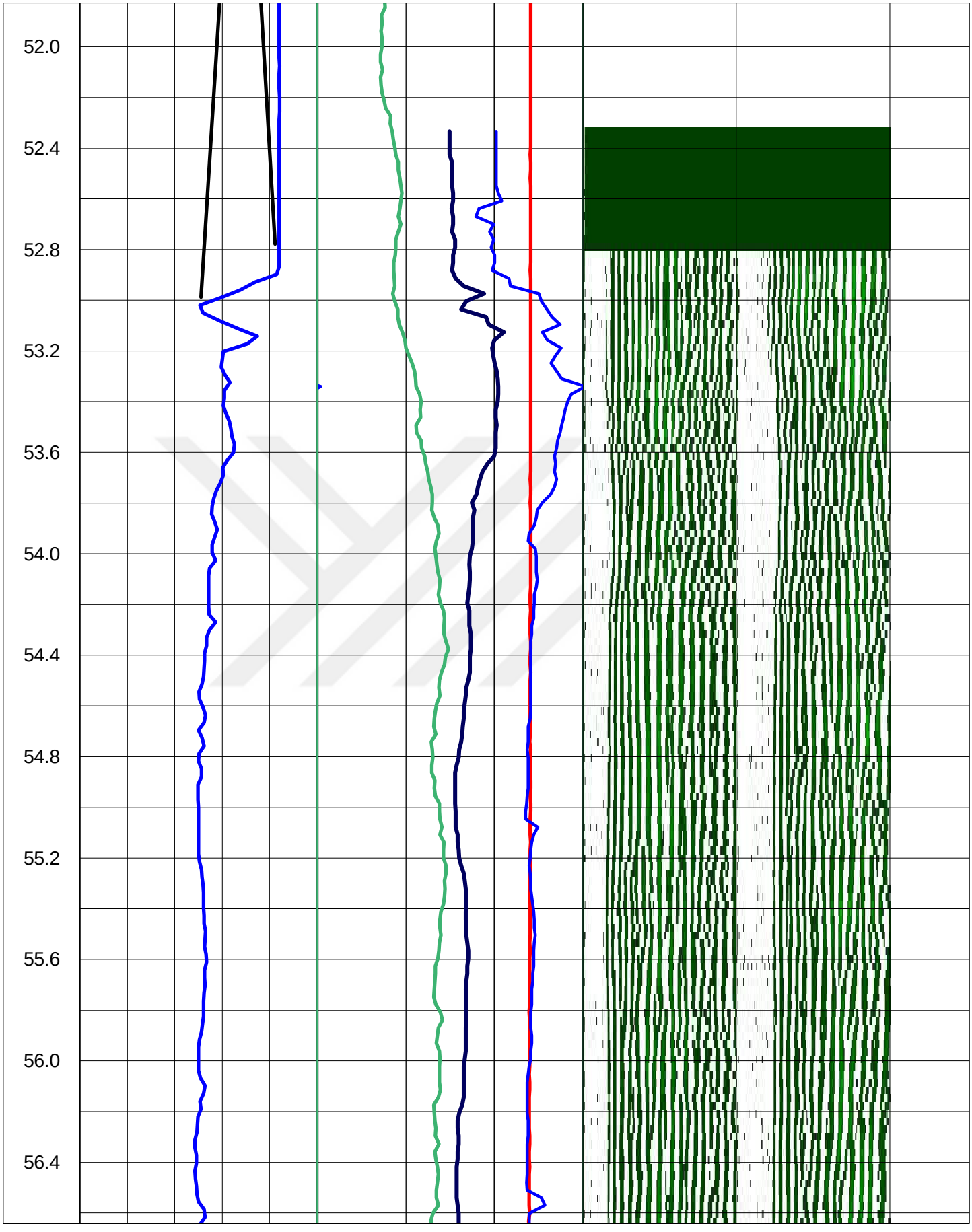
52.0
52.4
52.8
53.2
53.6
54.0
54.4
54.8
55.2
55.6
56.0
56.4

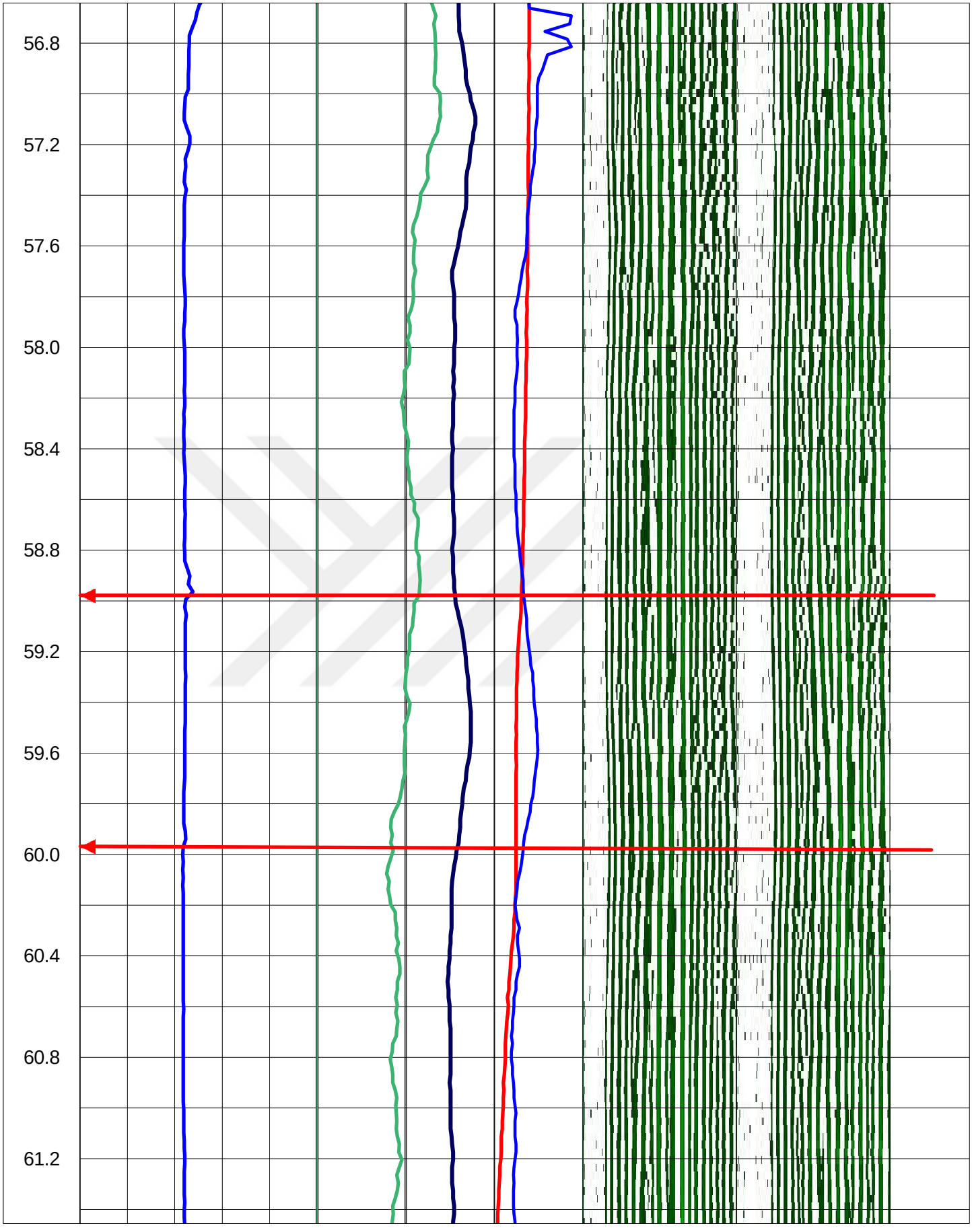
56.8
57.2
57.6
58.0
58.4
58.8
59.2
59.6
60.0
60.4
60.8
61.2

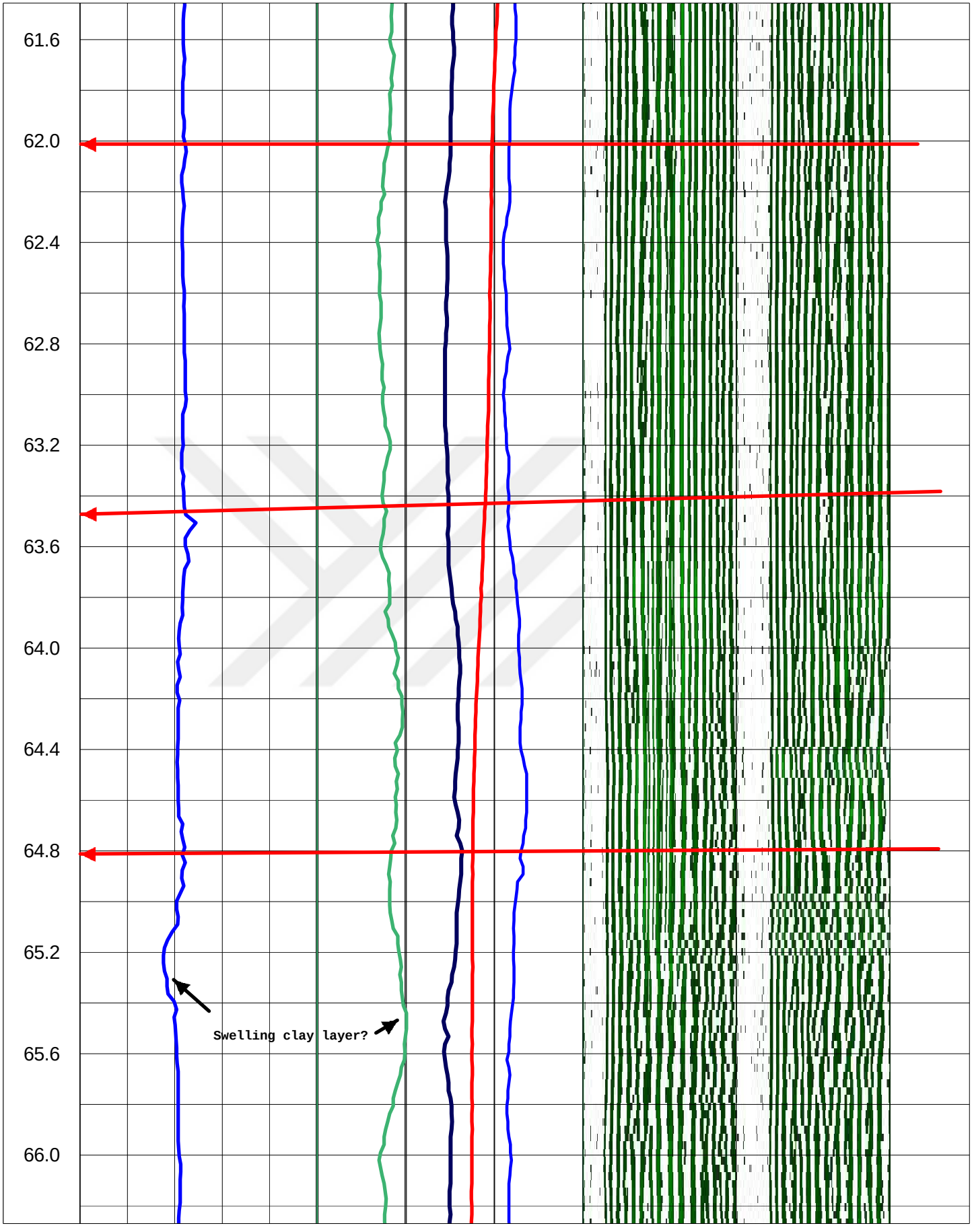
61.6
62.0
62.4
62.8
63.2
63.6
64.0
64.4
64.8
65.2
65.6
66.0
Swelling clay layer?

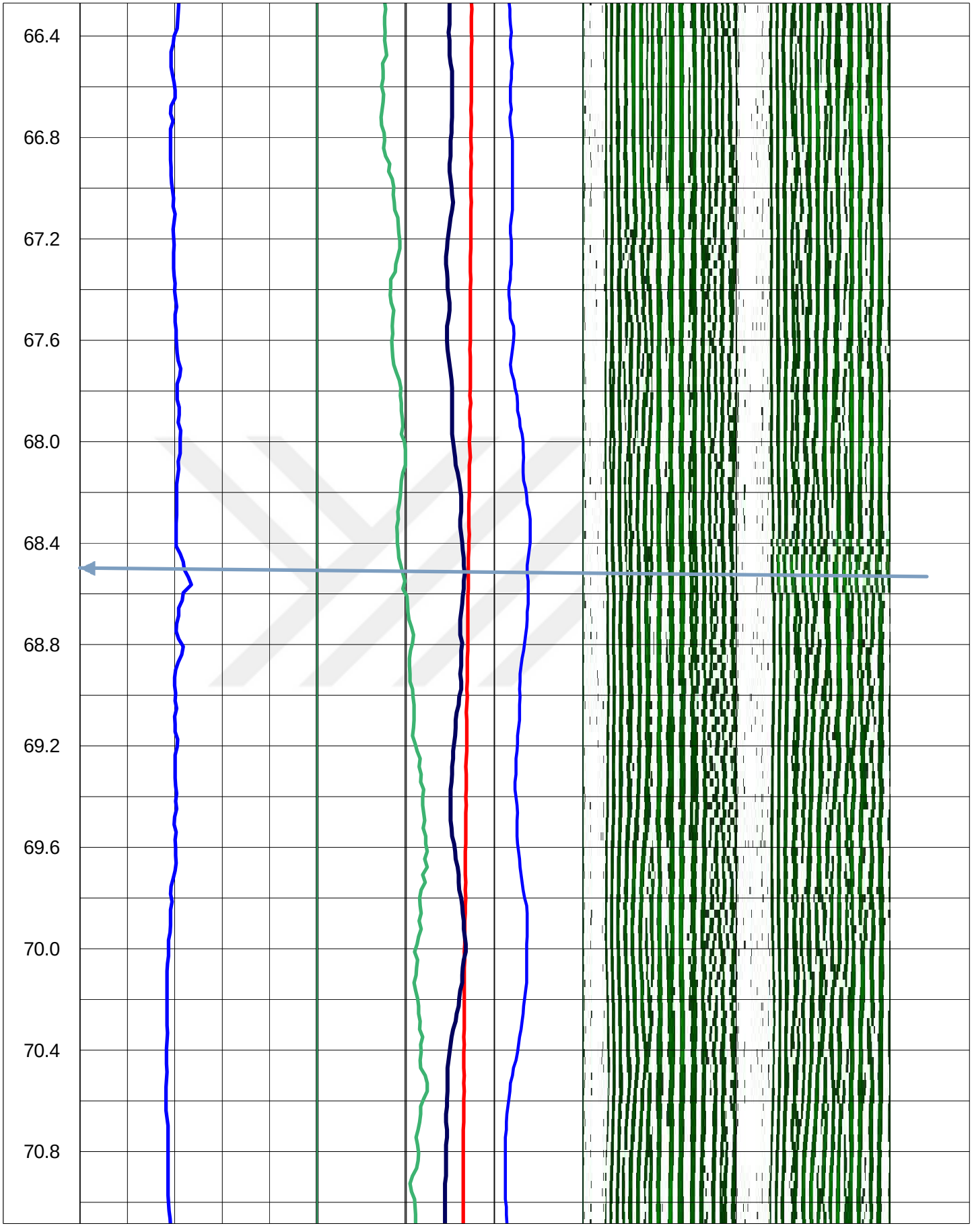
66.4
66.8
67.2
67.6
68.0
68.4
68.8
69.2
69.6
70.0
70.4
70.8

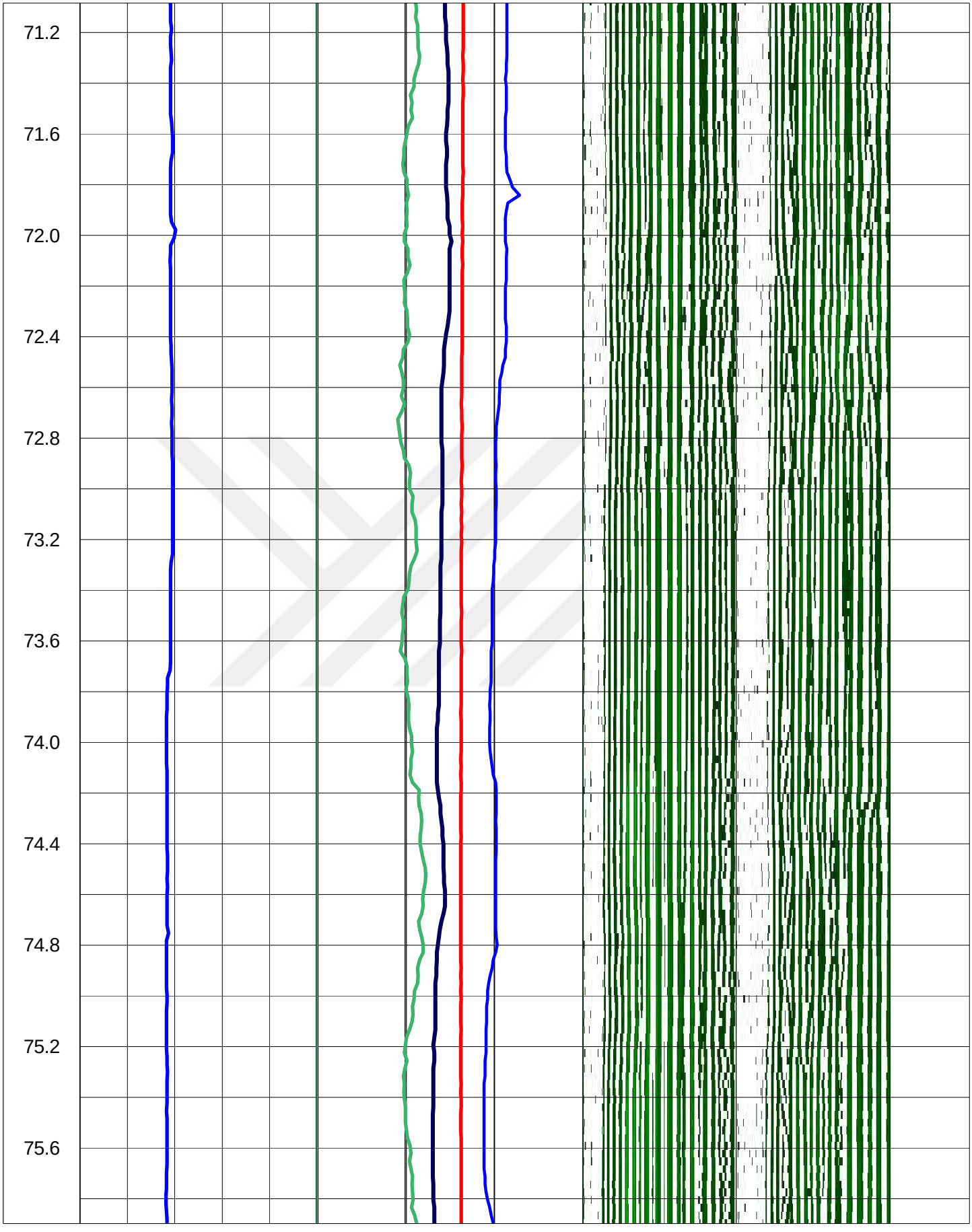
71.2
71.6
72.0
72.4
72.8
73.2
73.6
74.0
74.4
74.8
75.2
75.6

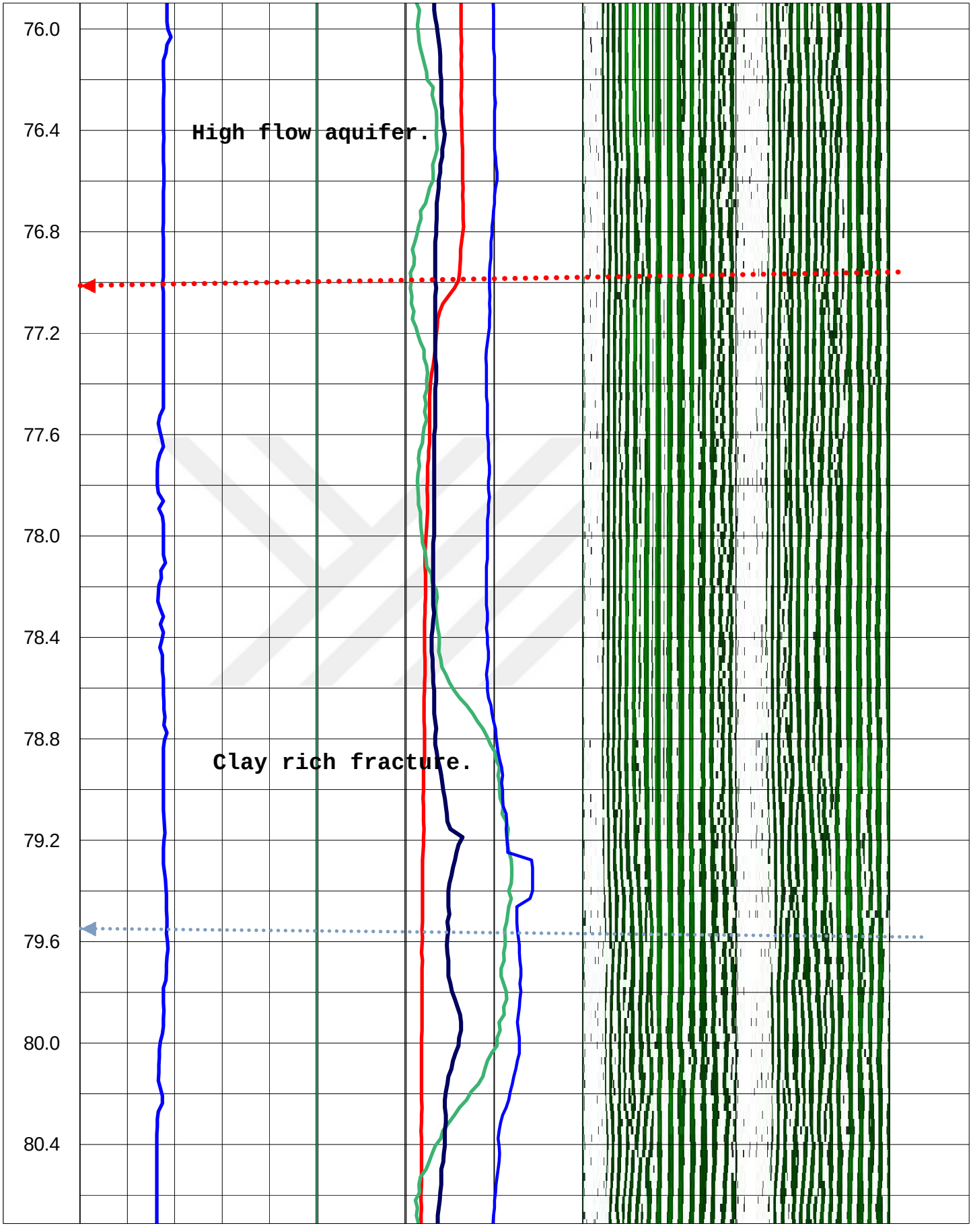
76.0
76.4
76.8
77.2
77.6
78.0
78.4
78.8
79.2
79.6
80.0
80.4
High flow aquifer.
Clay rich fracture.

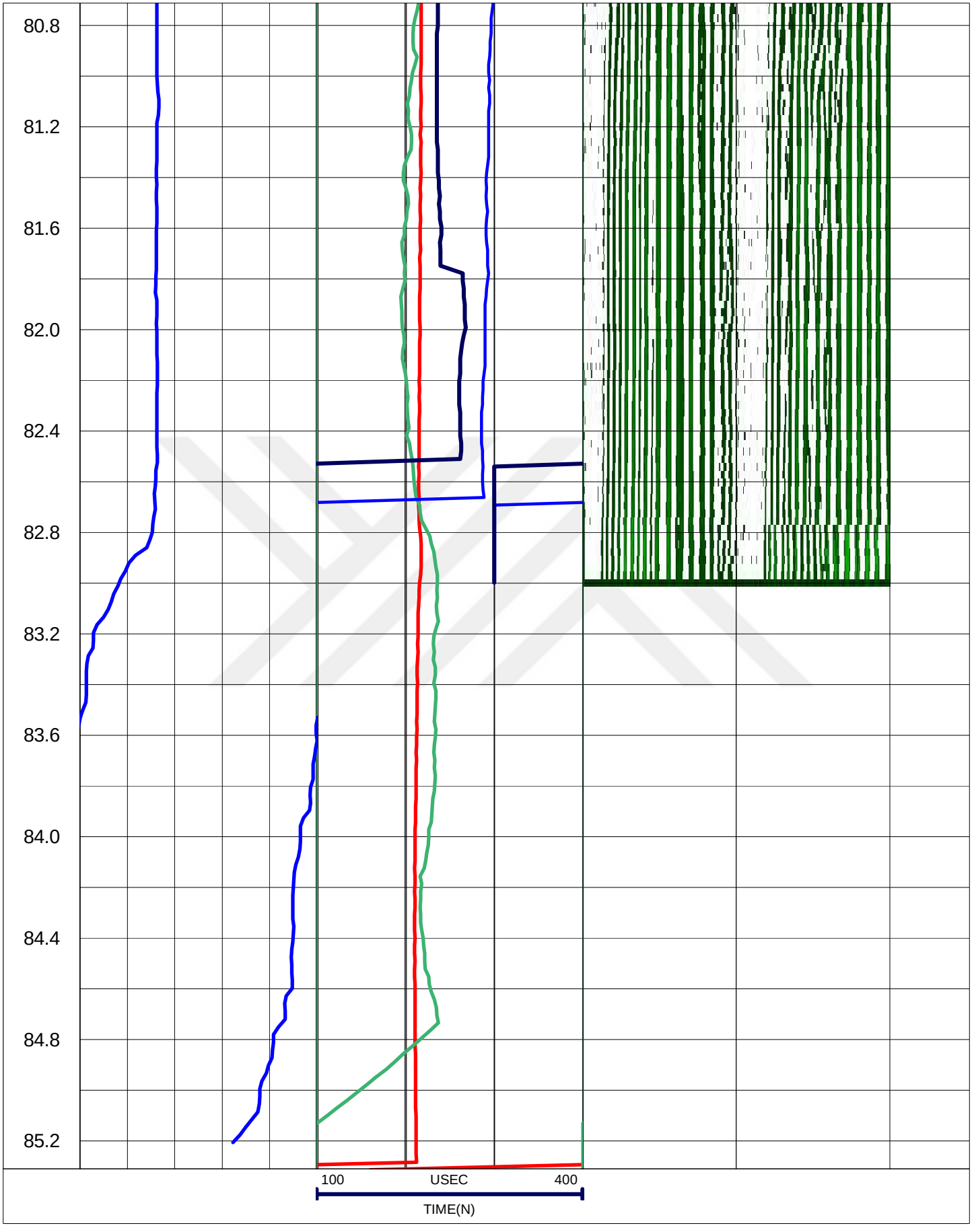
80.8
81.2
81.6
82.0
82.4
82.8
83.2
83.6
84.0
84.4
84.8
85.2
100
USEC
400
TIME(N)

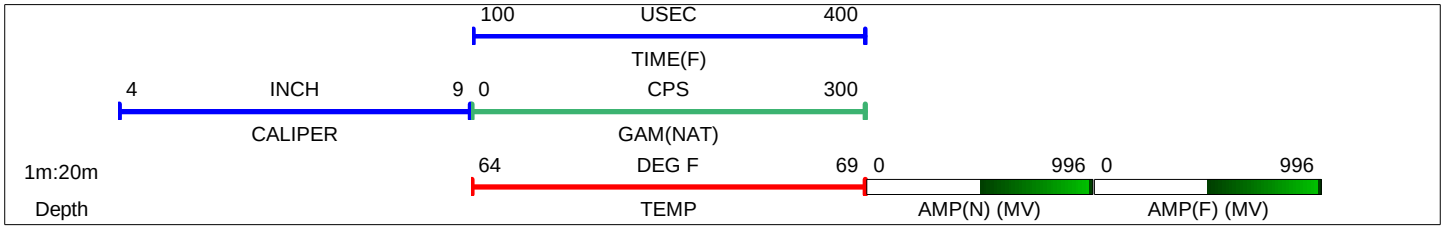
100
USEC
400
TIME(F)
4
INCH
9
0
CPS
300
CALIPER
GAM(NAT)
1m:20m
64
DEG F
69
0
996
0
996
Depth
TEMP
AMP(N) (MV)
AMP(F) (MV)

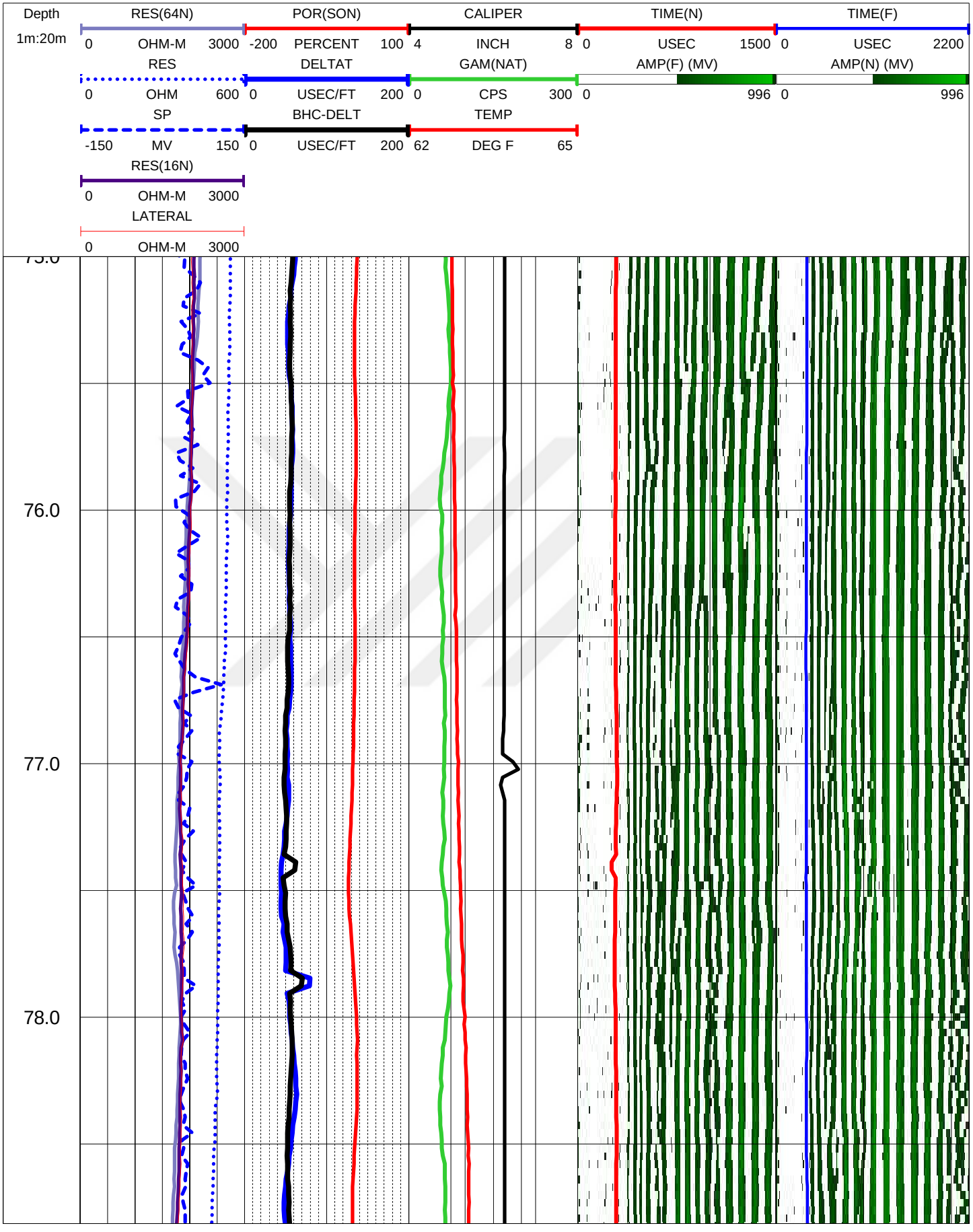
Depth
1m:20m
RES(64N)
0 OHM-M 3000
POR(SON)
-200 PERCENT 100
CALIPER
4 INCH 8
TIME(N)
0 USEC 1500
TIME(F)
0 USEC 2200
RES
0 OHM 600
DELTAT
0 USEC/FT 200
GAM(NAT)
0 CPS 300
AMP(F) (MV)
0 996
AMP(N) (MV)
0 996
SP
-150 MV 150
BHC-DELT
0 USEC/FT 200
TEMP
62 DEG F 65
RES(16N)
0 OHM-M 3000
LATERAL
0 OHM-M 3000
76.0
77.0
78.0

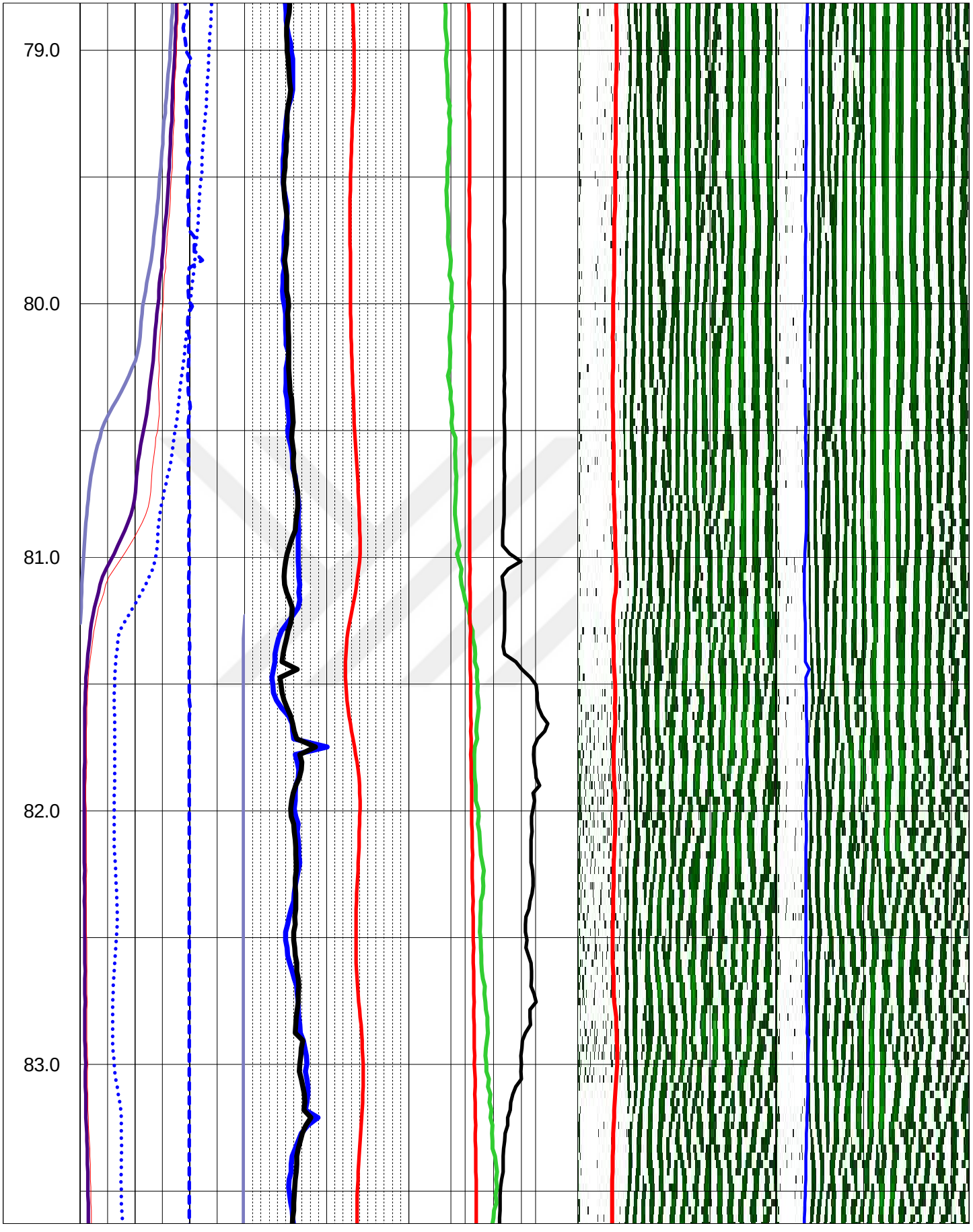
79.0
80.0
81.0
82.0
83.0

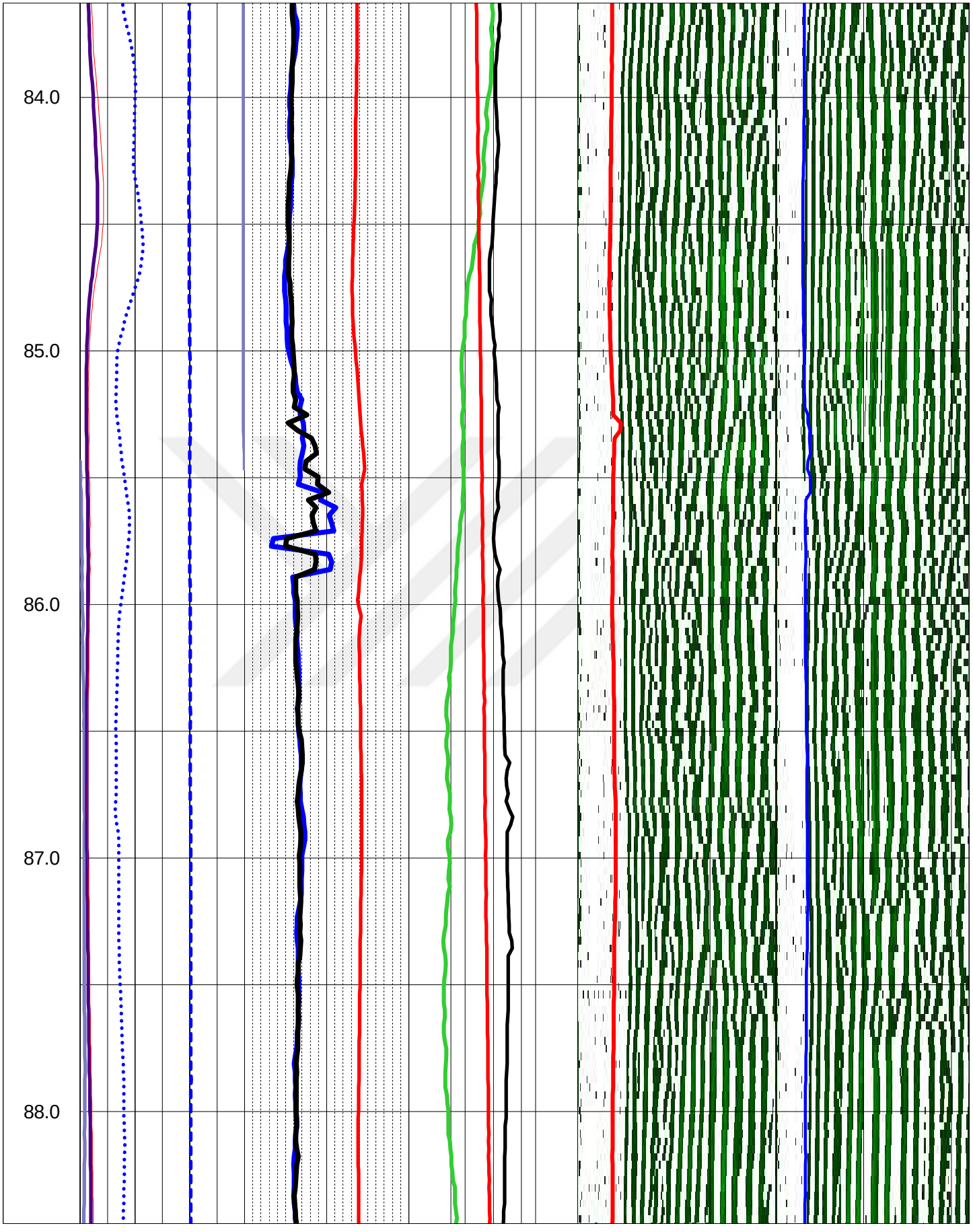
84.0
85.0
86.0
87.0
88.0

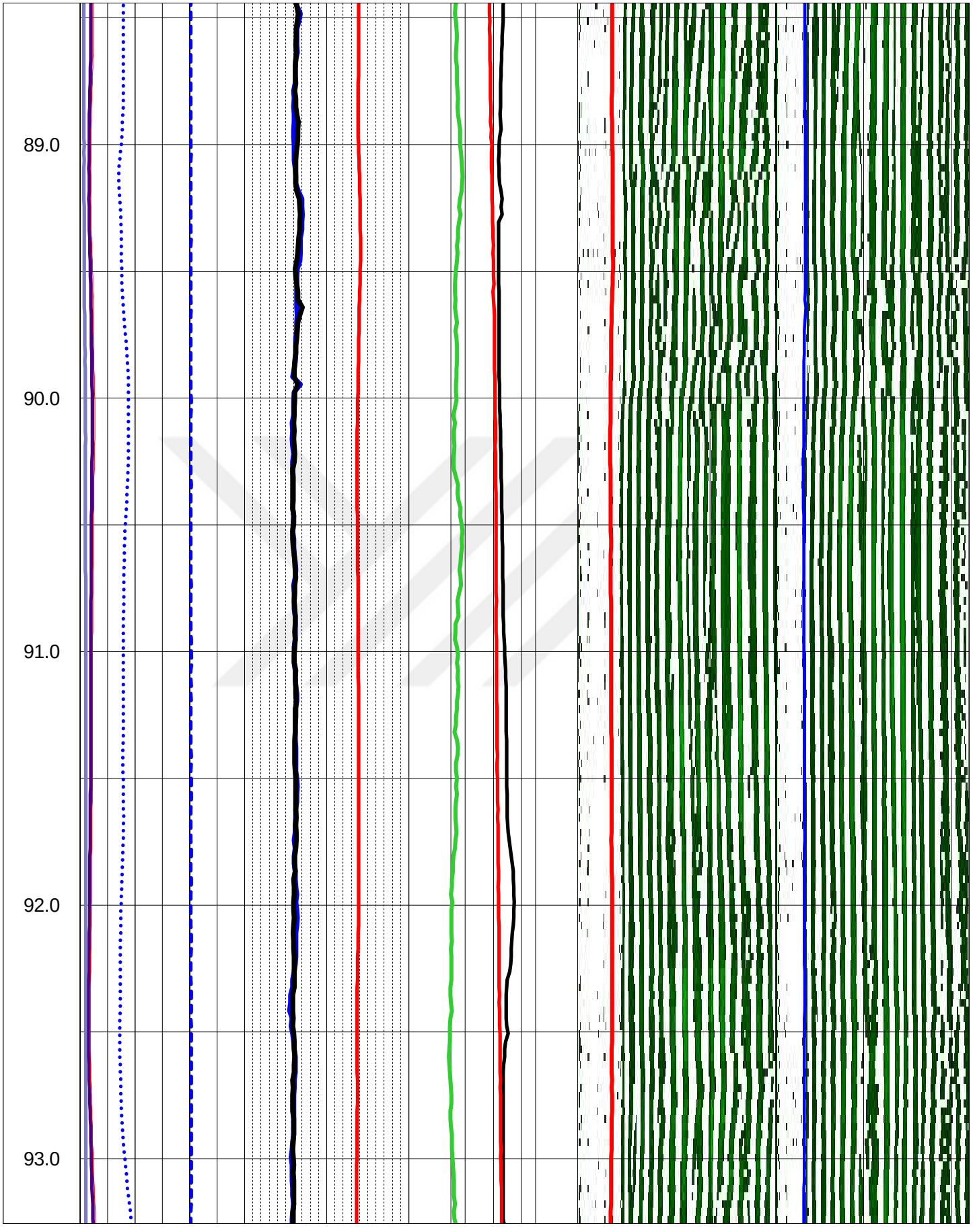
89.0
90.0
91.0
92.0
93.0

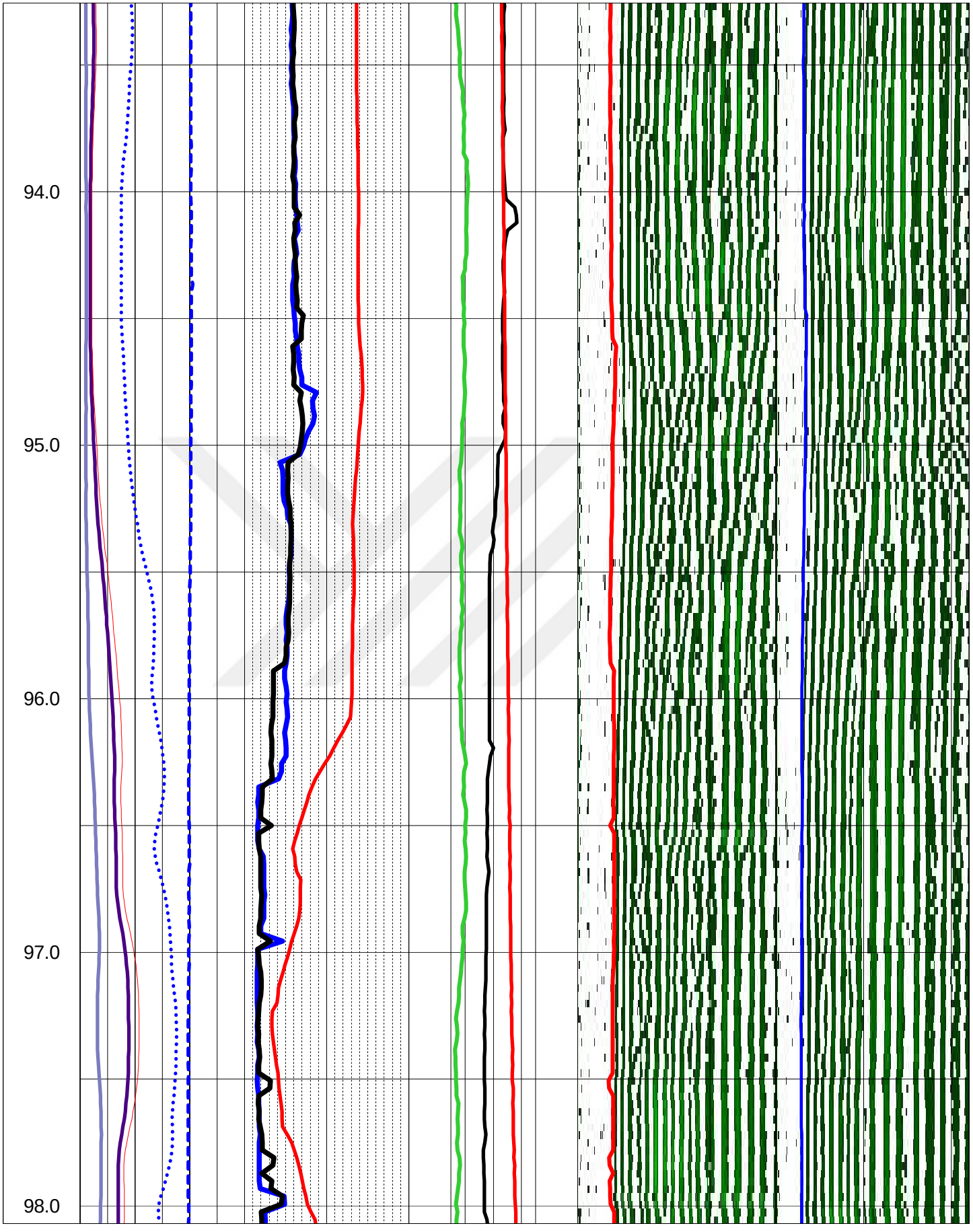
94.0
95.0
96.0
97.0
98.0

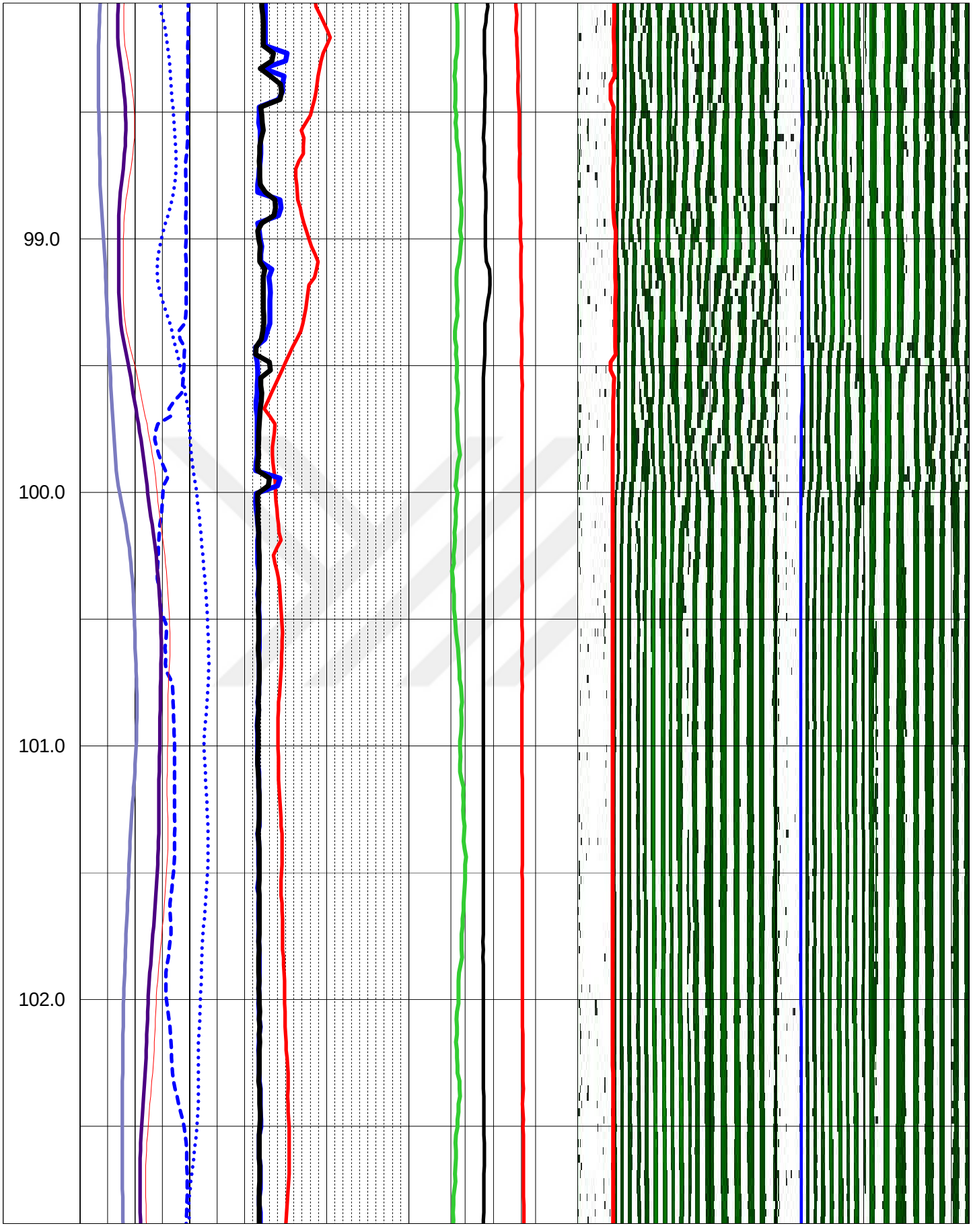
99.0
100.0
101.0
102.0

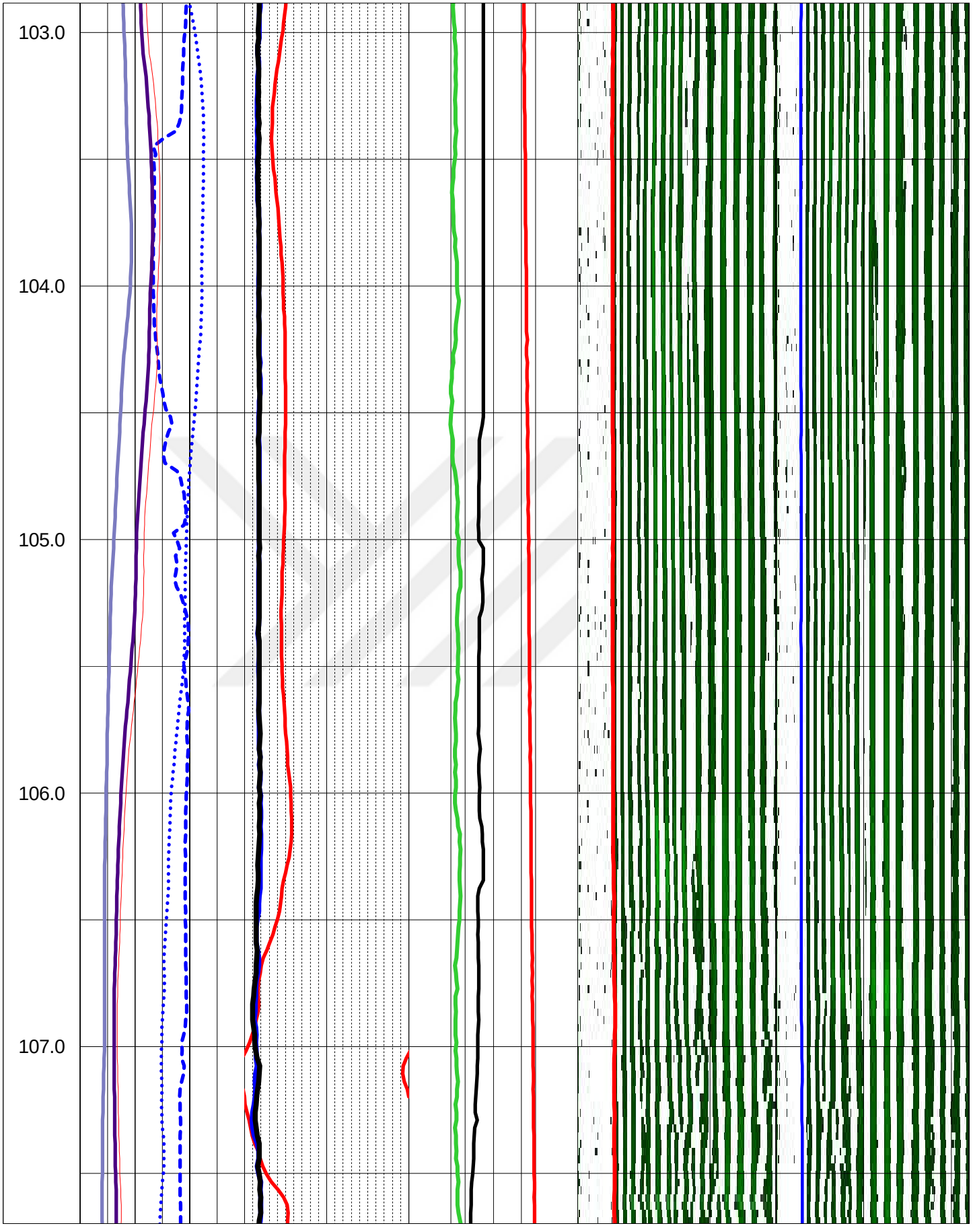
103.0
104.0
105.0
106.0
107.0

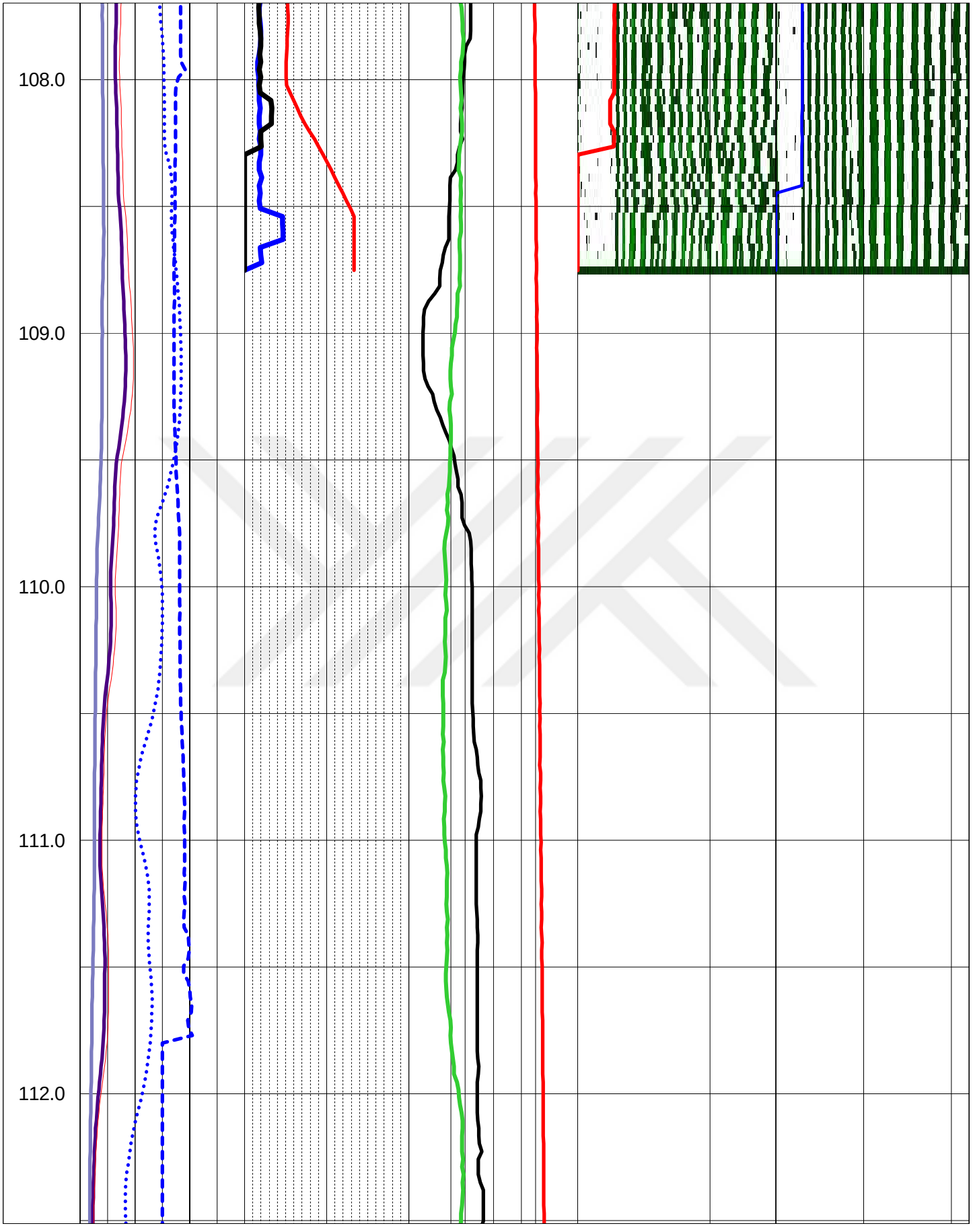
108.0
109.0
110.0
111.0
112.0

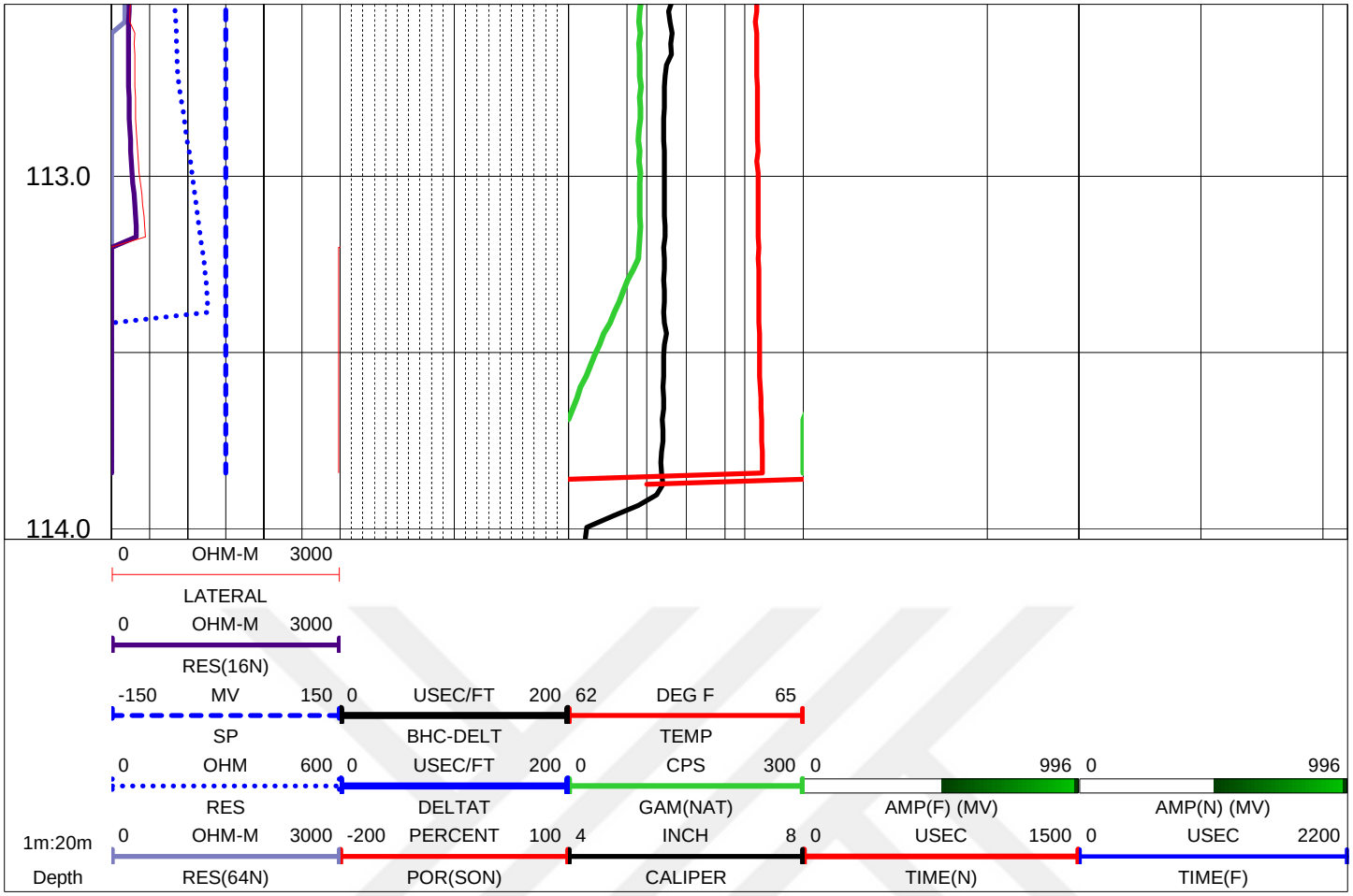
113.0
114.0
0 OHM-M 3000
LATERAL
0 OHM-M 3000
RES(16N)
-150 MV 150 0 USEC/FT 200 62 DEG F 65
SP BHC-DELT TEMP
0 OHM 600 0 USEC/FT 200 0 CPS 300 0 996 0 996
RES DELTAT GAM(NAT) AMP(F) (MV) AMP(N) (MV)
1m:20m
0 OHM-M 3000 -200 PERCENT 100 4 INCH 8 0 USEC 1500 0 USEC 2200
Depth RES(64N) POR(SON) CALIPER TIME(N) TIME(F)

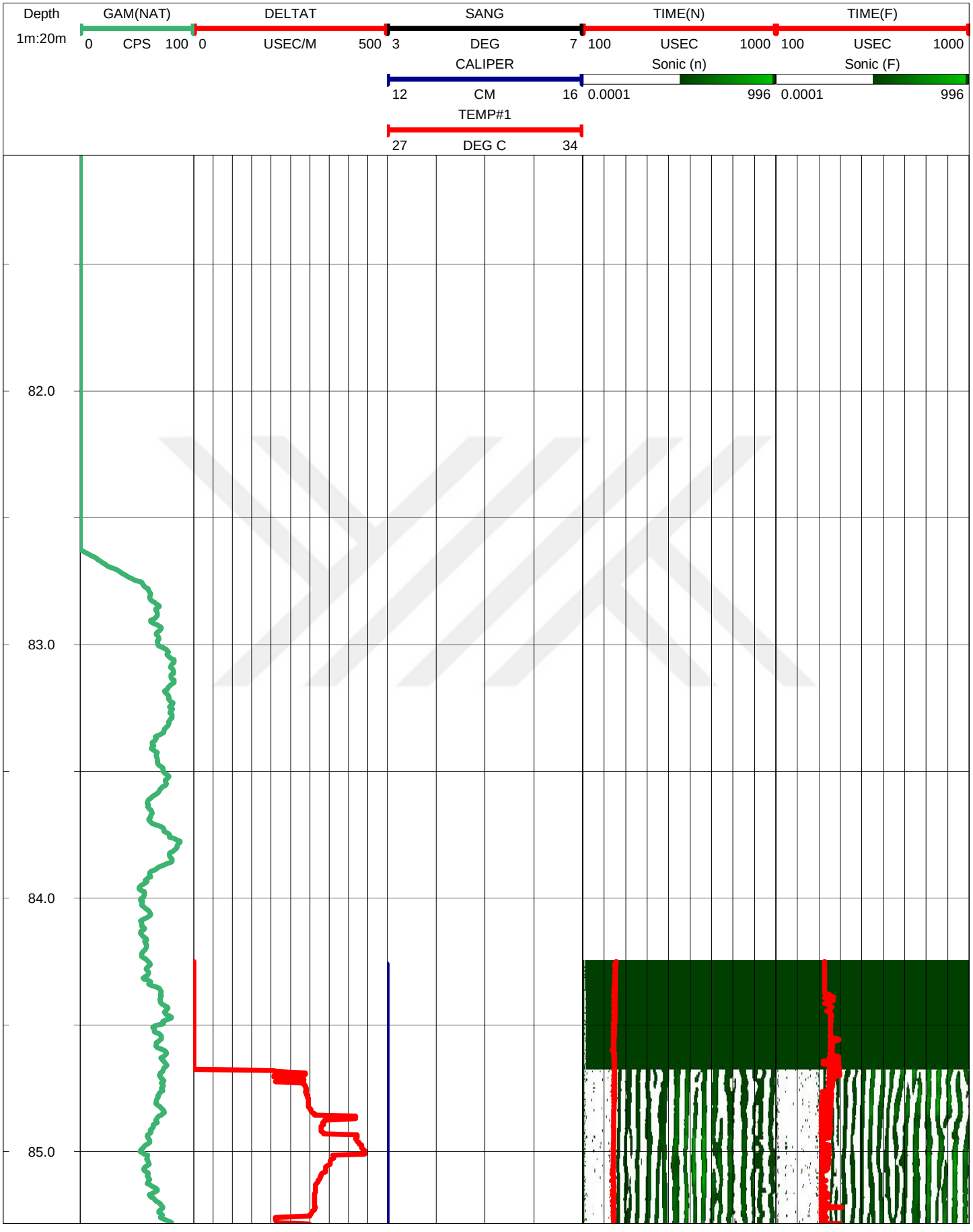
Depth
1m:20m
GAM(NAT)
0
CPS
100
DELTAT
0
USEC/M
500
SANG
3
DEG
7
TIME(N)
100
USEC
1000
TIME(F)
100
USEC
1000
CALIPER
12
CM
16
Sonic (n)
0.0001
996
Sonic (F)
0.0001
996
TEMP#1
27
DEG C
34
82.0
83.0
84.0
85.0

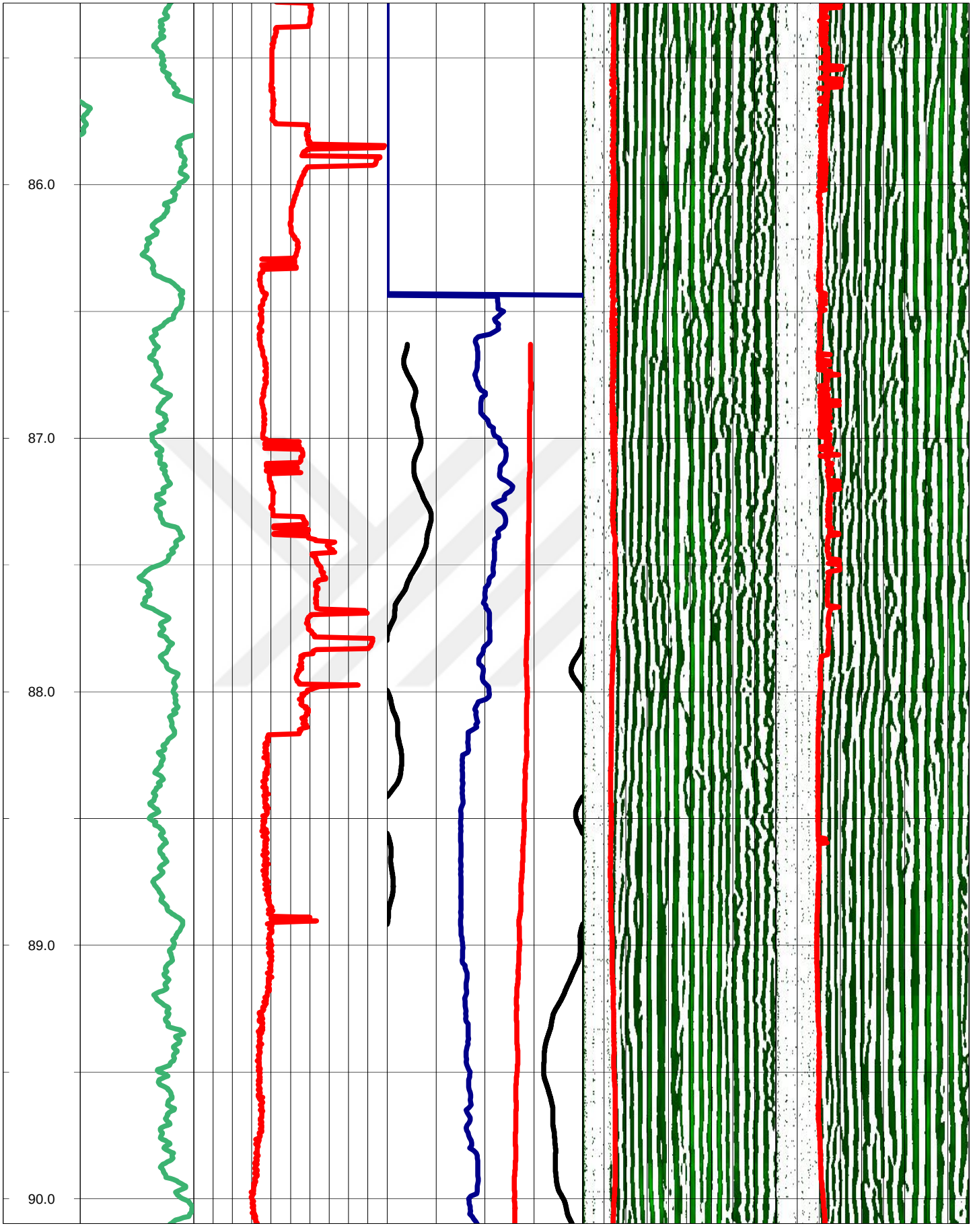
86.0
87.0
88.0
89.0
90.0

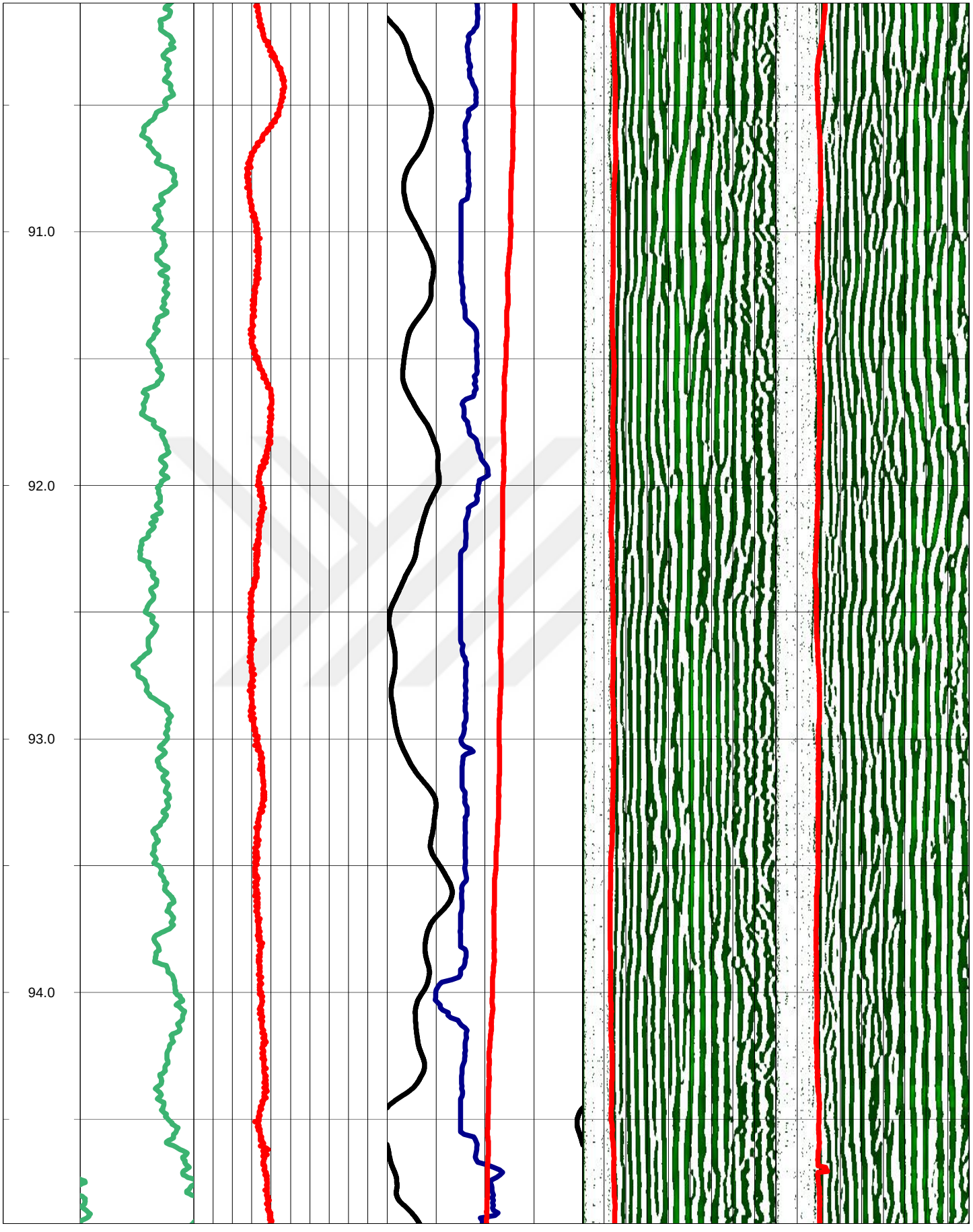
91.0
92.0
93.0
94.0

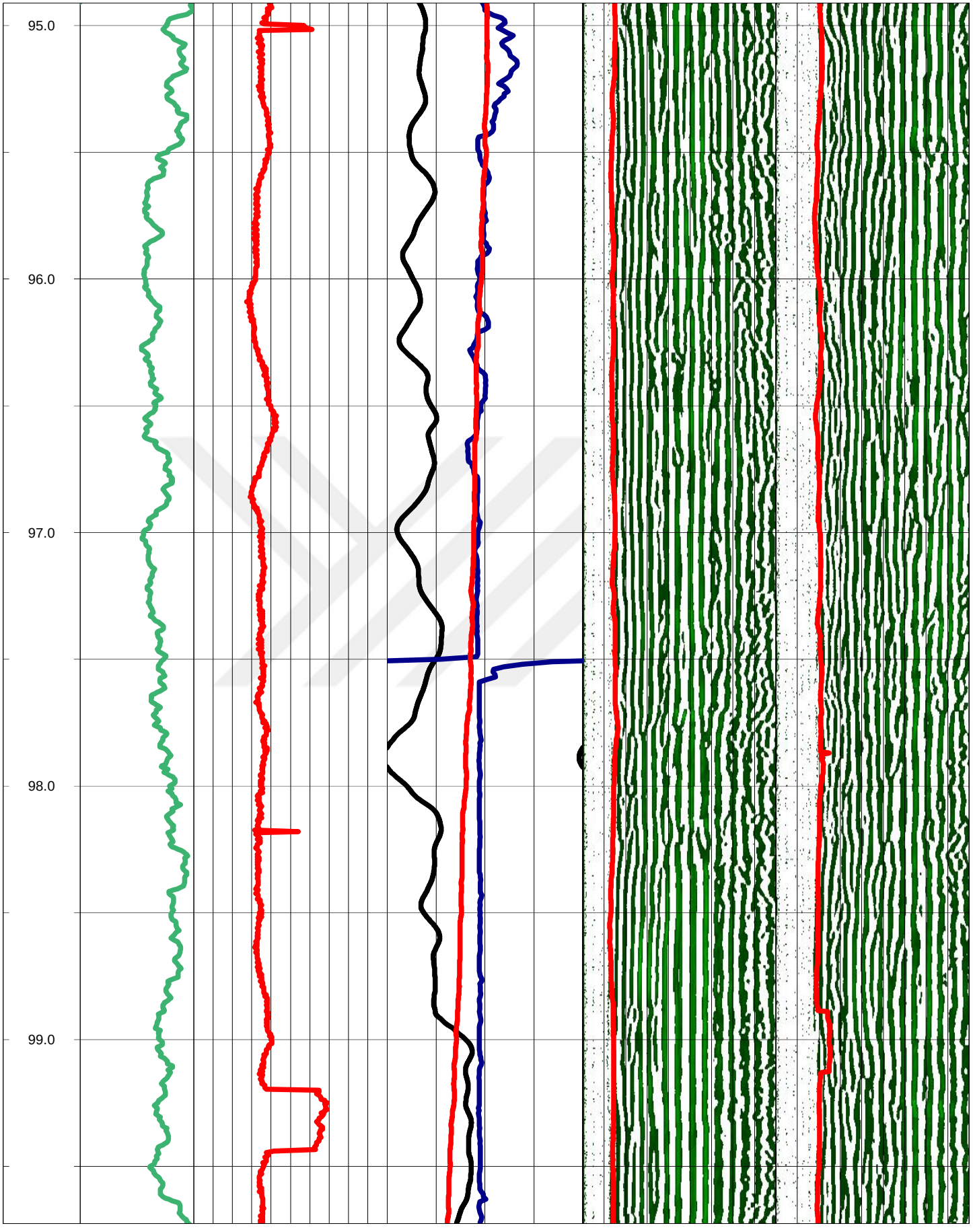
95.0
96.0
97.0
98.0
99.0

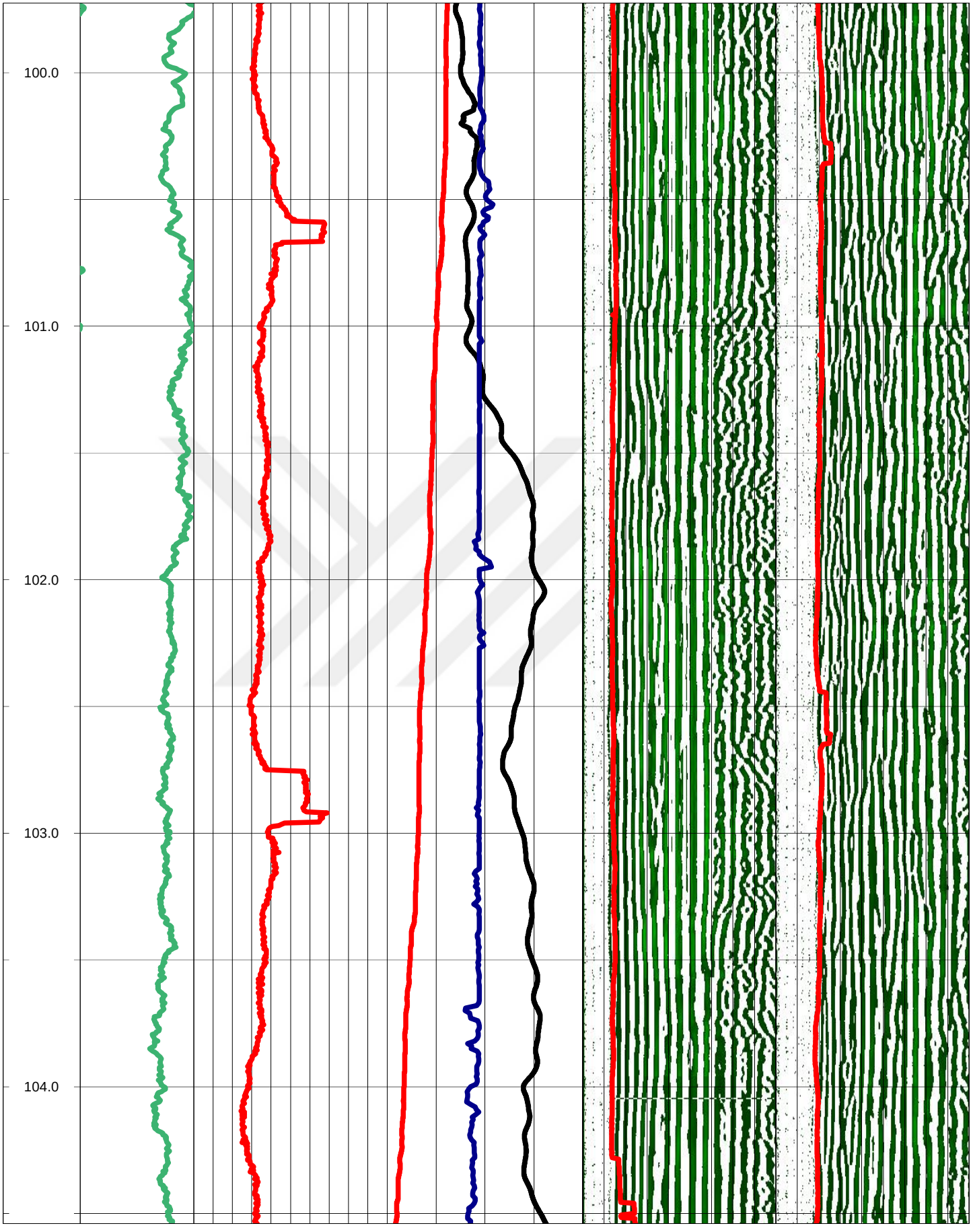
100.0
101.0
102.0
103.0
104.0

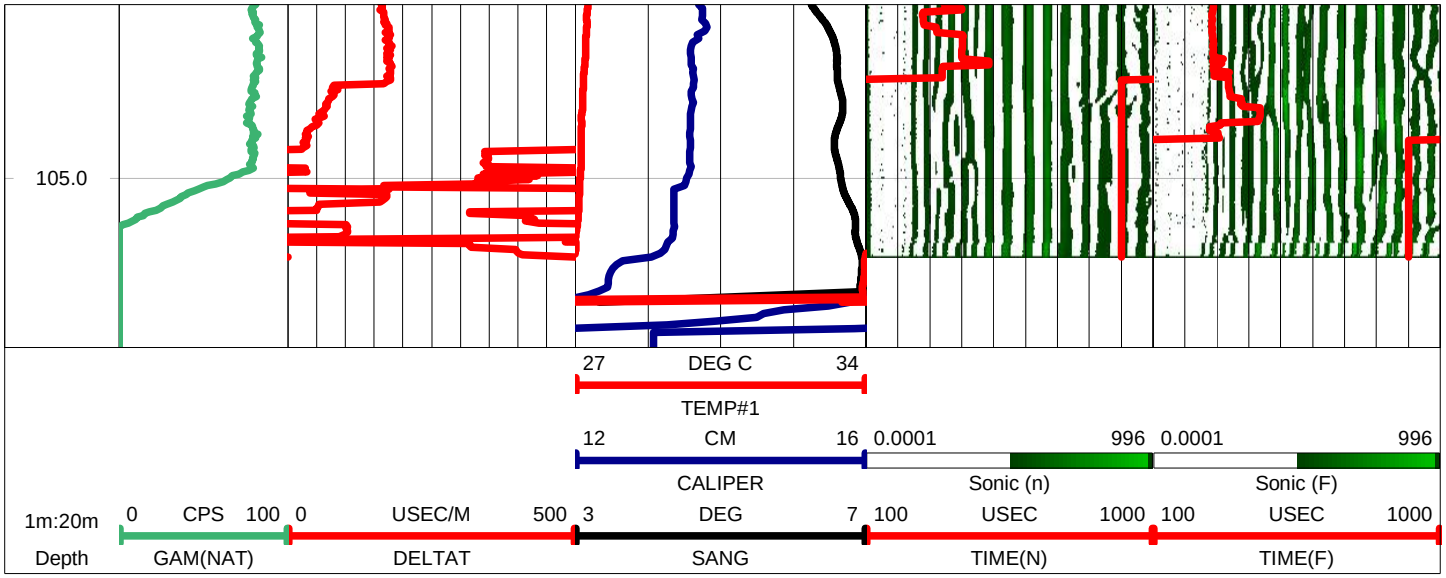
105.0
27
DEG C
34
TEMP#1
12
CM
16
0.0001
996
0.0001
996
CALIPER
Sonic (n)
Sonic (F)
1m:20m
0
CPS
100
0
USEC/M
500
3
DEG
7
100
USEC
1000
100
USEC
1000
Depth
GAM(NAT)
DELTAT
SANG
TIME(N)
TIME(F)